MODELLING BUSWAY OPERATION WITH MIXED STOPPING AND NON-STOPPING BUSES

Rakkitha Widanapathiranage

BSc (Civil Engineering)

Submitted in partial fulfilment of the requirements for the degree of Doctor of Philosophy

School of Civil Engineering and Built Environment

Science and Engineering Faculty

Queensland University of Technology

March 2015

Dedicated to Appachchi, Ammi, Akki, My Lovely wife Rupika and daughter Inuli

Keywords

BRT, busway, bus-bus interface, capacity, clearance time, delay, dwell time, efficiency, loading area, queue, reliability, South East Busway, transaction time.

Abstract

Bus Rapid Transit (BRT) systems are popular globally as they can provide high capacity, lower cost public transit solution that can significantly improve urban mobility for medium to large size cities. Earlier BRT systems were designed to operate on bus lanes only. In recent time, most sophisticated BRT systems have become popular, in particular segregated busways which have a separated carriageway for buses and therefore little or no disturbance by other traffic sources. This research analyses segregated busway performance using Brisbane's South East Busway (SEB) as a case study.

Stations on busway corridor ordinarily control line capacity, due to either queue spillback into the mainline upstream of the station, or the capacity of the bottleneck immediately downstream of the platform lane merge taper. Bus traffic turbulence is mainly a result of conflict as buses manoeuvre into and out of loading areas along the platform. As bus inflow to a station approaches capacity, queuing becomes excessive. Therefore, a practical capacity corresponding to an acceptable queue length needs to be defined for safe and efficient operation, which is a philosophy similar to that applied to other traffic facilities such as a minor approach on an unsignalised intersection.

Further, most busway stations on SEB accommodate both express and stopping bus services. The effect of stopping and non-stopping buses on mainline capacity is different from a basic mode of operation where all buses stop. However, no research was found in literature, which addresses this complex mode of operation. Hence, this research specifically addresses this research gap.

The operation procedure of SEB is complex; therefore a detailed investigation was conducted in order to select the best station for this study, considering the overall performance including all of its strategic elements. A scoping system considering all aspects was developed to select the best station for study, being Buranda. This research identified that dwell time, clearance time and station efficiency are the main parameters that affect station bus capacity. A series of surveys was designed as part of this study and conducted at Buranda to measure specific parameters and develop analytical tools.

It was identified that some drivers create a *temporary* loading area at the rear of the station platform during the peak hour, when the three formal loading areas are occupied. Increasing occupancy of *temporary* loading area is found here to reduce overall efficiency of the busway station platform. The applicability of this finding is important to busway operational procedures.

This research presents a novel methodology to estimate bus dwell time on a loading area at a station platform using smart card transaction data. The proposed method can estimate average dwell time and coefficient of variation of dwell time without the need for costly, manual field surveys. The empirical equations developed here are demonstrated to be simple yet robust.

A microscopic simulation model of Buranda station is developed in order to understand queue formation upstream of the station, and operation with a mixture of stopping and non-stopping buses. Empirical equations are developed for two modes of operation when all buses stop at the station and when some buses do not stop. These newly proposed procedures of estimating of both capacity and queuing are needed for traffic engineering analysis of busway facilities, particularly as some systems are now reaching capacity at certain stations and queue interaction between nodes arises. This can also facilitate analysis efforts to reduce additional passenger delays.

This study recommends that a practical degree of saturation of 0.8 should not be exceeded when estimating busway station design capacity under All-Stopping Buses (ASB) operation, for average dwell times between 10 and 60 seconds and coefficients of variation in dwell time between 0.4 and 0.6. In order to satisfactorily operate a busway station under ASB operation, the average upstream queue length should not exceed 6 buses for an average dwell time of 10 s, down to 3 buses for an average dwell time of 60 s, when the coefficient of variation of dwell time ranges between 0.4 and 0.6. Also the temporary loading area efficiency analysis identify that overall efficiency of the bus station reduce with increasing temporary loading area efficiency.

Table of Contents

List of Figures

List of Tables

List of Abbreviations

AIMSUN	Advanced Interactive Microscopic Simulator for Urban and Non-Urban Networks
AFC	Automatic Fare Collection
API	Application Programming Interface
ASB	All-Stopping Buses
AVL	Automatic Vehicle Location
BRB	Boggo Road Busway
BRT	Bus Rapid Transit
BSLC	Busway Loading Bus Capacity
BUZ	Bus Upgrade Zone
CBD	Central Business District
DoS	Degree of Saturation
EB	Eastern Busway
HCBs	High Capacity Buses
ITS	Intelligent Transportation System
K-S	Kolmogorov-Smirnov
LA	Loading Area
M3	Pacific Motorway
MSB	Mixed-Stopping Buses
MSL	Maximum Schedule Load Vehicle Capacity
NB	Northern Busway
NS%	Non-stopping bus percentage
NSB	Non-Stopping Buses (under MSB operation)
OLSR	Ordinary Least Squares Regression
OSB	On-Street Bus
QJBL	Queue Jump Bus Lane
QoS	Quality of Service
QSBS	Queen Street Bus Station
QUT	Queensland University of Technology
RMS	Root Mean Square
SB	Stopping Buses (under MSB operation)
SBBL	Set Back Bus Lane
SBIT	South Bank Institute of Technology
SEB	South East Busway
SEQ	South East Queensland
TCQSM	Transit Capacity and Quality Service Manual
TRB	Transportation Research Board
UQ	University of Queensland

Statement of Original Authorship

The work contained in this thesis has not been previously submitted to meet requirements for an award at this or any other higher education institution. To the best of my knowledge and belief, the thesis contains no material previously published or written by another person except where due reference is made.

QUT Verified Signature

Signature:

Date: 22/03/2015

Acknowledgements

It would never been able to produce this doctoral thesis without the Australian Postgraduate Awards scholarship provided by Department of Education and exceptional support from Queensland University of Technology (QUT).

First and foremost, I own my deepest gratitude to my principle supervisor, Associate Professor Jonathan M Bunker and Associate supervisor, Dr. Ashish Bhaskar. I greatly appreciate their outstanding guidance, encouragement, wisdom and caring support provided throughout this project. It was an honour and a pleasure to be one of their students. Their professional and far-thinking leadership ensured the study progress, timely completion and high standard of this thesis. The time spent working with my supervisors greatly shaped my professional identity and effectively made me the researcher I am today. For this I will be eternally grateful to them. Also I would like to thank Professor Edward Chung being my associate supervisor at the beginning of this research.

Secondly, I greatly appreciate the support and help received from TransLink Transit Authority, Department of Transport and Main Roads in particular Mr. Daniel Ng and Mr. Steve McEvoy. I also would like to thank Busway Operations, Department of Transport and Main Roads in particular Mr. John Ward and Mr. Peter Burns. Special thank goes to Mr. Hao Guo on developing smart phone survey application.

Thirdly, I would like to acknowledge Dr. Mark Robinson, Mater Private Hospital on successfully conducting my shoulder surgery. I also acknowledge QUT Disability Support Unit on providing me relevant work station equipment and financial supports on buying them. The support from QUT medical centre, particularly Dr. Timothy Staunton-Smith is highly appreciated. Special thanks go to COR Rehabilitation and Mater Hospital Allied Clinic.

Fourthly, I would like to thank my beloved wife Rupika Bandara and daughter Inuli Widanapathiranage on their support and courage. Without their support this PhD would be a miracle. I also acknowledge support from my family in Sri Lanka; WP Thilakarathe (dad), P Seelwathi (mum) and Nilanka Roshini (sister) for their understanding, support and encouragement at all times. I hope I have not failed their expectations.

Last but not least, I would like to extent my thanks to all my friends and survey team who supported me during the entire three years of this PhD both in academic and in daily life: Shiran Jayakody, Bhagya Jayasinghe, Hasitha Damruwan, Hasitha Nayanajith, Supipi Kumari, Sandya Wasanthi, Rajitha Nawarathna, Cynthujah Vivekananthan, Buddhi Wijesiri, Lakshika Kalhari, Sampath Dareeju, Thilan Jayathilake, Maura Atapattu, Lanka Dissa Bandara, Nadeeka Migunthanna, Nandika Migunthanna and Chandima Gunwardana. They proved that our friendship is beyond the bounds of distance, time and circumstances. Without help and friendship from these people, this PhD would have been a rough ride.

Chapter 1: Introduction

1.1 Research Background

Bus Rapid Transit (BRT) systems are popular globally as they are generally more economical than other rapid transit systems like Light Rail Transit (LRT). BRT is an innovative, high capacity, lower cost public transit solution that can significantly improve urban mobility for medium size to large cities. This stable, integrated system uses buses or specialized vehicles, roadways or dedicated lanes to promptly and efficiently transport passengers to their destinations, while offering the flexibility to meet transit demand. BRT systems can easily be customized to community needs and incorporate state-of-the-art, low-cost technologies that result in more passengers and less congestion (UNHSP, 2013).

The greatest challenge to BRT as a transit mode is its comparison with LRT and Metro systems. Initially, it was believed that capacity of BRT system was limited to 12,000 p/h (FTA, 2008). However, after opening of Bogotá's TransMilenio BRT system in Colombia in 2000, a capacity of 35,000 p/h was realised, which is significantly higher than the nominal 19,000 p/h capacity of a fully grade separated LRT system (TCRP-90, 2003). While LRT has certain operational advantages, overall BRT has been considered by many to be superior with respect to capacity, mobility, and cost.

Another significant challenge facing BRT is its comparison with conventional On-Street Bus (OSB) service. Being operated in general traffic lanes, OSB faces more delay, reduced speed, higher travel time than BRT system (UNHSP, 2013). However, its main advantage is that it does not require a separate, expensive right-of-way.

This thesis uses as its case study the BRT facility in Brisbane, Australia, which is identified as a busway system. Its design and planning was largely modelled on Ottawa's BRT system in Canada (Rathwell & Schijns, 2002). The first section of Brisbane's busway system, between Brisbane Central Business District (CBD) and Woolloongabba station opened in year 2000; in time for 2000 the Olympic Games

Football matches (Figure 1-1). Further development extended the South East Busway (SEB) to Eight Mile Plains in 2001; followed by development of the Boggo Road Busway (BRB) to University of Queensland in 2009, the Eastern Busway (EB) to Langlands Park station in 2011, and the Northern Busway (NB) to Kedron in 2012. At present, the SEB is 16 km long and consists of 11 busway stations (Figure 1-1) (Widanapathiranage, Bunker, & Bhaskar, 2013a). Further extension of SEB is planned from Eight Mile Plains to Springwood, while the EB is planned to be eventually extended from Langlands Park to Capalaba via Coorparoo and Carindale (TransLink, 2007, 2010).

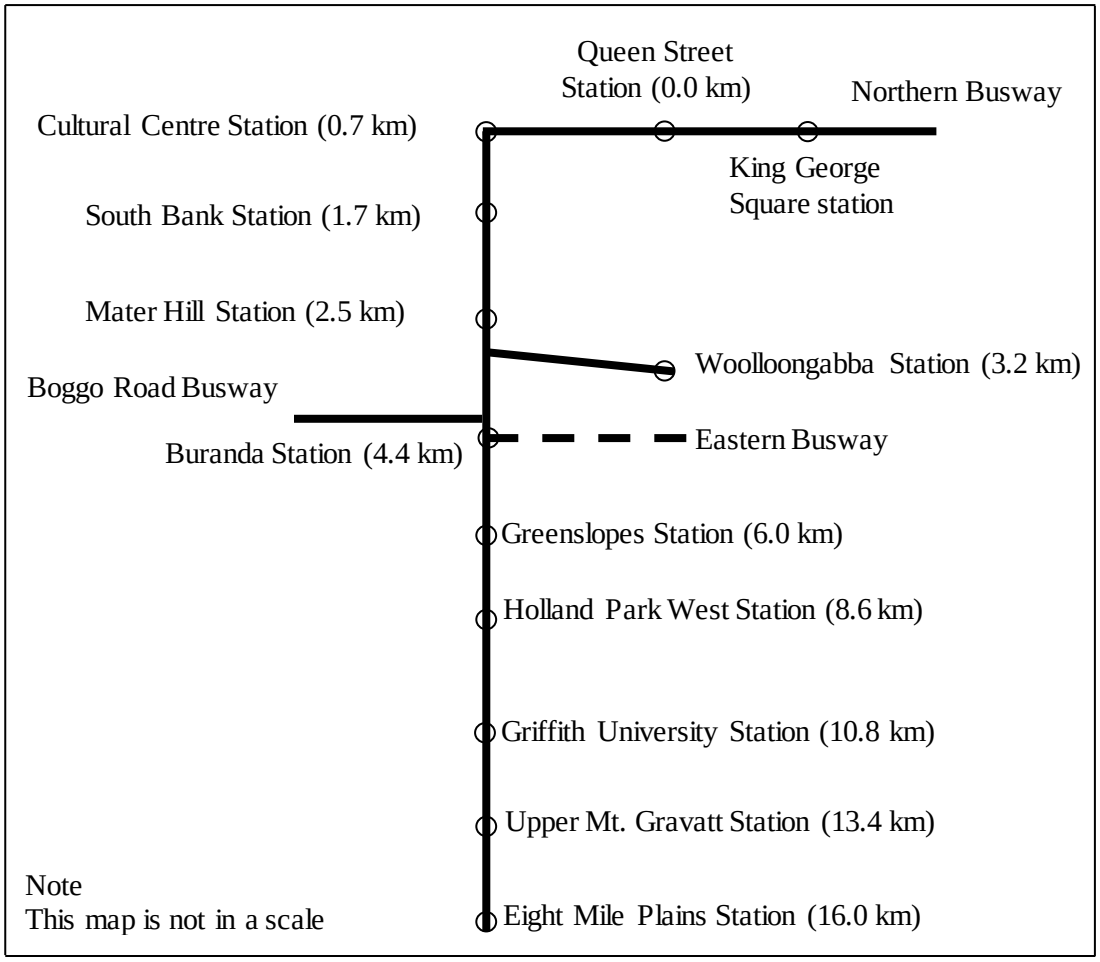

Figure 1-1: Schematic Diagram of the SEB

1.1.1 Research Motivation

There has been a 180 percent increase in patronage on major bus routes since Brisbane's South East Busway opened in year 2000. Moreover, more than 70 percent of network passengers use some part of a Busway in their journey. In 2009, 18,000 p/h were carried on the SEB's maximum load segment in the busiest morning peak (Lucas, 2009). With South East Queensland region's population forecast to grow

from 3.1 million in 2009 to 4.4 million in 2031, and because of growth in easy and reliable services compared to other available transport modes, demand on the SEB continues to increase (TransLink, 2011).

The SEB mostly operates with direct bus service between suburbs and the CBD (Golotta & Hensher, 2008). Buses from suburban areas access the busway through one of many access intersections near busway stations and then continue to Brisbane CBD. This is reversed for outbound services. During peak hours (especially mornings and evenings) the volume of buses and their interference on each other cause traffic congestion at certain busway stations, particularly those near the CBD where buses experience their maximum load segments and / or highest dwell times due to maximum passenger boarding and alighting flows. As well as reducing bus efficiencies, this tends to increase passenger crowding at these stations, increasing travel time and reducing service comfort and reliability.

Jaiswal, Bunker, and Ferreira (2010) found that increased passenger crowding on a Brisbane BRT platform led to increased service times per passenger, which heightens bus service time. This in turn has a feedback effect of reduced bus throughput capacity. This is further confounded near the CBD by at-grade intersections of the busway with surface streets carrying general traffic.

Most SEB busway stations have linear off-line loading areas (three loading areas per station) to allow buses to overtake the stopping buses (Widanapathiranage, Bunker, & Bhaskar, 2013b). Therefore, busway stations are crucial from an operational standpoint as they are the only sections on a busway where buses can overtake dwelling or otherwise stopped buses. Due to high volumes of buses, recurrent congestion occurs at several stations on the SEB during weekday peak periods.

Mainline capacities of a busway (bus/h) are predominantly dependent on busway station capacity, due to either queue spillback into the mainline upstream of the station, or the capacity of the bottleneck immediately downstream of the platform lane merge taper. Bus traffic turbulence is mainly a result of conflict as buses manoeuvre to pull into and out of a loading area along the platform. As bus inflow to a station approaches capacity, queuing becomes excessive. Therefore, a practical capacity corresponding to an acceptable queue length needs to be defined for safe and efficient operation, which is a philosophy similar to that applied to other traffic facilities such as a minor approach on an unsignalised intersection.

Limited research has been conducted on impacts of busway station operation on the line capacity of a busway. Therefore, this research is intended to address this gap by considering a case study station on the SEB.

Further, most busway stations in Brisbane accommodate both express and stopping services. The effect of stopping and non-stopping buses on mainline capacity is different from a more basic mode of operation with all buses stopping. No research was found in literature, which addresses this more complex mode of operation. Hence, this research specifically addresses this research gap.

1.2 Research Aim

The central aim of this research is to improve existing methodologies of quantifying busway corridor performance, particularly under the conditions unique to the busway system of Brisbane, Australia.

1.3 Research Hypothesis

The central hypothesis of this thesis is that busway facility operation can be analysed more effectively and reliably using mathematical models, which are developed from computer simulations which were calibrated and validated using field data under varying operational conditions.

1.4 Research Questions

This research is guided by the following four questions, which flow from the above mentioned research aim and hypothesis:

1. Using Brisbane's SEB as a case study, how does an existing busway facility perform when analysed using existing standard procedures and how accurate is capacity estimation under high demand conditions?
2. How can we improve existing procedures, where necessary, to more accurately estimate capacity with respect to queuing?
3. How can we improve existing procedures, if necessary, to more accurately estimate capacity with stopping and non-stopping operation?
4. How can we estimate the variables that affect busway performance measurement in a simple and effective way?

1.5 Objectives

The following key objectives of this research have been established to achieve the research aim by responding to the research questions:

1. Review the literature on busway facility operation and feasibility studies also identify suitable methods and metrics to measure capacity and reliability. (RQ1)
2. Investigate overall performance of SEB to select a busway station for this thesis.
3. Analyse the existing performance of SEB by targeting Buranda Station since it experiences high passenger exchange. As the demand of the system increased substantially after opening of EB in late 2011, Buranda is ideal to measure and investigate performance changes since that time. (RQ4)
4. Develop a microscopic traffic simulation model test bed of Buranda busway station using methods identified from objective 1 to measure operational conditions for both all buses stopping and mixture of buses stopping regimes under a range of operating conditions. (RQ2, RQ3)
5. Demonstrate the use of Automatic Fare Collection (AFC) data to effectively estimate dwell time, which is a key parameter of busway station performance measurement. Real time data are used to develop simple and effective mathematical models which are validated with literature. (RQ4)
6. Use this simulation model to generate data reflective of a range of operational conditions. Use statistical analysis of the data to generate and calibrate mathematical models to estimate capacity and upstream bus queue length under varying inflow for both all-stopping and mixed-stopping regimes. (RQ2, RQ3)
7. Develop recommendations for future busway planning, operational analysis and management.

1.6 Scope and Limitations of the Research

One of the main contributions of this research is to investigate the applicability of AFC data to measure bus dwell time in an easy and simple way. The models developed in Chapter 6 account for two door buses since more than 88 percent of buses that use the SEB have two doors (Otto, 2008). The scope of the research is limited to off line busway station operation which is the main type of operation for SEB. In addition, this research based on developing dwell time models under all-stopping and mixed-stopping bus operational modes.

The other motivation of this research is to study BRT facility operation with mixed-stopping and non-stopping buses and hence define a practical bus capacity. However, the practical bus capacity of a BRT facility will be improved by introducing High Capacity Buses (HCBs) or introducing new operational methods (such as trunk and feeder operation system); but these paths are beyond the scope of this research.

The investigation of practical bus capacity is limited to existing busway infrastructure. Analysis of operation under modification to existing infrastructure or construction of new infrastructure is beyond the scope of this research. Practical bus capacity is investigated for average dwell times between 10 s and 60 s and coefficient of variation of dwell times between 0.4 and 0.6.

1.7 Significance of the Research

Public transport demand in South East Queensland (SEQ) is growing rapidly. Forecast population growth means transport trips will increase from about 10 million a day in 2006 to more than 15 million a day by 2031 (TransLink, 2011). Brisbane's busway system has incorporated some short term solutions such as expansion of express Rocket and high frequency Bus Upgrade Zone (BUZ) services and other additional services to accommodate growing public transport demand. However, this increase in services has been argued by some as a contributing factor to bus congestion on Brisbane's busway network and with it decreased reliability of the system (Golotta & Hensher, 2008).

This study helps to increase the disciplinary knowledge by identifying impacts of busway station operation on line capacity under mixed-stopping and non-stopping bus operation. This study is interesting yet significantly important to transport

planners (such as in Brisbane busway) who are constantly try to achieve bus network operation optimal capacity with customer satisfaction.

1.8 Thesis Outline

Remainder of this thesis consists of another seven more chapters. Figure 1-2 shows the structure of thesis.

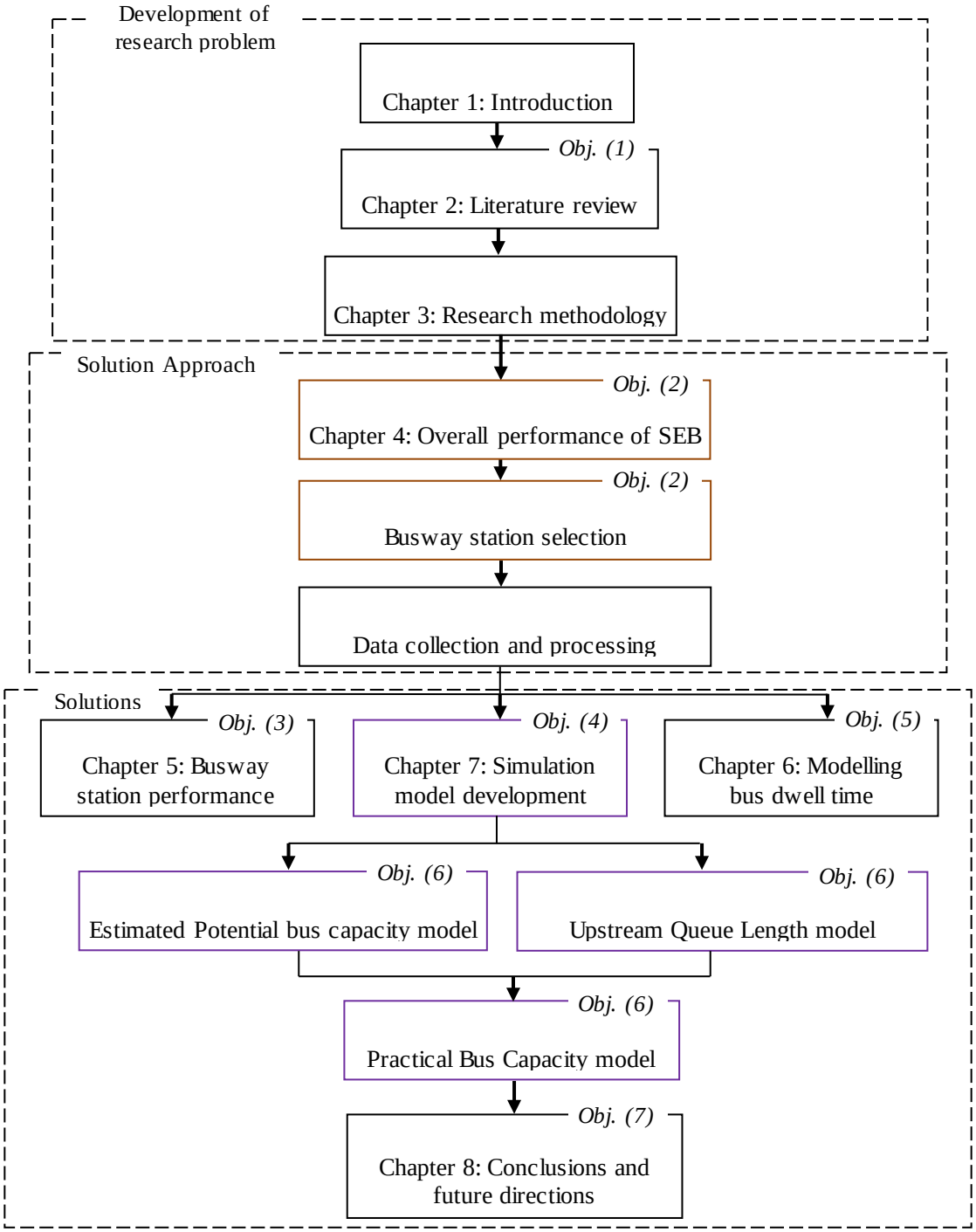

Figure 1-2: Thesis Structure

A brief outline of each Chapter is given bellow.

Chapter 1 (this chapter) presents the background, research motivation, research aim, research hypothesis, research questions and research objectives. Subsequently, scope and significance of the research are presented. Finally, an outline of the thesis is discussed.

Chapter 2 further discusses literature relevant to the research hypothesis and research questions. Then identified knowledge gaps in busway capacity analysis and other operational characteristic analysis are presented.

Chapter 3 elaborates on the methodology proposed in this research to answer research questions identified in Chapter 1.

Chapter 4 investigates the overall performance of SEB and then select a busway station to conduct in detail analysis.

Chapter 5 presents analysis of busway station performance by targeting a busway station in SEB. In particular, this chapter proposes an improved method to analyse busway station efficiency.

Chapter 6 describes the development of estimating key operational variables, which impact on capacity and queuing, using AFC data.

Chapter 7 describes the development of BRT facility potential capacity models for all-stopping and mixed-stopping operation. Thereafter, Chapter 7 analyses the queue formation busway bottlenecks (busway station) and the practical bus capacity with acceptable queue length and demand for both stopping and mixed-stopping operation.

Chapter 8 concludes by presenting a summary of the outcomes of the work conducted in this study, followed by suggestions for future work.

1.9 Publication from this Research

This research has yielded four peer reviewed conference papers. One journal article was submitted with revisions and an additional four journal articles are being prepared. In addition, a report titled “Investigating the SEB overall performance” was published. A complete list of publications is given below.

Journal article (under review)

1. Widanapathiranage, Rakkitha, Bunker, Jonathan M., & Bhaskar, Ashish (2015) Modelling the BRT station capacity and queuing for all stopping busway operation. Public Transport: Planning and Operations, 7(1), pp. 21-38.

Conference papers (peer reviewed)

1. Widanapathiranage, Rakkitha, Bunker, Jonathan M., & Bhaskar, Ashish (2015) Analyzing busway station potential capacity under mixed stopping and non-stopping operation. In Perk, Victoria (Ed.) Transportation Research Board 94th Annual Meeting Compendium of Papers, Transportation Research Board of the National Academies, Washington, D.C.
2. Widanapathiranage, Rakkitha, Bunker, Jonathan M., & Bhaskar, Ashish (2014) Modeling Bus Rapid Transit station bus queuing for Bus Rapid Transit station bus operation analysis. In Weeks, Jennifer (Ed.) Transportation Research Board 93rd Annual Meeting Compendium of Papers, Transportation Research Board of the National Academies, Washington, DC, USA.
3. Widanapathiranage, Rakkitha, Bunker, Jonathan M., & Bhaskar, Ashish (2013) Modelling busway station dwell time using smart cards. In Australasian Transport Research Forum 2013 Proceedings, Australasian Transport Research Forum, Queensland University of Technology, Brisbane, QLD.
4. Widanapathiranage, Rakkitha, Bunker, Jonathan M., & Bhaskar, Ashish (2013) A microscopic simulation model to estimate bus rapid transit station bus capacity. In Australasian Transport Research Forum 2013 Proceedings, Australasian Transport Research Forum 2013, Queensland University of Technology, Brisbane, QLD
5. Widanapathiranage, Rakkitha, Bunker, Jonathan Michael, & Bhaskar, Ashish (2013) A microscopic simulation model to estimate Bus Rapid Transit (BRT) station service capacity with mixed stopping and non-stopping bus operation. In OPTIMUM 2013: International Symposium on Recent Advances in Transport Modelling, 21-23 April 2013, Mantra on Salt Beach Resort, Kingscliffe, NSW Australia.

Report

1. Widanapathiranage, R., Bunker, J. M. & Bhaskar, A., (2014) Case study: South East Busway (SEB), Brisbane, Australia.

Chapter 2: Literature Review

2.1 Overview

This chapter reviews the necessary literature in the field of dwell time estimation, Bus Rapid Transit (BRT) facility capacity and reliability measures. The chapter begins (section 2.2) by defining BRT in its various forms. The role of the station in overall operation of the BRT facility is examined in section 2.3. Section 2.4 discusses the theory of the facility reliability. This chapter closes by identifying knowledge gaps in relation to BRT station and facility operational modelling and capacity estimation (Section 2.5).

2.2 Bus Rapid Transit (BRT) Arrangement

2.2.1 BRT Definition

BRT is an emerging rapid transit mode. It has both advantages and disadvantages compared to the other rapid transit modes. Usually, BRT are operating from small to medium size cities, as well as along moderately used corridors in larger cities. There are various definitions of BRT. The United States Transportation Research Board's (TRB) Transit Capacity and Quality Service Manual 2013 (TCQSM 2013) (TRB, 2003b) defines bus rapid transit as a flexible, rubber-tired rapid transit-mode that incorporates stations, vehicles, services, running ways and Intelligent Transportation System (ITS) elements into an integrated system with a strong positive identity that evokes an unique image.

2.2.2 Types of BRT Facilities

Figure 2-1 classifies the types of BRT systems in use. The most common types of BRT are bus lanes, transitway and segregated busways.

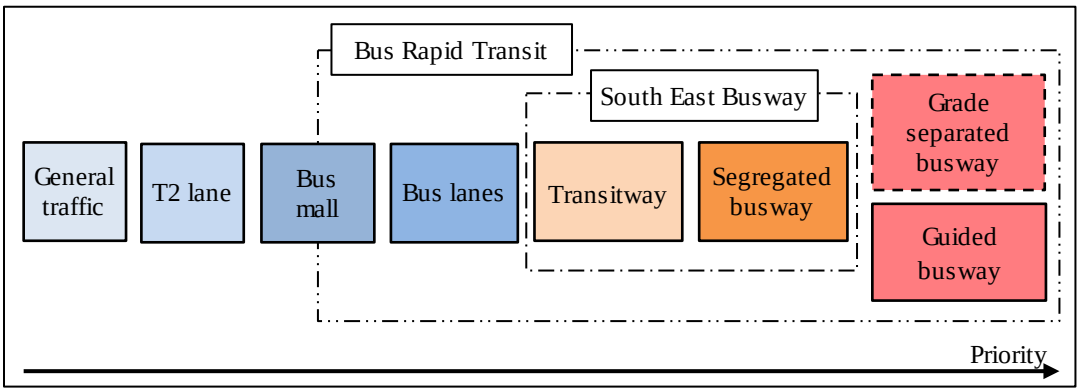

Figure 2-1: Bus Rapid Transit System classification

General Traffic

Buses that are operating in general traffic move without any priority (Figure 2-2). These services operate with the lowest priority hence overall performance is lowest.

Figure 2-2: Buses operating in general traffic
(base: http://busautralia.com)

T2 lane (Transit lane)

This is similar to buses in general traffic, but has the priority on operating T2 lane during designated peak periods (Figure 2-3).

Figure 2-3: Buses operating in T2 lane
(source: http://busautralia.com)

Bus Mall

Bus mall can be argued as either a BRT facility or general traffic facility. Usually, a bus mall consists of a series of bus stops situated close to each other with skip-stop operation of buses. Figure 2-4 shows Brisbane CBD's Adelaide Street bus mall. The main advantage of a bus mall is that it can process quite large number of buses; however the reliability can be low.

Figure 2-4: Buses operating in bus mall
(base: http://busautralia.com)

Bus lane

Bus lanes are exclusively designed for bus movement only. This enables greater speed than other transit facilities mentioned above (Figure 2-5). However, bus lanes interact with general traffic at intersections.

Figure 2-5: Buses operating in bus lane
(base: http://busautralia.com)

Transitway

A transitway is a traffic lane reserved for bus use only and gives moderate improvement to transit speed and reliability. Transitways are similar to bus lane operation, but are separate from general traffic by a kerb lane (Figure 2-6). A section

between Queen Street Bus Station (QSBS) portal and the Melbourne Street portal of SEB is a typical transitway section (refer Section 4.3.2).

Figure 2-6: Buses operating in transitway
(base: http://busautralia.com)

Segregated busway

Segregated busways are exclusive right of way for buses which can provide greater improvement in transit speed and reliability; but are expensive to build and maintain (FTA, 2008). Brisbane's and Ottawa's busway systems are example of segregated busways (Figure 2-7).

Figure 2-7: Segregated busway
(base: http://juts.janes.com)

Guided busway

Another form of busway is a fixed guide way for buses (FTA, 2008). In this form, once a bus (usually equipped with side-mounted guide wheels) enters the guide way, the bus driver needs only control the speed of the bus as the steering is controlled by the guide way. The benefit of guided busways over grade separated

busways is the high average speed. Adelaide's O-Bahn (Figure 2-8) is an example of such a system (Currie, 2006).

Figure 2-8: Guided busway
(base: http://busautralia.com)

In theory busways can be fully grade separated meaning that buses operate with no disturbances from other traffic, intersections, ramps, etc. Despite being unrealistic, this is the maximum reliable operation that a BRT facility can operate. According to the BRT classifications mentioned above, guided and segregated busways closely match performances of fully grade separated busways.

Considering BRT facilities mentioned above, we selected segregated busway section in SEB (section between Melbourne Street portal tunnel and Eight Mile Plains busway station) for this study. When this thesis specifically talk about busway, it represents segregated busways while term "BRT" use for general discussion for the remainder of this thesis.

2.2.3 Busway and Busway Station

A busway corridor is a linear corridor containing multiple segments, which carries one or more bus routes (Widanapathiranage et al., 2013c). A segment is defined as a section of BRT facility between two nodes that influences the traffic operation of the BRT line. Examples of a node include a BRT station where buses are able to stop and dwell to serve passenger exchange (boardings and/or alightings) (Figure 2-9 (a)), signalized intersection (Figure 2-9 (b)), unsignalized intersection (Figure 2-9 (c)), on-ramp and off-ramp (Figure 2-9 (d)).

(a) (b)

(c) (d)

Figure 2-9: BRT facility nodes
(base: http://cotteeparker.com.au, http//: wikipedia.org , http://weekendbrisbane.com.au, http:// skyscrapercity.com)

In this study, a station is defined to be directionally separated such that buses cannot overtake across the oncoming side of the roadway. It has a linear platform in each direction to serve passenger exchange. The platform contains multiple and off-line linear loading areas. In each direction, the roadway contains a platform stopping lane with an upstream pull-out taper and a downstream merge taper, plus an adjacent passing lane (Widanapathiranage et al., 2013c). A loading area is defined as a portion of the platform stopping lane, either marked or unmarked, which is designated for bus stopping and dwelling to serve passenger exchange.

Stations are one of the main features of a BRT facility (FTA, 2007). In BRT systems like that of Curitiba, Brazil, stations are nodes between surrounding land uses and feeder services that offer a reasonably comfortable and secure location to access BRT services and interchange with feeder services (TRB, 2003a). Stations may also provide a number of other functions in common with stations of other rapid transit modes including heavy rail and light rail, such as bicycle racks, park and rides, drop-off points, information boards and ticket machines.

2.3 BRT Capacity Theories

Capacity represents the maximum passenger volume that a BRT facility can transport during a given time period. Capacity of a system or facility gives a maximum ability to perform for public transport (Vuchic, 2005). Two different capacity measures are important to estimate BRT Capacity and they are BRT facility vehicle capacity and BRT facility line service capacity.

2.3.1 Vehicle Capacity

Vehicle capacity is the maximum number of spaces for passengers that a transit unit (bus) can accommodate. Vehicle capacity can be calculated in three different methods; seats plus standing, seats only and the ratio of passenger per seat (Vuchic, 2005). Seats plus standing spaces are suitable for high volume bus services where bus service is primarily designed to service on relatively less lengthy routes (especially in city suburban areas). This capacity depends on the standard use for floor area per standee.

2.3.2 BRT Facility Capacity

There are various transit capacity methods available in literature. However, some methods have drawbacks or they are not entirely expressing the true BRT operation (detail discussion included in section 2.3.5). Conversely, the procedure of estimating BRT facility capacity is described fairly well in TCQSM 2013.

The capacity of a BRT corridor is estimated by considering the busiest station of the BRT facility (TRB, 2013). TCQSM 2013 identified these busiest station as a critical bus stop of the BRT facility (TRB, 2013). However, the capacity of a busway station may vary depending on passenger demand, bus route characteristics and busway station size.

According to TCQSM 2013, station capacity is dependent on the loading area (Figure 2-10) capacity and the efficiency of each loading area (TRB, 2013). Each of these is now presented in logical sequence.

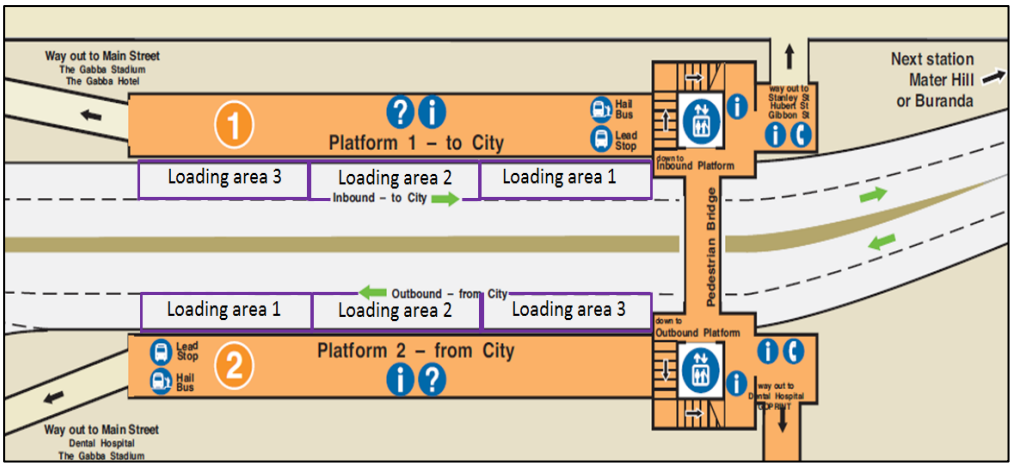

Figure 2-10: Typical busway station in SEB
(base: http//:translink.com.au)

Loading Area Capacity

Combination of dwell time and clearance time gives the time that bus occupies the loading area. The true theoretical loading area capacity (B_l) of can be estimated deterministically as follows,

$$B_l = \frac{3600}{t_c + t_d} \qquad \text{Equation 2-1}$$

where:

B_l = Loading area bus capacity (bus/h)

3600 = Number of seconds in one hour

t_c = Average clearance time (s)

t_d = Average dwell time (s)

Average clearance time is the time that needed to a dwelled bus clear its own length by moving out of the platform plus the time for a queued bus to replace it in the loading area. Average dwell time is the time that required a bus to service passengers which includes the time of maximum passenger flow time of all door channels, door opening and closing time and boarding lost time. Detail discussion of dwell time and clearance time is discussed in section 2.3.3.

Additional elements were introduced in TCQSM 2013 (TRB, 2013) methodology to calculate design loading area capacity. Section 2.3.4 gives the detail discussion of TCQSM 2013 loading area design capacity.

Loading Area efficiency

Loading area efficiency was first introduced in the first edition of TCQSM 1999 (TRB, 1999) to reflect that buses interfere with each other's ability to position into a loading area. It can be defined as follows for an off line three loading area platform. On the platform, efficiency of the rearmost, in this case third, loading area is 100 percent as it can always be occupied by a bus. Efficiency of loading area 1 is given by,

$$E_{LA1} = \frac{T_{2,3} - T_{1,b}}{T_{2,3}}$$ Equation 2-2

where,

E_{LA1} = Efficiency of loading area 1

$T_{2,3}$ = Total time that loading area 2 OR loading area 3 OR loading areas 2 and 3 are occupied during time *T*.

$T_{1,b}$ = Total time that loading area 1 was empty while a bus occupied loading area 2 OR loading area 3 OR both loading areas 2 and 3.

Efficiency of loading area 2 is given by,

$$E_{LA2} = \frac{T_3 - T_{2,b}}{T_3}$$ Equation 2-3

where,

E_{LA2} = Efficiency of loading area 2

T_3 = Total time that loading area 3 is occupied during time *T*

$T_{2,b}$ = Total time that loading area 2 was empty while a bus occupied loading area 3 during time *T*

T = Analysis period (3600 s)

Bus Station Capacity

Theoretical capacity of the bus station with three loading area can be estimated by (Jaiswal et al., 2007),

$$B_s = E_{LA1} B_{LA1} + E_{LA2} B_{LA2} + E_{LA3} B_{LA3}$$ Equation 2-4

where:

B_s = Bus stop bus capacity (bus/h)

E_{LA1}, E_{LA2},E_{LA3} = Efficiency of loading area one, two and three, respectively

$B_{LA1}, B_{LA2}, B_{LA3}$ = Loading area one, two and three bus capacities, respectively.

For an off line three loading area platform, the third loading area efficiency ought to be 100 percent because the bus at the front of the queue on platform area entry ought to have immediate access to it, once it is vacated. However, Widanapathiranage, et al. (2013a) found that sometimes there is just enough space at the end of a platform after the third loading area, for a fourth bus to stop and dwell in front-door only mode to serve passengers. This is called *temporary* loading area and its efficiency depends on the demand of BRT facility and driver behaviour. Further discussions and analysis of *temporary* loading area are discussed in Chapter 5.

Practical Bus Station Capacity

The practical capacity of a busway station corresponds to the practical degree of saturation in order to maintain acceptable upstream design bus queue lengths.

Hidalgo et al. (2013) suggested a method to estimate practical capacity of a busway station. However, their method is not suitable for most of BRT facilities as it is specifically designed to TransMilenio BRT system in Bogotá, Colombia. TransMilenio system is operating under trunk and feeder method where stations are situated within 500 m with two berths. The designed capacity of a station is 80 bus/h (with articulated and bi-articulated buses); however, a BRT system like in Brisbane, busway stations is occupied more regularly by buses. For an instant Buranda busway station in SEB is experiencing 220 bus/h during morning peak period plus 30 percent of non-stopping buses (94 bus/h). Therefore, the practical capacities of each BRT facility are different with respect to bus operation and busway station attributes.

Other drawback of this method is they did not consider a bus station with multiple berths. Even though Hidalgo et al. (2013) used dwell time as passenger boarding or alighting time, dwell time need to be refined all the components associated with dwell time including door open and closing time and boarding lost time (section 2.3.5). Therefore, this research is focused on estimating busway station practical capacity and Chapter 8 discusses the practical busway station capacity.

2.3.3 Factors Affecting Theoretical Busway Station Capacity

Clearance time

For the buses stopping on a kerb lane, this is the time needed to start up and leave the stop after doors have closed plus the time for a queued bus to replace it in

the loading area. For the buses stopping in a bay, the clearance time (t_c) also includes the time spent waiting for a gap of sufficient length in the adjacent traffic. TCQSM 2013 suggests the clearance time range between 10 - 20 seconds when data is not available for estimating facility capacity (TRB, 2013). Section 5.5.1 provides the analysis of clearance time.

Dwell time

Vehicle dwell time (t_d) is an important determinant of system performance and the passenger service quality of public transport systems. It is a part of vehicle running time and has a large influence on operational speed. Particularly for frequent services, the vehicle dwell time becomes a major component of vehicle headways and causes constraints to the system capacity.

Dwell time variability

Depending on fluctuations in passenger demand between buses and between routes, not all buses stop for the same amount of time at a stop. In addition, infrequent events such as wheelchair, passenger inquiry with driver or bicycle loading have the potential to significantly increase a given bus's dwell time at a stop. The coefficient of variation of dwell times (c_v) can be shown as follows;

$$c_v = \frac{\text{standard deviation of dwell time}}{\text{average dwell time}} \qquad \text{Equation 2-5}$$

Based on field observations of bus dwell times in several U.S. cities, $c_v$typically ranges from 0.4 to 0.8, with 0.6 recommended as an appropriate value in the absence of field data (TRB, 2013). Section 5.5.1 provides dwell time and coefficient of variation of dwell time analysis.

Existing dwell time models

TCQSM 2013 highlighted that dwell time is an important measure in capacity and service planning. TCQSM 2013 defines dwell time as the time a bus to serve for passenger boarding and alighting. This typically considers the average time that bus spent at bus stop to serve passengers including time for door openings and door closing (TRB, 2013). Bus dwell time directly affects vehicle travel time, and thus the fleet size is required to provide service based on scheduled headway.

TCQSM 2013 gave a standard value for dwell time calculation with passenger service times of 3.5 s with smartcards and 4.2 s with magnetic stripe tickets (TRB, 2013). In addition to that, crowded situations and bus type differences are accounted by adding or subtracting 0.5 s to or from each service time.

Earlier research on dwell time is mainly focused on manually collected data and used to find the impact of fare type, boarding and alighting passengers, crowding, and vehicle configuration. Levinson (1983) found that dwell time is equal to 5 s plus 2.75 s per boarding or alighting passenger in a no-fare bus system until passengers exceed the seating capacity, at which point the service time increases. Guenthner et al. (1983) found a 10 s to 20 s penalty for each stop plus a 3 s to 5 s penalty for each passenger boarding or alighting. However, most of early dwell time models were developed by using limited samples.

Stop-delay time may be further subdivided into delay time associated with bus deceleration, time to open and close doors, delay time associated with bus acceleration, and passenger boarding and alighting time (Wu and Murray, 2005). Wu et al. (2005) mathematically modelled first three delay components to estimate delay time at a stop with the function of door opening and closing time, bus cruise speed, acceleration rate and deceleration rate. The dwell time of a bus stop is assumed as linearly changing with passenger boarding and alighting time.

Jaiswal et al. (2009) introduced time lost into the dwell time model. The time lost by the bus is a loading area specific parameter and is included to account for the requirement that the passenger walk along a lengthy BRT station platform to reach the bus entry door. The differences between boarding and alighting times at three loading areas at one station were analysed in their research. They have come up with following conclusions: a) passenger per boarding time was 5.9 s, b) the least time lost resulted from the mid-loading (the second) area, while the greatest time lost resulted from loading at the third area and c) 85 percent of the time lost calculated for each of the three loading areas was 7.2 s, 4.5 s, and 8.7 s (Jaiswal et al., 2009, Jaiswal et al., 2010).

More recently, bus dwell time analysis was carried out using on-board video by Fricker (2011), and he developed a linear relationship for the dwell time as number of standees of the bus, number of passengers alight from front door and number of

boarding passengers. However, a value for number of passengers alight from front door was not included in this research.

Li et al. (2012) introduced dwell time estimation models for BRT stations using traditional survey method. They found that dwell time follows a logarithmic normal distribution with a mean of 2.56 s and a variance of 0.53. However, conducting a long survey to see the dwell time distribution is time consuming and costly.

Even though there are some good dwell time models found in the literature, they have limited applicability. Therefore, a simple and robust model to estimate dwell time is required. Accordingly, Table 2-1 shows the comparison of dwell time model attributes.

Table 2-1: Comparison of dwell time models

Method	Dwell time model (t_d)	Remarks
Levinson, 1983	$t_d = 5.0 + 2.75\ N$ N= number of passengers board and alight	2.75 s per passenger service dwell time model for no fare system with buses not exceeding seating capacity
Guenthner & Sinha, 1983		dwell time 10 s - 20 s per stopping 3 s - 5 s per boarding and alighting
Wu et al., 2005	Delay time at busway station $\delta_i = k_i + 0.5\mathrm{v}_i\left(\frac{1}{\alpha_i} + \frac{1}{\beta_i}\right)$ δ_i = delay time at a i^{th}stop k = door opening and closing time v = bus cruise speed α = acceleration rate β = deceleration rate	k = 3 s v = 40 km/h α = 1.33 m/s^2 β = 1.33 m/s^2
Jaiswal, et al., 2009	$DT_n = P_b t_b + P_a t_a + t_{oc} + LT_n$ DT_n= n^{th} loading area dwell time P_b,P_a= number of passenger boarding and alighting t_b,t_a= service time per passenger boarding and alighting t_{oc} = door opening and closing time (2 - 5 seconds) LT_n = n^{th} loading area bus lost time	Average passenger boarding 5.9 s Bus lost time for loading area one, two and three 7.2 s, 4.5 s and 8.7 s
Fricker, 2011		dwell time changing linearly with number of standees of the bus

		and passenger boarding and alighting from front door
Li, Duan, & Yang, 2012		Dwell time distribution follows lognormal distribution with mean of 2.56 and variance of 0.53
TCQSM 2013	$t_d = t_{pf,max} + t_{oc} + t_{bl}$ t_d = average dwell time $t_{pf,max}$ = maximum passenger flow time of all door channels t_{oc} = door opening and closing time t_{bl} = boarding lost time	service time per passenger 3.5 s with smartcards and 4.2 s with magnetic stripe tickets default dwell time: 60 s at a downtown stop (transit centre), 30 s at a major outlying stop and 15 sat a typical outlying stop

As mentioned in the TCQSM 2013 (Table 2-1), bus channel lay out needs to be carefully considered. Usually the boarding door of a bus is wider (or same in size) than rear doors. This allows passengers to board using two channels if a bus with adequate facility such as AFC system. However, alighting is limited at front door to a single channel because there is not enough space inside the bus for two passengers alight simultaneously. As far as alighting process is considered in three axle 14.5 m bus (Figure 2-11), there are two designated alighting channels exists at rear door where passengers in back and middle sections of the bus can use these separate channels to alight without any disturbance. Figure 2-11 demonstrates number of door channel layout of Brisbane SEB buses.

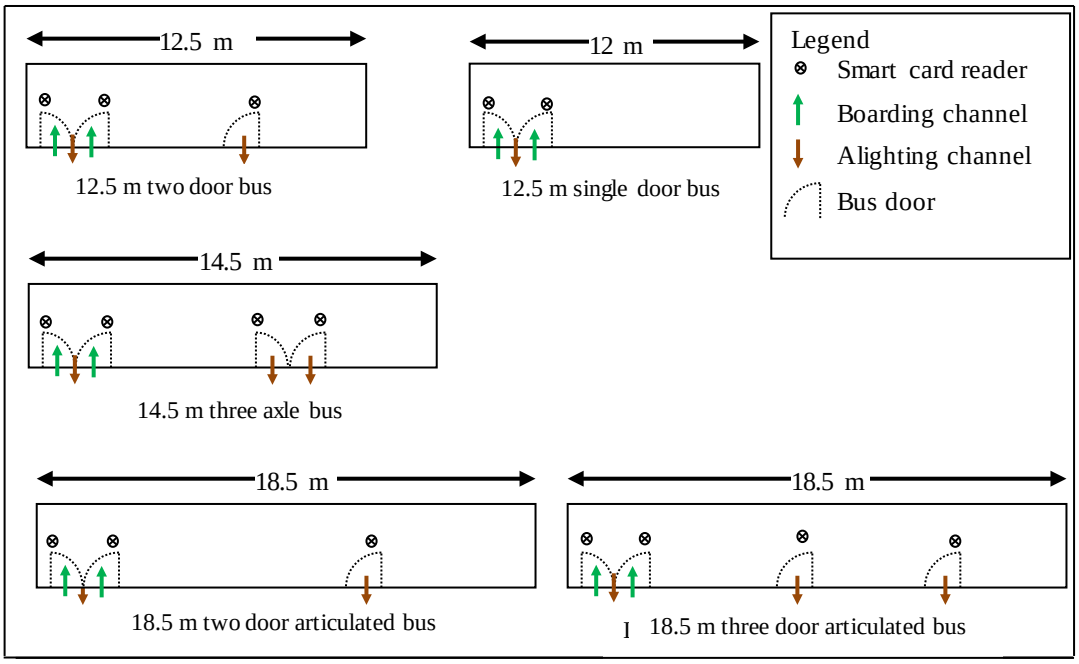

Figure 2-11: Bus channel layout

Dwell time Estimation

Dwell time at stops is understood to be an important component, which can impact travel time in transit systems and particularly on bus operations (Milkovits, 2008). Since dwell time being an important parameter in busway capacity analysis, there are several implemented methods to estimate dwell time. However, the TCQSM 2013 method is the best model to estimate dwell time as it accounts all delay components which relate to dwell time more importantly including boarding lost time.

The conventional method for dwell time estimation uses field surveys. However, this method is costly and requires high human resourcing. Therefore, the most current dwell time estimations were conducted using Automatic Fare Collection (AFC) or Automatic Vehicle Location (AVL) data.

Dwell Time Estimation Using AFC Data

Smart card fare collection system is a mode of AFC where it has overtaken other fare collection systems such as magnetic strip and paper tickets due to its reliability to both transit passengers and operators. Smart card transaction data gives the opportunity to find transaction time at particular bus stop for specific buses individually (Sun and Xu, 2012). Since Brisbane busways use AFC, this research investigates the possibility of estimating dwell time using AFC data. Detail analysis of dwell time estimation is described in Chapter 6.

2.3.4 Design Busway Station Capacity

BRT facility design capacity (bus/h) is differs from theoretical capacity, in that it represents an achievable flow rate (bus/h) under stipulated repeatable, safe working conditions resulting in a maximum achievable frequency with minimum headway. Usually, BRT facility capacity governs by the weakest link (or node) of facility such as busway station, signalised or unsignalised intersections.

Operating margin was first introduced by the TCQSM 1999 to account non-reliability for capacity estimation. When the operating margin is excluded as in Equation 2-1, true theoretical capacity can be estimated; which represents a condition when loading area failures occur continuously.

The design loading area capacity is given in the TCQSM 2013 method as (TRB, 2013);

$$B_l = \frac{3600}{t_c + t_d + t_{om}}$$ Equation 2-6

where:

B_l = Loading area bus capacity (bus/h)

3600 = Number of seconds in one hour

t_c = Average clearance time (s)

t_d = Average dwell time (s)

t_{om} = Operating margin (s)

Operating margin is a buffer introduced to make design-capacity estimation with the intention of avoiding loading area failures (section 2.3.4). As mentioned above, the design busway station capacity is affected by not only dwell time and clearance time but also in operating margin, dwell time variability and failure rate.

Failure Rate

Bus loading area capacity is maximized when a bus is available to move into a loading area as soon as the previous bus vacates it. However, achieving this condition is difficult due to several reasons as follows (TRB, 2013):

1. Bus travel speeds can reduce, due to the time spent waiting for a loading area to become available.
2. Bus schedule reliability suffers because of the additional delays.
3. Buses block traffic in the street while waiting to enter the bus stop.

The more often that bus stop failure occurs, the higher the bus throughput over the course of the hour, but the more severe the operational problems. The failure rate is used in combination with dwell time variability and the average dwell time to provide an operating margin. Lower the failure rate greater the operating margin and schedule reliability and lower loading area capacity. Conversely, when the failure rate is greater, operating margin and schedule reliability becomes lower with greater loading area capacity (TRB, 2013).

However, failure rate is not a parameter in the estimation of theoretical capacity of a busway station (or loading area) (section 2.3.2), which is the core of this research.

TCQSM 2013 defined bus stop failure rate as (TRB, 2013);

$$Z = \frac{t_{om}}{\sigma_{t_d}} = \frac{t_i - t_d}{\sigma_{t_d}} \quad \text{Equation 2-7}$$

where;

Z = Standard normal variate corresponding to a desired failure rate

t_{om} = Operating margin (s)

σ_{t_d} = Standard deviation of dwell times

t_i = Dwell time value that will not be exceeded more often than the desired failure rate (s)

t_d = Average dwell time (s)

where, operating margin (t_{om}) can be shown as (TRB, 2013);

$$t_{om} = \sigma_{t_d} Z = c_v t_d Z \quad \text{Equation 2-8}$$

where;

c_v = Coefficient of variation of dwell times

2.3.5 Other Existing BRT Station and Bus Stop Capacity Models

There are important BRT station and bus stop capacity models available in literature. Some of them are opt for a different approach than the conventional TCQSM 2013 method to estimate design stop capacity depending on different operation procedures.

BRT line service capacity is dependent on the bus capacity of its critical segment. In turn, critical segment capacity is controlled by one of its two adjacent nodes, which may take the form of a controlled intersection or a station, acting as a bottleneck (Levinson and Jacques, 1998). Station bus capacity may be influenced by factors including spacing, location, design and operation. Accordingly the analyst requires a robust methodology in order to estimate bus capacity considering these potential bottlenecks.

Fernández (2007) introduced the concept called capacity of divided bus stops. A divided bus stop contains berths that are separated to reduce bus interference and consequently increase bus capacity. It was found that weaving distance between nearby stop points should be designed by considering the influence of downstream stop queue length and the combination of passenger demand of stopping points.

Kwami et al. (2009) investigated the quantitative impact of bus bays on curb lanes capacity of roadway. They introduced new concepts of bus impact time occupancy ratio and bus impact times. Relationships among bus deceleration time, bus acceleration time and bus impact time were established when buses manoeuvre to pull into and out of the bays. They found that bus bays have significant impact on curb lanes capacity. As well as with the increase in bus arrival frequency, the actual curb lane traffic capacity decreases showing that both bus impact time and bus arrival frequency affect curb lane capacity.

Jaiswal et al. (2009) introduced Busway Loading Bus Capacity Model (BSLC) with lost time variables. Results showed that TCQSM 2013 model gives higher values than BSLC as the introduced model accounts lost time variable which accounts higher delay time for buses.

Hidalgo et al. (2013) introduced a method to estimate theoretical maximum number of passengers in bus lanes where maximum capacity per hour equals to maximum buses per hour per lane in to passenger per bus multiply with bus degree of saturation in to number of lanes. Further, they introduced a method to estimate maximum theoretical passenger capacity as a multiple of maximum buses per hour per platform, number of platforms per express buses and passenger per bus. However, this method is not considering the efficiency of platform area and limited for maximum of 60 buses per hour per platform (Hidalgo et al. 2013). In a real BRT station operation with multiple loading areas this amount is far greater.

Moreover, the procedure for estimating BRT line service capacity is defined by the US Transit Capacity and Quality Service Manual (TRB, 2013) where line service capacity is controlled by capacity of buses through the busiest stop. This method is suitable when the system is operating under its capacity and all the buses are stopping at that critical station. However, some systems include operation where express buses pass the critical station, resulting in a proportion of non-stopping buses. It is important to understand the operation of the critical busway station under this type of operation, as it affects busway line capacity. However, research on such busway lane capacity of BRT operation is scarce.

For BRT facilities the procedure simplifies when the absence of immediately adjacent signalized intersections which removes the need to apply a green time ratio. The design capacity is based on applying an operating margin to average dwell time

that corresponds to a desired failure rate, which is defined as the probability of a bus queue waiting to access a loading area occupied by a dwelling bus.

One drawback of the TCQSM 2013 procedure is that it does not explicitly address bus queuing upstream of the platform area at a BRT station, where queues have been observed in this study to form rather than at each loading area along the station platform. Further, the actual length of bus queues cannot be readily estimated using the existing procedure. However, actual queue lengths are useful when undertaking traffic engineering for a BRT facility, for instance in addressing queue spillback to other features on the line.

2.3.6 Microscopic Traffic Simulation Capacity Analysis

Microscopic simulation modelling provides a controlled environment, where different traffic scenarios can be simulated and sensitivity analysis of different parameters on traffic and its behaviour can be analysed (Widanapathiranage et al. 2013b). Microscopic traffic simulation on busway station can efficiently represent the real world situation and reproduce its behaviour under a controlled environment and hence has been extensively used in transport research (Widanapathiranage et al. 2014). This simulation modelling approach can be used to measure stop or station capacity as well as other performance measures.

Microscopic traffic simulation modelling in Bus operation

Some useful researches have been conducted to investigate bus operation and queueing. Fernández, (2010) modelled bus stops and a light rail station using the PASSION microscopic model under mixed traffic conditions. It was found that the stop cannot operate at its absolute capacity because upstream bus queuing developed even at low degree of saturation, suggesting that no more than one vehicle queue would be acceptable during a short period of time.

Hidas et al., (2009) analysed the bus operations by using microscopic simulation technique in a bus corridor and evaluate various alternative operational and traffic management scenarios to accommodate the expected growth in bus numbers in Sydney. Challenges they came across during simulation model developments was modelling of “Dead Running” (running out of service, unavailable for passengers) buses. Since most of corridors experiencing dead running buses during peak periods, they modelled them as separate services running on a frequency calculated from the

inbound or outbound services. Further, during the simulation, they observed that there was a conflict between the buses being generated from a bus stop and the inbound buses servicing the same bus stop. This led to buses blocking each other and an eventual break down of the model. To overcome this problem, a set of clone bus stops were created on top of existing bus stops (one for inbound and the other for outbound service).

AUSTROADS (2012) uses AIMSUN (Advanced Interactive Microscopic Simulator for Urban and Non-Urban Networks) microscopic simulation software to simulate both Queue Jump Bus Lane (QJBL) and Set Back Bus Lane (SBBL) models. QJBL model considered both "with departure-side merge lane" and "without a departure-side merge lane". Further, SBBL Models are introduced to simulate signal priority in the models by placing detectors at the end of the bus lane.

In this research AIMSUN is used as a simulation tool to achieve the objectives identified in Chapter 1. AIMSUN is given a priority to replicate BRT operation by allowing to create reserved public transport lanes and public transport lines (TSS, 2010). Moreover, factors affecting BRT operation (dwell time, bus station stopping priority, lane changings, giveaway and vehicle attributors) can be changed directly using AIMSUN while some them (dwell time distribution and headway distributions) can be changed by using AIMSUN API (*Application Programme Interface*). Details of AIMSUN model development is provided in Chapter 7.

2.3.7 Unsignalised Intersection Queuing Analogy

Queuing at unsignalised intersection is an important parameter to measure the quality of traffic flow. Usually queuing is depending on the degree of saturation (demand and capacity). Highway Capacity Manual 2000 (HCM 2000) methodology consists of an equation that predicts the 95^{th} percentile queue length for major street left-turns and minor street movements with the function of movement flow rate, capacity and average delay per vehicle (TRB, 2000).

Adopting unsignalised intersection queuing theory for BRT operation

BRT station operation can be better understood through applying some features of traffic queuing theory. Specifically, the whole BRT station is analogous to a multi-channel server system, where each of the multiple off-line loading areas along the platform represents a server. These servers are only partially parallel, as bus-bus

interference prevents each of the loading areas from operating completely independently. Microscopic traffic simulation modelling is ideal to represent this bus-bus interference phenomenon. Widanapathiranage et al., (2013b) introduced bus-bus interference on BRT station for off line three loading area platform. Detail discussion is presented in Chapter 7.

The BRT station multi-channel server system contains an inflow immediately upstream of the platform area, the loading areas as the server system causing constriction, and an outflow immediately downstream of the platform area. Queuing into the server system may occur immediately upstream of the platform area.

As mentioned in section 2.3.5 TCQSM 2013 does not explicitly address bus queuing upstream of the platform area at a BRT station. Therefore, this research is developed a method to estimate upstream queue length by considering unsignalised intersection analogy hence develop a method to estimate Practical Bus Station Capacity (Chapter 7).

2.4 Busway Reliability

Day to day, and within day, variability in traffic flow and congestion levels cause variations in travel time and makes prediction of bus journey time uncertain. Variations in passenger demand also cause variation in dwell time at bus stops. Buses do not always run on the schedule, leading to bunching especially on short headway routes. Operators may also have insufficient spare capacity to cover for service breakdowns (Liu and Sinha, 2006). These all contribute to unreliability of bus service. The factors affecting bus reliability can be classified as in Table 2-2.

Table 2-2: The factors affecting bus reliability (Liu & Sinha, 2006)

Characteristics	Descriptions
Traffic characteristics	Traffic composition, day to day and within day variation in travel demand and traffic congestion levels.
Route characteristics	Length of the route, number of intersections, number of stops on the route, volume of passenger activity, seasonality, time of day, number of lanes, location of the bus stops, provision of bus lanes (whether in short stretches or all along the route) and direction of travel.
Passenger characteristics	Passenger volume at stops, variability in passenger volume, passenger route choice and passenger arrival distributions
Bus operational characteristics	Fleet maintenance, ticketing system, scheduling system, staff shortages, fleet availability, and variability in driver behaviour and experience

However, this research is targeting on busway operation; only bus station reliability and bus service reliability are considered.

2.4.1 Bus Station Reliability

Usually, bus station reliability is associated with failure rate (section 2.3.4) and upstream queue back from platform.

Upstream queue

When the demand of BRT facility becomes higher (greater than capacity) queue can be formed of the upstream section of the platform. Because of this excessive demand, buses have to wait on upstream section, resulting lower reliability of bus station. Moreover, passenger travel time can exceed due to queue at bus station. However, there is limited research conducted to analyse the effect of bus queuing to bus station reliability. Therefore, this research is designed to address this knowledge gap. Detail discussion of queue estimation is described in Chapter 7.

2.4.2 Bus Service Reliability

The term reliability can be used to covering all aspects of service, including safety, punctuality, regularity, cleanliness, passenger comfort, documents and security (TRB, 2013; Liu and Sinha, 2006). Six types of bus reliability measures are commonly used:a

- On-time performance
- Headway adherence (the consistency or "evenness" of the interval between transit vehicles)
- Excess wait time (the average departure time after the scheduled time)
- Missed trips (i.e., scheduled trips not made)
- Percent of scheduled time in operation (for automated systems)
- Distance travelled between mechanical breakdowns

Usually, first three bus reliability measures are incorporated all kind of delay and unreliability. First two reliability components account for headway reliability transit service.

Headway Reliability

Headway reliability is directly connected with on-time performance and the regularity of headways between successive transit vehicles. Irregular headways cause in uneven passenger loadings, with a late transit vehicle collecting with its regular passengers plus passengers that have arrived early for the following vehicle, which may lead to the following vehicle running early. Some of the passengers may miss that service, creating additional demand on the extra peak service, resulting in bus bunching and irregular headways. This phenomenon is irritating both to passengers of the bunched buses and to passengers waiting for other buses who see several buses for another route pass by while they wait for their own bus (TRB, 2013). Such peaks in passenger demand may result in buses reaching the Maximum Schedule Load (MSL) and having to bypass subsequent stops due to inadequate bus capacity, further exacerbating bunching. Maintaining the scheduled headways and providing regularity help to reduce passenger discomfort by minimizing the average passenger wait time (Lin et al., 2008).

On-time Performance

On-time performance is mainly used to measure reliability of longer headway transit services. It is measured in specific time point (busway stations, transfer centres) along the busway corridor. On-time performance defines “on-time” as a departure from a time point as one minute early to five minute late or an arrival at the route terminal up to five minute late (TRB, 2013). Measurement of on-time performance can be applied to routes that have headways longer than 10 minutes.

Headway Adherence

Headway adherence is used to determine the reliability when transit service operating at headways of 10 minutes or less (TRB, 2013). Usually headway adherence can be used to measure the bus bunching effect. Bunching can occur when two or more vehicles on the same route arrive together (or in close succession) followed by long gap between vehicles. Normally these lead vehicle over crowded. Therefore, some passengers down on the line may have to wait for the next bus. On the other hand, the trailing vehicle does not have many passengers to collect and it might come to the stop early or wait at stop to neutralize early arrivals. As transport operators' point of view, trailing vehicles represent wasted capacity, and more time is needed at the end of the route for schedule recovery, which increases the route's cycle time and thus potentially increases operating costs. Headway adherence is based on coefficient of variation of headways (C_{vh}) of transit vehicles serving a particular route arriving at a stop, and is calculated as follows:

$$C_{vh} = \frac{\text{standard deviation of headways}}{\text{mean scheduled headway}} \qquad \text{Equation 2-9}$$

Headway deviations are measured as the actual headway minus the scheduled headway.

Excess wait time

A variety of performance measures can be defined based on relationships between when passengers arrive at a transit stop, when the transit vehicle is scheduled to depart, and when it actually departs. Excess wait time measures can be defined based on passenger arrivals times and vehicle departure times (TRB, 2013). They include excess wait time, excess platform waiting time, potential waiting time and budgeted waiting time.

2.5 Conclusion

Based on literature review, important findings were made in estimating BRT facility capacity, platform efficiency and dwell time. Figure 2-12 shows the gap in knowledge based on BRT facility capacity estimation from the literature.

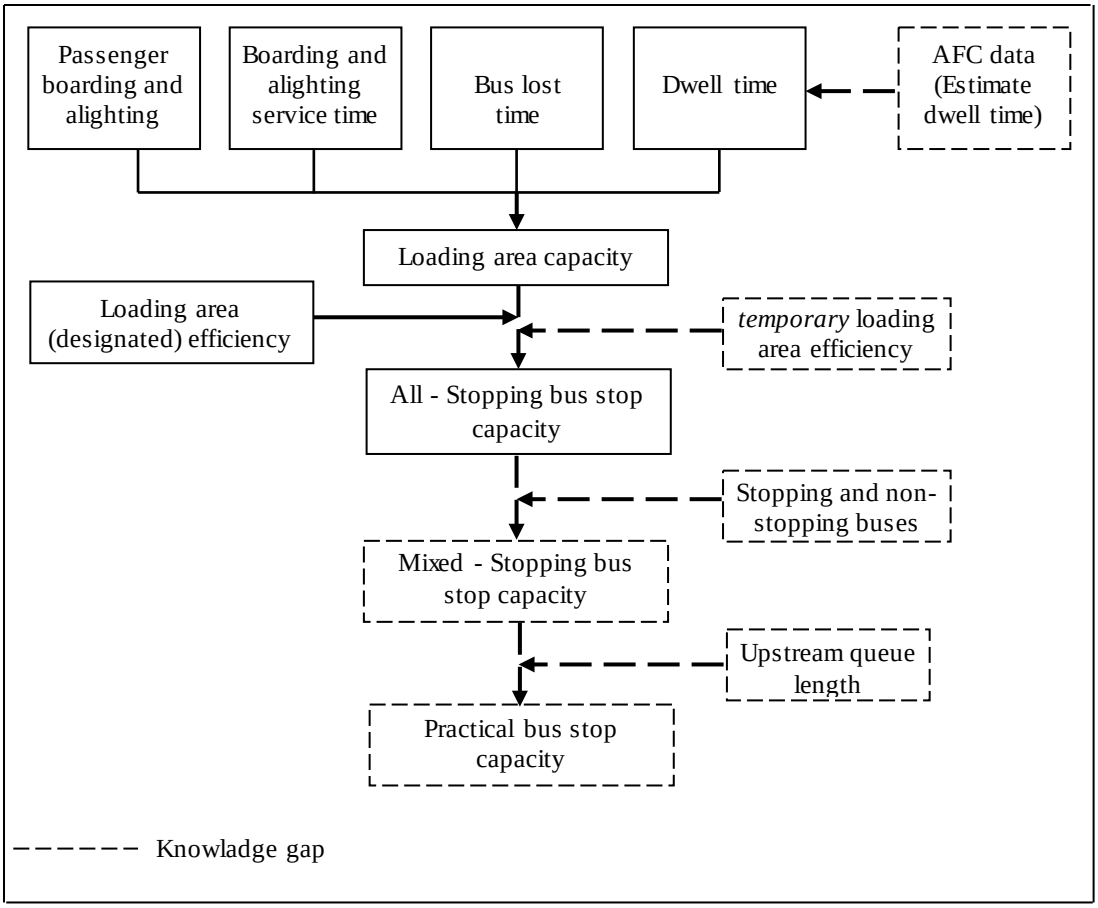

Figure 2-12: Knowledge gap in busway station capacity analysis

The most important finding of the literature review is that the existing methodologies for analysing busway station capacity are not suitable. The TCQSM 2013 method is based on simple bus stop operation; however, the actual operation of busway station is far more complex. Instant key aspects are that TCQSM 2013 (or in other literature) does not provide guidance on the operation of mixed-stopping and non-stopping bus operation. Moreover, TCQSM 2013 does not provide a means of estimating longitudinal queuing upstream of the station in regard to capacity analysis. Finally, it was found that existing methods did not provide a method to estimate designed practical capacity of a BRT facility. Therefore, this research is designed to fill these knowledge gaps.

Apart from the major findings of the literature, research gaps were identified.

The standard procedure for estimating loading area efficiency is only applicable for designated loading areas. Depending on demand of the BRT facility and other requirements mentioned in section 2.3.2, *temporary* loading area can be created. Therefore, these *temporary* loading areas cannot be treated as designated loading

areas. *Temporary* loading area can cause huge impact on bus stop capacity when the system reaches to its threshold limit especially during rush hour periods. This research is developed a methodology to estimate offline *temporary* loading area efficiency (Chapter 5).

Further, literature review highlighted that dwell time analysis needs to be simple and effective since dwell time is predominant component of bus stop capacity analysis. In this research a model is developed to estimate dwell time using AFC data (Chapter 6). TransLink's SEB has been selected to conduct this research (Chapter 4). Chapter 3 discusses methodology of this research.

Chapter 3: Research Methodology

3.1 Overview

This chapter presents the development of a comprehensive research methodology to estimate critical busway station capacity and practical design busway station capacity with respect to the knowledge gaps identified in Chapter 2 regarding the quantification of busway corridor performance for a BRT (segregated busway) system unique to Brisbane, Australia.

This chapter opens with fundamental appreciation of busway station operation. Methodological approach to evaluate busway corridor performance with regard to "mixed express and local services" and "busway station queuing" is discussed in Section 3.3. Section 3.4 presents data collection and field Surveys procedures plus instruments. Participants and ethics of the research are presented in Section 3.5. The chapter closes with the conclusion.

3.2 Fundamental Appreciation of Busway Station Operation

As mentioned in Chapter 2, busway stations in Brisbane are main interface between passengers and bus services where busway station capacity depends on loading area capacity, loading area efficiency and other variables (Section 2.3). It was observed by Jaiswal et al. (2010), most passengers wait near front loading areas. They introduced a boarding lost time variable by studying this phenomenon for dwell time estimation at a busway station, which has since been incorporated in to the capacity methodology of the TCQSM 3rd Edition (TRB, 2013).

Buses arrive to platform servicing as first come first serve order (Figure 3-1). With this type of bus operation and off-line linear loading areas, the front and middle loading areas can be blocked due to variation of dwell time. For an instance, if last loading areas occupies while front is vacant, this block the front loading area (Figure 3-2). Ultimately, this reduces the efficiency of loading areas.

Figure 3-1: Buses servicing platform in first come first served order
(base: http://commons.wikimedia.org)

When the demand of the busway station is high during peak periods, circumstances can arise when there can be just enough space for a bus to pull in and dwell using only front door by creating an additional *temporary* loading area (Figure 3-2).

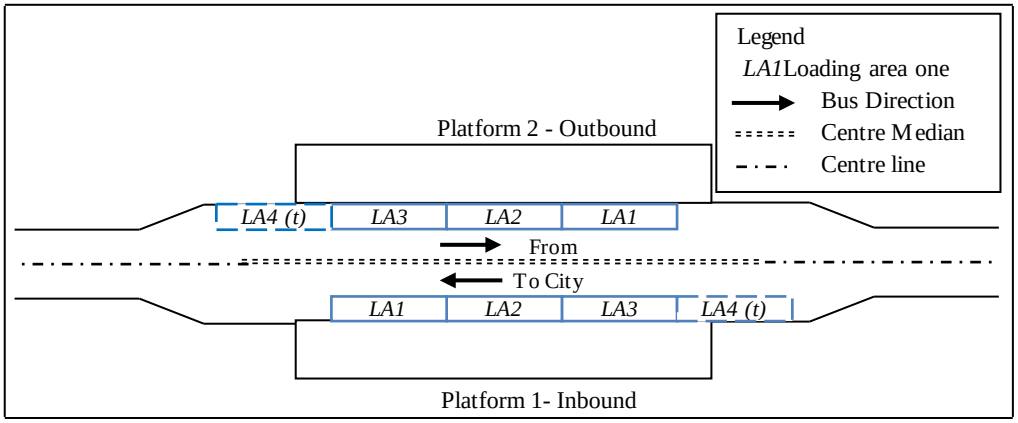

Figure 3-2: *Temporary* loading area; LA4 (t)

Smart card ticketing is used on Brisbane's busway system. This transaction system affects boarding and alighting times, which in turn affect dwell time. Usually, smart card passengers must tag on using their valid smart card when boarding and tag off when alighting. Each bus is equipped with two smart card readers (two channels) per door (Figure 3-3).

Figure 3-3: Smart card readers inside the bus
(base: http//:brisbanetimes.com.au)

Passengers can alight from either front or rear doors but boarding is only permitted through the front door. All fare processing occurs off-board. Passengers who use smart cards can top up their smart cards online, at news agent or through ticket machines located at bus station platforms (Figure 3-4).

Figure 3-4: Ticket machine located in busway station platform
(base: http//:danielbowen.com)

3.3 Methodological Approach

Figure 3-5 is a schematic diagram that outlines the methodological approach to this research.

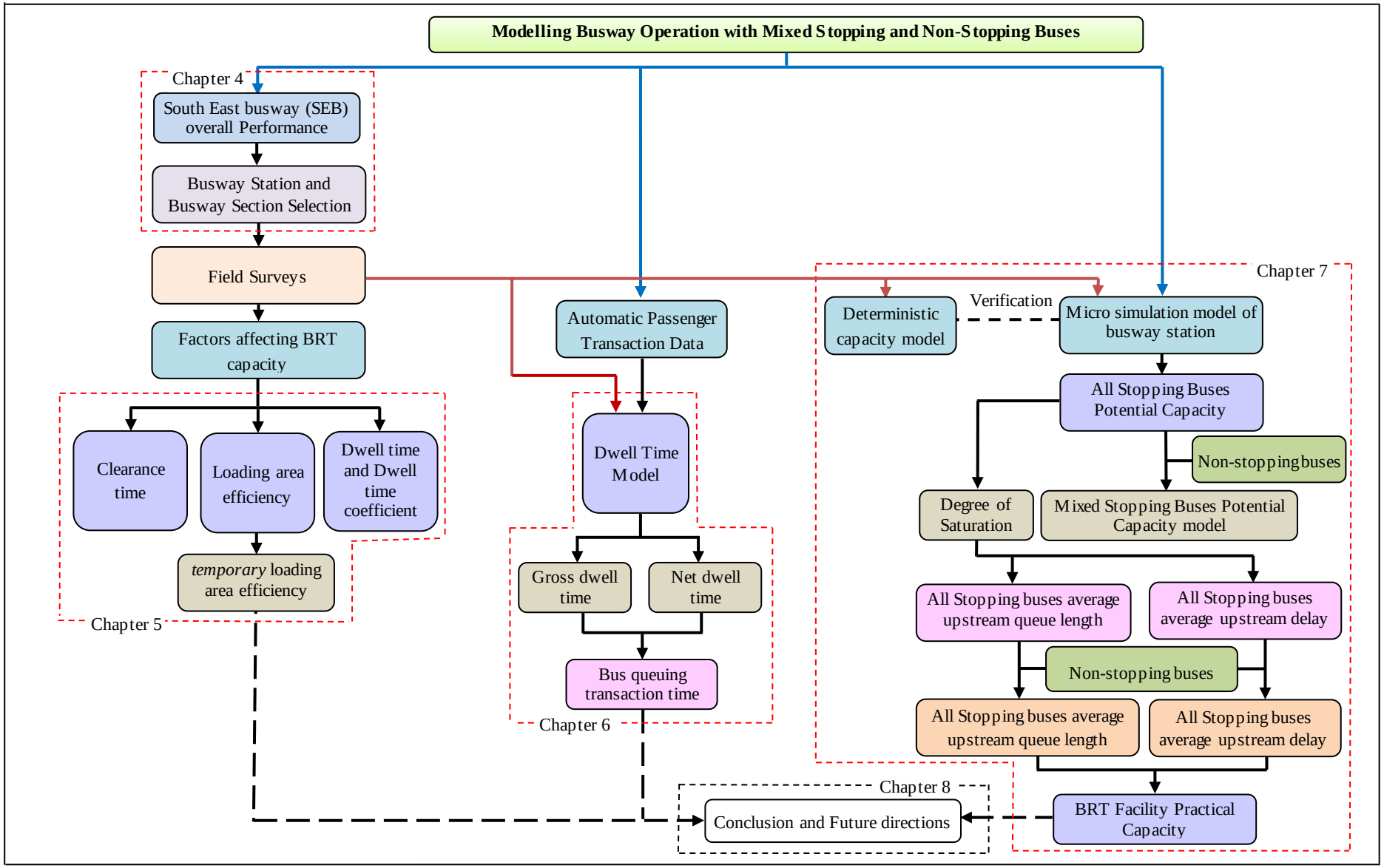

Figure 3-5: Schematic diagram of the research

As was mentioned in Chapter 2, the standard procedure for estimating BRT line service capacity is prescribed in TCQSM (TRB, 2013). However, some systems (such as Brisbane's busway system) include operation where express buses (or non-stopping buses) pass a critical station, resulting in a proportion of non-stopping buses. It is important to understand the operation of a critical station under this type of operation, as it affects busway capacity. However, research on estimating busway capacity with the above mentioned operating procedure is scarce.

Another limitation of the TCQSM 2013 methodology is that it does not explicitly address bus queuing upstream of the platform area at a busway station. We have observed queues to interact horizontally amongst the loading areas and upstream of the platform, rather than as "vertical queues" at each loading area along the station platform as implied by the TCQSM 2013 methodology. Further, the actual length of bus queues cannot be estimated using the existing methodology. It is useful to be able to estimate actual queue lengths when undertaking traffic engineering for a BRT facility, for instance in addressing queue spillback to other nodes on the line.

It is also feasible that the maximum acceptable queue length could be prescribed as a means of estimating a station's limiting service bus capacity. Therefore, this research is designed to estimate busway station capacity and upstream average queue length with respect to two distinct modes of operation; all-stopping buses, and mixed-stopping buses. Hence, a methodology to estimate busway design potential capacity is proposed.

It is not feasible to develop empirical models from real data alone to estimate busway station capacity and queue length for following reasons:

- It is difficult to realize potential capacity of a given busway station because most operate below capacity due to conservative scheduling. Those which have been observed to reach potential capacity only do so for a short period of time there by giving limited data.
- Usually busway stations operate within a limited range of degree of saturation and therefore, display a limited range of queue length.

In contrast to empirical modelling of real data alone, microscopic simulation modelling can efficiently represent the real world situation and reproduce its behaviour under a controlled environment and hence has been extensively used in

transport research (NBRTI; TRB, 2013; UNHSP, 2013; Widanapathiranage et al., 2013a). Microscopic simulation provides opportunities for controlled experiments where by detailed analysis of various operating conditions on a busway can be performed.

Microscopic simulation modelling allows us to estimate capacity and queue length across a broad range of conditions and testing scenarios. In this research, Advanced Interactive Microscopic Simulator for Urban and Non-Urban Networks (AIMSUN) is used as a simulation tool. This platform has been used extensively for commercial and research and validated in literature (Chen et al., 2010; Siddique et al., 2006; Tian et al., 2010; Widanapathiranage et al., 2013b, 2014). Its *Application Programme Interface* (API) capability provides opportunities to acutely control simulation modelling under very specific environments.

For realistic representation of the network and reproduction of network behaviour, the parameters for the microscopic simulation model need to be calibrated with real data. Accordingly, real data were collected using field surveys and then microscopic simulation model was validated with deterministic TCQSM capacity model. Detailed discussion of simulation model development is described in Chapter 7 (Figure 3-5).

Actual busway operation must be investigated and analysed as far as its overall performance is concerned to carefully select busway station and segment. The selected busway station can then be used to collect the necessary data in order to develop a microscopic simulation model. Detailed investigation of Brisbane's South East Busway (SEB) is provided in Chapter 4 (Figure 3-5) for this purpose. Prior to collecting data at the selected busway station for microscopic simulation modelling, the existing performance and variables affecting busway station capacity must be examined to gain a complete understanding of busway station operation.

The standard procedure of estimating loading area efficiency mentioned in Chapter 2 does not represent the situation when a *temporary* loading area is occupied. For instance, if we consider a platform with three off-line loading areas, the efficiency of any given loading area needs to consider the separate cases of a three loading area platform without a *temporary* loading area, and a four loading area platform with a *temporary* loading area. Detailed analysis of loading area efficiency estimation is given in Chapter 5 (Figure 3-5). Further, Chapter 5 provides dwell time and

clearance time characteristics since they are dominant parameters in busway station capacity estimation (Li et al., 2012; TRB, 2013, Widanapathiranage et al., 2013c).

Various dwell time estimation methods are discussed in Chapter 2. In this study we estimate dwell time and its properties at a busway station using smart card data. Development of dwell time models requires calibration and validation using field survey data of actual dwell times, and an appreciation of another component of transaction time (time between first and last transaction), being the bus time in queue. Detailed analysis of dwell time is presented in Chapter 6.

The methodology described in this chapter is based on the operation of the SEB; however, the method can be applied for different bus operational characteristics. Empirical equations to estimate the temporary loading area efficiency, which are introduced in Chapter 5, can be applied to bus stops with online loading areas with buses being processed on a first in first out fashion The methodology of the dwell time estimation model using Automatic Passenger Transaction data can be used at a range of stop types from simple bus stops to busway stations with online loading areas. The BRT facility Practical Capacity model developed in this research considers a bus queue formation model analogous to traffic queuing at an unsignalised intersection. The model is valid for bus stops with single or multiple loading areas. The model could be improved in the future by considering the effects of near side and far side intersections. Chapters 5, 6 and 7 described these considerations.

3.4 Field Surveys, Data Collection and Instruments

Data gathering was conducted in five stages during the research period from 2011 to 2014. Pilot surveys were first conducted to analyse the existing performance of SEB by using stop watches to measure dwell time, clearance time and loading area efficiency. A manual counting method was used to count boarding and alighting passengers to minimize error and abide by station owner, TransLink's observation policy. The pilot study was conducted in May 2011, which is one of the busiest months of passenger demand in Brisbane. Data were collected using pre-prepared observation sheets. For latter surveys (second, third, fourth and fifth) a smart phone application was used to increase the efficiency of data collection and processing. Figure 3-6 shows an image of the smart phone application.

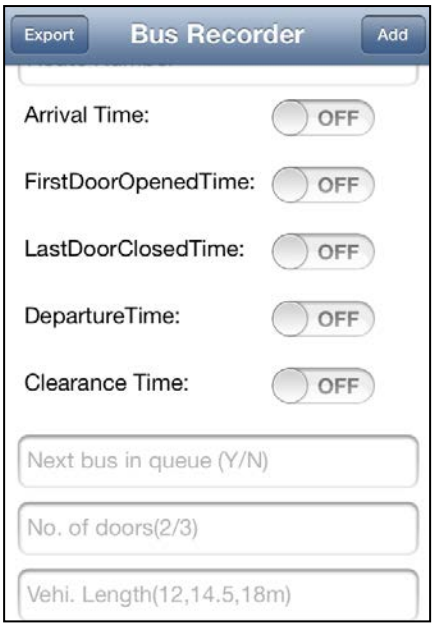

Figure 3-6: Smart phone application developed to conduct surveys

The second set of field surveys was conducted between 16/04/2013 and 18/04/2013. These surveys were conducted to evaluate the performance of the study busway station (refer Chapter 5) and to develop a comprehensive model to estimate dwell time using smart cards transactions (refer Chapter 6). The third and fourth sets of data were collected in May 2013 (18/05/2013 to 20/05/2013) and in August 2013 (20/08/2013 to 22/08/2013) respectively, to further validate the proposed dwell time models. The final survey was conducted in February 2014 to further evaluate study station performance (refer Chapter 5).

Surveyors avoided wearing high visibility clothing as per busway filming policies so dark coloured but identifiable QUT shirts were worn. In addition, surveyors were instructed not be closer to passengers in platform to avoid any interference.

3.5 Participants and Ethics

This research was carried out with microscopic traffic simulation software and field surveys. During the field surveys no data was gathered which could identify any particular individual or their personal details. The human data collection was limited to factors necessary for development of the busway operation models which are the subject of this study; specifically, headcounts and processing times.

Video recordings and field surveys were two possible means of data collection. Field surveys were chosen due to video recording being prohibited by TransLink Division

of Queensland Department of Transport and Main Roads. Notwithstanding, this research required ethical clearance to conduct surveys. This research obtained the approval to conduct surveys on busway station platform from QUT Human Research Ethics Committee. The Ethics Category stipulated by the Committee was "Human - Low Risk" and approval number that was given is 1300000074 (refer Appendix B).

3.6 Conclusion

This chapter identified microscopic traffic simulation modelling as the means to address the main analytical research objective. A method is proposed to estimate BRT facility design capacity by incorporating capacity and queue lengths for both stopping and mixed-stopping patterns.

In addition, a method to estimate dwell time using smart card transaction data was proposed. Further, the existing busway station efficiency estimation technique is improved when the *temporary* loading area in action. These works lead to next chapters of busway station performance evaluation, analysis and microscopic simulation.

Chapter 4: Case Study Outline: South East Busway (SEB)

4.1 Overview

This chapter provides a detailed description of the South East Busway (SEB), Brisbane, Australia. The primary goal of this chapter is to select a busway section (with busway station) to achieve the research objectives mentioned in Chapter 1. Figure 4-1 shows the chapter's structure.

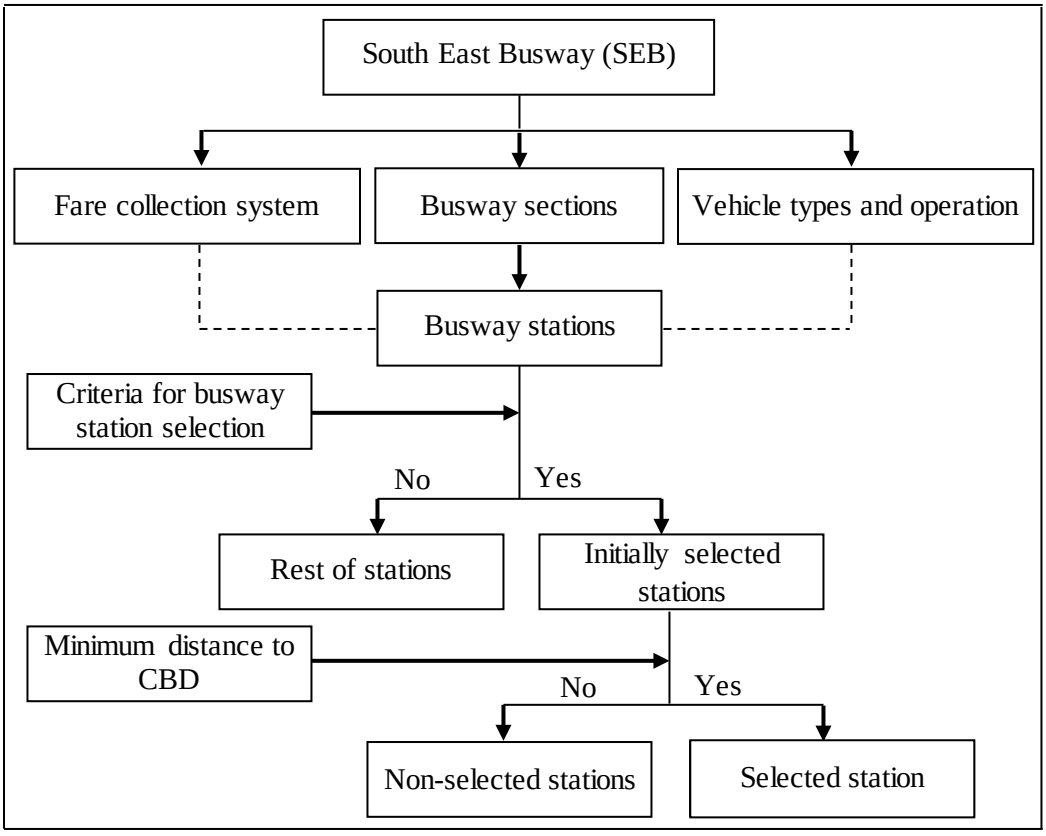

Figure 4-1: Chapter structure

This chapter begins by providing the background to SEB (Section 4.2). Section 4.3 describes each SEB section. Bus operation types are discussed in Section 4.4. Section 4.5 gives the insight of bus characteristics of SEB. Fare collection methods of SEB and the role of smart card system are presented in Section 4.6. Finally, Section 4.7 describes the selection of busway station for the remainder of this research.

4.2 South East Busway (SEB) Background

As mentioned in Chapter 1, the first section of SEB between the existing Queen Street Bus Station in Brisbane's CBD and Woolloongabba station was opened in 2000. This first section of busway to open was 3.2 km in length. This section consists of Queen Street, Cultural Centre, South Bank, Mater Hill and Woolloongabba busway stations (Figure 4-2). In 2001, the SEB was extended to its present terminus of Eight Mile Plains, which is 16 km south of the CBD terminus of Queen Street Bus Station. The SEB now incorporates ten busway stations. It consists of a two-lane, two-way road with pull-off lanes at stations and is designed to support 50 km/h travel speed in inner urban areas and up to 90 km/h in suburban areas. SEB contains approximately 1.6 km of underground sections, both bored and cut and cover tunnels, which allow buses to travel rapidly and directly, which in turn reduces bus operating cost and attracts more riders due to time saving (Currie, 2006; Golotta et al., 2008).

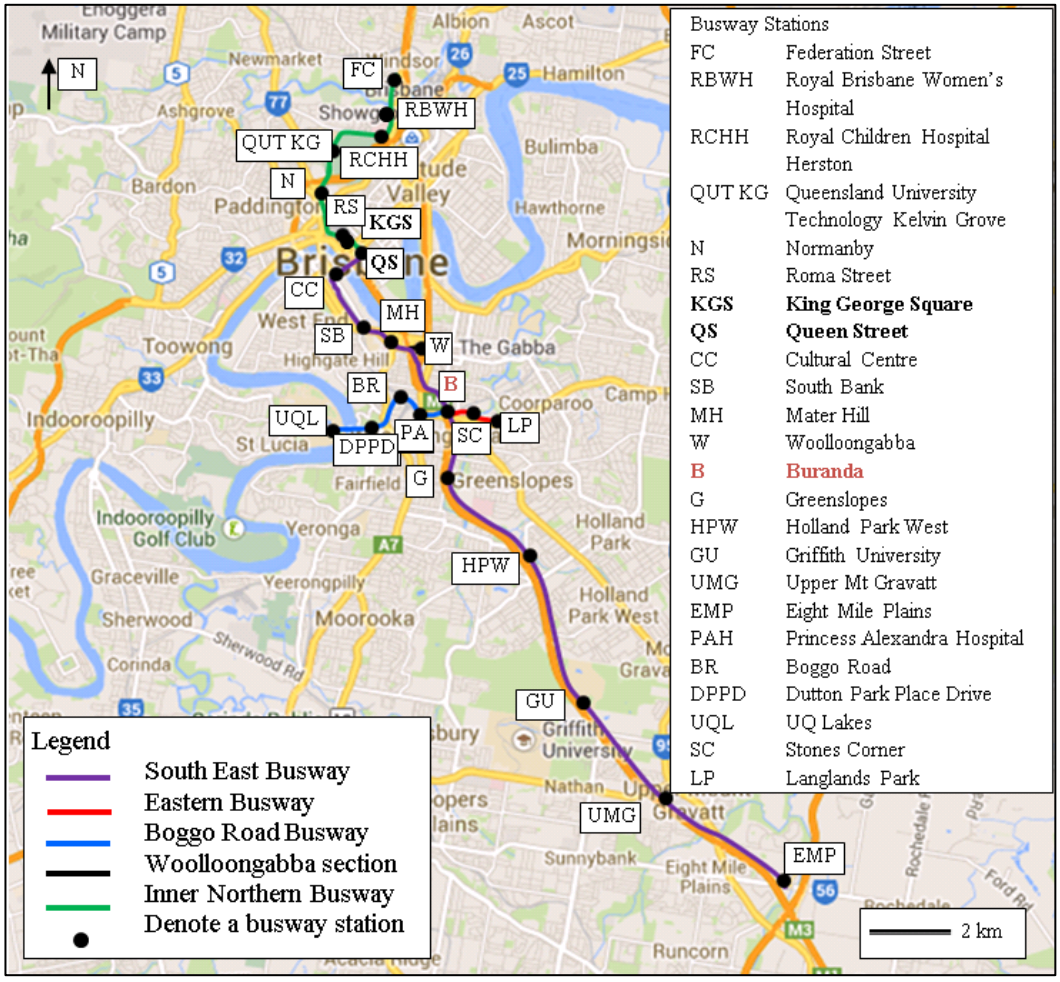

Figure 4-2: SEB bus network, Brisbane, Australia (base: google map)

In 2009 the Boggo Road Busway (BRB) was opened, followed by the Eastern Busway (EB) in 2011. These branch busways connect to the SEB main line at opposite ends of Buranda busway station, as shown in Figure 4-2.

The 4.4 km BRB provides important network access to University of Queensland (UQ), which is Brisbane's second largest passenger destination (Widanapathiranage et al., 2013b). BRB contains four busway stations (Princess Alexandra Hospital, Boggo Road, Dutton Park Place Drive and UQ Lakes). Three bus routes use BRB to connect from eastern and southern suburbs to UQ as do two routes from the CBD and Woolloongabba. Even though, the BRB conveys only five routes, each operates on 5 min to 6 min average headway per direction during peak periods and 10 min to 15 min average headway per direction during off-peak periods. In addition, five routes use part of the BRB, including one cross town route, one route to UQ lakes station via West End and three all stops routes (refer Figure 4-17). The maximum load segment of BRB is the Eleanor Schonell Bridge between Dutton Park Place Drive and the UQ Lakes terminus.

The 1.05 km long EB incorporates two busway stations; Stones Corner and Langlands Park. While being short, this busway is an important component of the network as it connects directly to the Old Cleveland Road on-street bus corridor, which serves a substantial number of routes (refer Figure 4-17) and high throughput. The maximum load segment of EB is generally between Stones Corner and Buranda stations.

All buses which serve the SEB are managed by Queensland Government's TransLink Division, which uses smart card fare technology for efficient passenger exchange and seamless multi-modal transit system operation.

4.2.1 Busway Stations

Busway stations are the most visible element of Brisbane's Busways, and are considered by planners as critical to the system's success (Golotta, et al., 2008; Lucas, 2009). These stations usually have a platform in each direction that facilitates multiple linear loading areas (three, and in some major stations four) to serve alighting and boarding passengers. Busway stations are designed with an open platform (generally 5 m deep and 55 m long), large shelter and elevators, and stairs with an overhead bridge to allow for access between the two platforms and in some

cases onto the surrounding pedestrian system. Having higher passenger exchange capacities and higher passenger amenities, busway stations are significantly different from enhanced kerbside bus stops. Consequently, busway stations have proven to attract more passengers (TransLink, 2012a).

Figure 4-3: Standard Brisbane busway station

Brisbane's predominantly template-designed busway stations include attributes such as shelter, advanced fare collection system, level boarding, lighting and security, seating facility, etc. The main advantages of this design are attractiveness, comfort and convenience and higher capacity than on-road stops. Figure 4-4 shows the typical template of a SEB busway station.

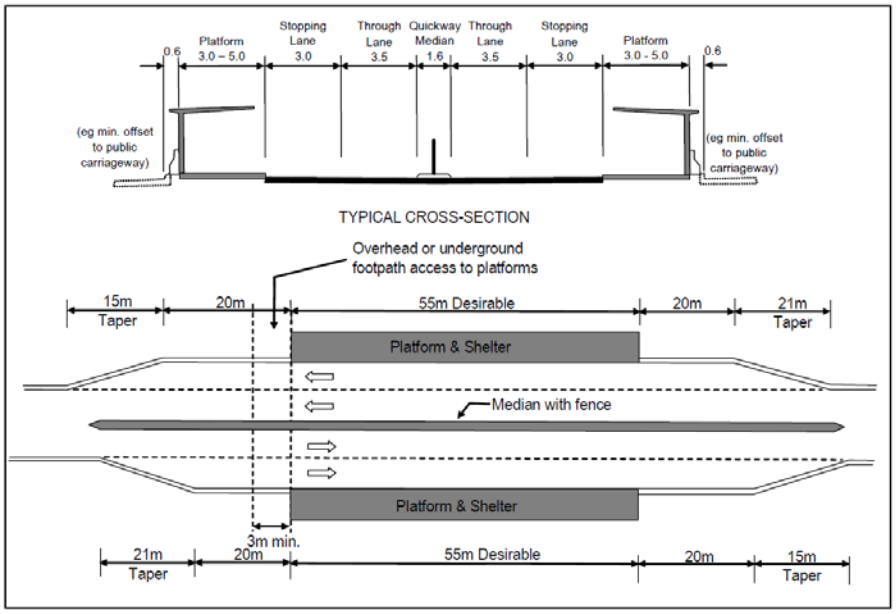

Figure 4-4: Brisbane station typical cross section (FTA, 2008)

All SEB busway stations have linear off-line loading areas to allow buses to overtake stopping buses (Figure 4-4). Accordingly, busway stations are critical in operation as they are the only sections where buses can pass others. Further, busway stations are the points of passenger access to transit service. Therefore, spacing, location, design and operation of stations significantly influence transit system performance.

Traffic congestion is recurrent at some stations on the SEB during peak periods because of conflict between manoeuvring buses. Stations can constrict bus flow as demand reaches station capacity, resulting in some buses queuing in the upstream travel lane until they are able to access a vacant loading area. On certain occasions, buses block the passing lane during their dwell time. This is particularly so for long buses (18.5 m articulated or 14.5 m three axle buses).

4.3 South East Busway (SEB) Strategic Elements

SEB has been analysed by section and station, in order to select the most suitable busway station for this study. Detailed discussion of each is given below.

4.3.1 Queen Street Bus Station

Queen Street Bus Station (QSBS) is the Brisbane CBD's primary urban bus terminus. It is an underground station beneath a commercial pedestrian mall and a major CBD shopping centre in the city heart. Its southern access from its portal to SEB is via a ramp to the major signalised at-grade intersection of North Quay / William Street / Victoria Bridge / QSBS portal. This is a complex intersection catering for many general traffic, bus, and pedestrian movements.

Its northern access to the Inner Northern Busway is underground via King George Square station (Figure 4-5).

QSBS provides direct connections to the heart of CBD from southern and eastern suburbs via the SEB, and the Centenary, Indooroopilly, and Kenmore corridors via other access facilities (Luke et al., 2000). It is the inner terminus of many of the city's BUZ (frequent) routes.

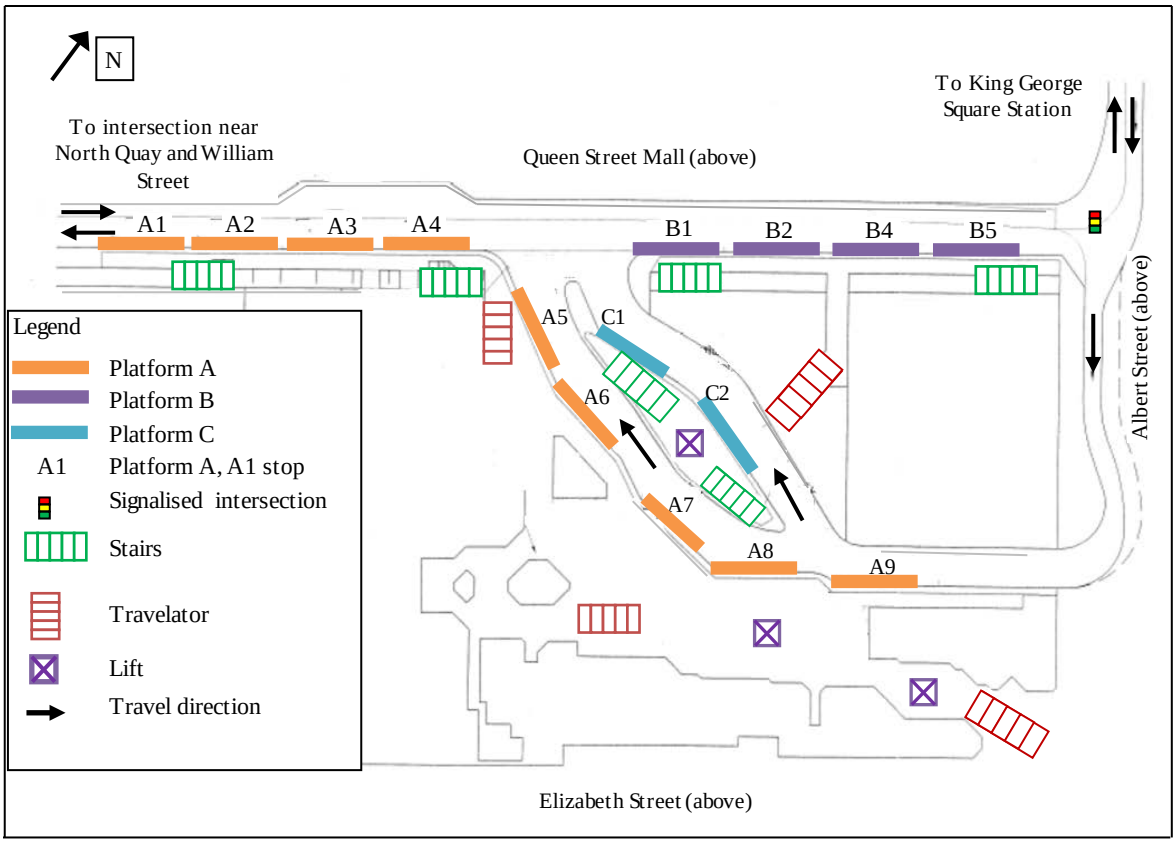

Figure 4-5: Queen Street Bus Station (QSBS) layout

4.3.2 Queen Street Bus Station Portal to Melbourne Street Portal Busway Access Intersection

The section between the QSBS portal and the Melbourne Street portal is a transitway section whereby buses operate in on-street bus lanes. This section limits the capacity of SEB due to various constraints. This section contains the Cultural Centre station (chainage 0.4 km). Despite having a passing lane and four loading areas per direction, this station has significant geometric constraints on its tapers at both ends. This station is the busiest along the SEB due to following reasons.

- The majority of bus routes to and from SEB, BRB, EB, and West End pass through Cultural Centre station (refer Figure 4-17).
- Some northern and western suburbs routes use Cultural Centre as their inner terminus (BCC, 2007) (refer Figure 4-17).
- This station is the dominant network passenger transfer station.

Cultural Centre station is adjacent to the signalised intersection of Melbourne Street / Gray Street (40 m south west of Cultural Centre), which itself is geometrically and

operationally challenging, with numerous general traffic, bus, and pedestrian movements. The signalised intersection of Melbourne Street / SEB portal (110 m south west of Cultural Centre) is also a complex intersection catering for general traffic, bus, and pedestrian movements. In particular, buses travelling in opposing directions have little space to manoeuvre past each other while making a right angle turn into / out of the portal, and space for only two to three queued buses is available between this intersection and the Melbourne Street / Gray Street intersection. South Brisbane railway station is situated just south to the Cultural Centre station and passenger interchange is possible via Gray Street.

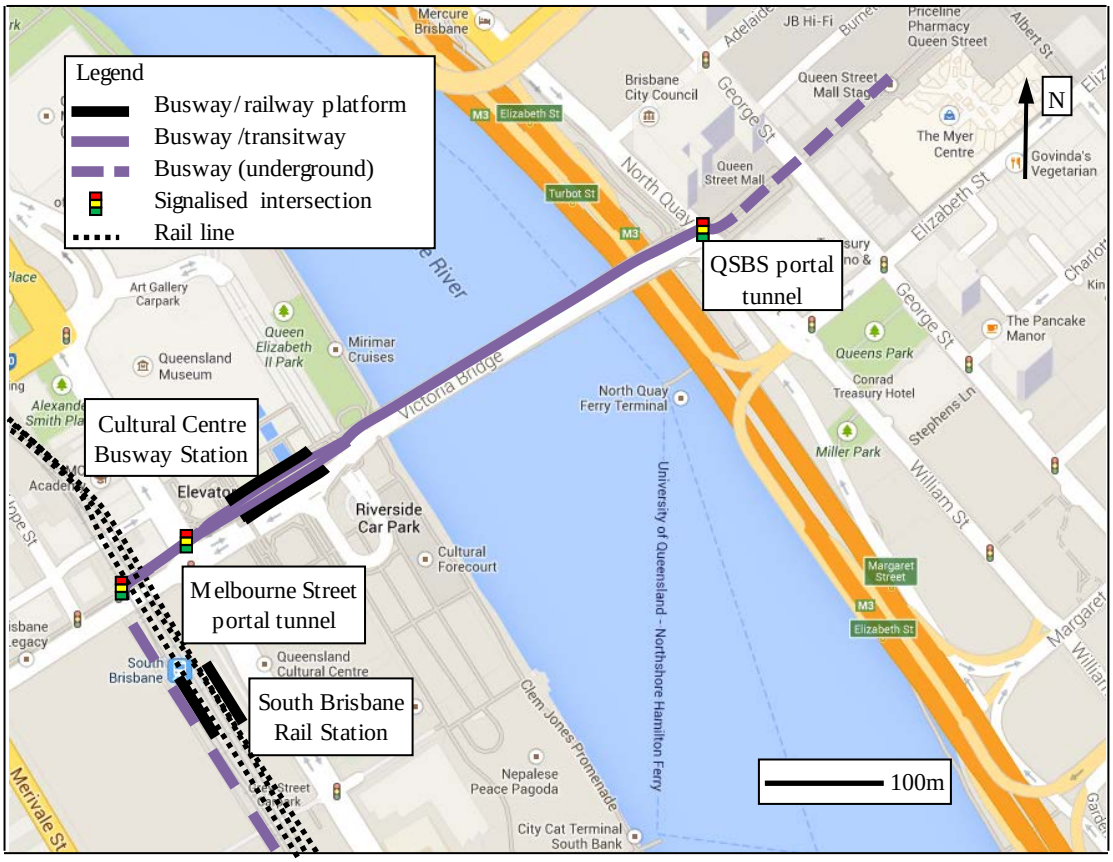

Figure 4-6: Transitway section between Melbourne street portal and Queen Street tunnel (base: google map)

4.3.3 Melbourne Street Portal Busway Access Intersection to South Bank Busway Station

This section contains South Bank busway station (chainage 1.7 km), which is one of the inner core stations (Figure 4-7). This station was constructed adjacent to South Bank railway station, to cater for a significant level of passenger interchange.

South Bank busway station is a high demand station due to its vicinity to adjacent passenger generators such as three high schools, South Bank Institute of Technology (SBIT), Queensland University of Technology (QUT), South Bank campus - Griffith University, and South Bank Parklands.

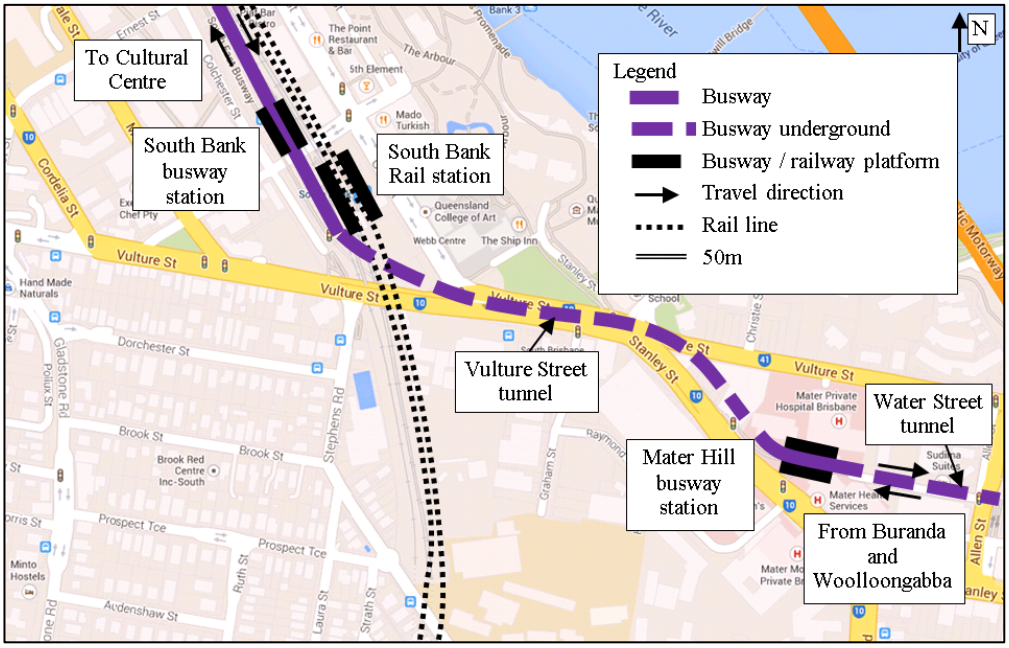

Figure 4-7: South Bank and Mater Hill busway stations
(base: google map)

4.3.4 South Bank Busway Station to Mater Hill Busway Station

Mater Hill station (chainage 2.5 km) is the southernmost inner core station (Figure 4-7). It is located between the Vulture Street tunnel and Water Street tunnel and is straddled by the Mater Private Hospital. It is a high use station due to its proximity to the Mater Hospitals, Griffith University, QUT, two private high schools, South Bank, and a commercial precinct. It also serves as a transfer station between certain southern and eastern bus routes.

Its station platform length is 45 m, which is less than the normal busway station platform length of 55 m, due to geometric constraints. Although the station has three designated loading areas in each direction, buses in the third loading area often are only able to serve passengers using the front door, while the rear door is kept closed due to its overhang past the platform. This station operates satisfactorily most of the time except for some portions of peak periods. Queue spillback into the Water Street tunnel occurs during the inbound morning peak (07:30 - 08:30), and spillback into

the Vulture Street tunnel occurs during the afternoon school peak period (14:45 - 15:30), and evening peak period (16:30 - 17:30).

4.3.5 Water Street Tunnel Portal to Woolloongabba Busway Spur Intersection

The signalised intersection of SEB / Allen Street Busway access, which is 170 m south of Mater Hill station and immediately to the south of the Water Street tunnel portal, and the unsignalised intersection of SEB / Pacific Motorway south ramp, which is a further 170 m to the south, together provide access between SEB and the Captain Cook Bridge for numerous peak period express routes. Queue spillback occurs occasionally during the morning peak period at the SEB / Allen Street access intersection (Figure 4-8) due to a congested northbound on-ramp to the Captain Cook Bridge on the Pacific Motorway (M3).

The signalised intersection of SEB / Woolloongabba Busway Spur is located 80 m south of the SEB / Pacific Motorway south ramp intersection. Queue interaction is not presently problematic between these two intersections. The signalised intersection operates below capacity during both weekday morning and evening peaks.

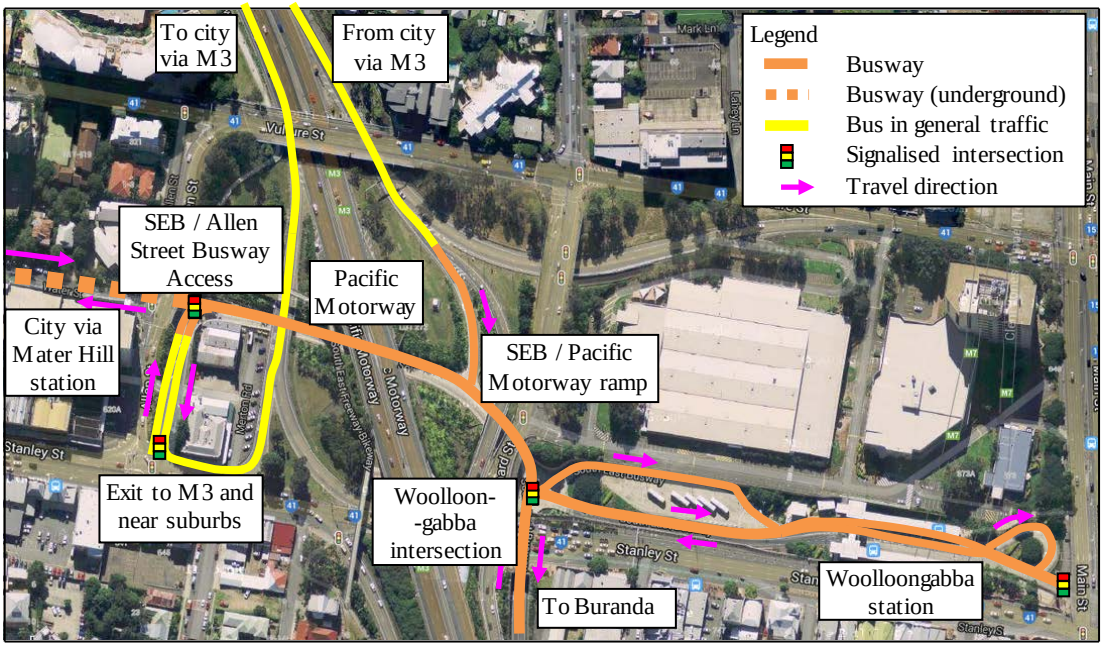

Figure 4-8: Water Street Tunnel portal to signalised intersection of Ipswich Road / Main Street / Stanley Street / Woolloongabba access
(base: google map)

4.3.6 SEB / Woolloongabba Busway Spur Intersection to Woolloongabba Busway Station

This section consists of Woolloongabba station (chainage 3.2 km), a bus parking facility and turnaround facilities (Figure 4-8). Many eastern suburbs and some southern suburbs bus routes join the busway at the signalised intersection of Ipswich Road / Main Street / Stanley Street / Woolloongabba access, which is located immediately to the east of Woolloongabba station.

Woolloongabba station is the primary transit node serving the Brisbane Cricket Ground (the 'Gabba). Further, Woolloongabba busway station is important since it includes the 'Gabba Transit Oriented Development, access to nearby midrise office complexes, government services, and a driver layover facility located just north of the station. It also serves as a significant transfer station between certain southern and eastern bus routes (refer Figure 4-17). This station mostly operates satisfactorily however, buses entering the busway via Stanley Street experience on-street congestion during the morning peak period.

4.3.7 SEB / Woolloongabba Busway Spur Intersection to Cornwall And Juliette Street Ramp

This section consists of the signalised intersection of SEB / BRB Harrogate Tunnel portal at its north end, the Buranda Busway Station (Chainage 4.4 km), the signalised intersection of SEB / O'Keeffe Street access / EB Cowley Tunnel portal, and at the southern end two south-facing ramps to access the major road network at the Cornwall Street / Juliette Street couplet (Figure 4-9).

Buranda station is an important bus-rail interchange with a suburban railway station on the Cleveland urban rail line situated on ground level above (Figure 4-9) (Translink, 2012b). Furthermore, bus-bus interchange activities are high at Buranda due to interchange between outer urban buses with CBD buses, outer urban buses or middle urban buses with cross country buses, and urban buses or middle urban buses with UQ buses. This is a high demand station due to its proximity to Princess Alexandra Hospital, the Stones Corner and Buranda commercial / community precincts, and Buranda State Primary School.

The SEB / BRB Harrogate Tunnel portal signalised intersection, which is 270 m to the north of Buranda Station, connects high number of buses to UQ from SEB

southern and northern directions. Bus queuing can occur between this intersection and Buranda station platform in the outbound direction during the evening peak period, due to busway station operation.

Bus routes from EB connect to the SEB at the signalised intersection of SEB / O'Keeffe Street access / EB Cowley Tunnel Portal, which is 130m to the south of Buranda Station. Bus queuing on the south approach to this intersection commonly occurs during the morning peak period due to high bus flow rates. Moreover, queuing spillback from Buranda station into this intersection is prevalent due to station operation (Figure 4-9).

The SEB / Cornwall Street / Juliette Street south facing ramp junctions are 110 m and 370 m to the south of the SEB / O'Keeffe Street access / EB Cowley Tunnel portal intersection respectively. These ramps provide access for a high number of buses joining SEB from Greenslopes and Garden City suburbs (refer Figure 4-17).

Buranda station experiences high passenger exchange and some bus queuing on the inbound platform during the morning peak period and on the outbound platform during the peak period. Although there are three loading areas on the platform, a fourth *temporary* loading area sometimes occurs during peak periods when bus drivers are able to pull into it and dwell using only the front door to serve passengers with the rear door kept closed due to overhang.

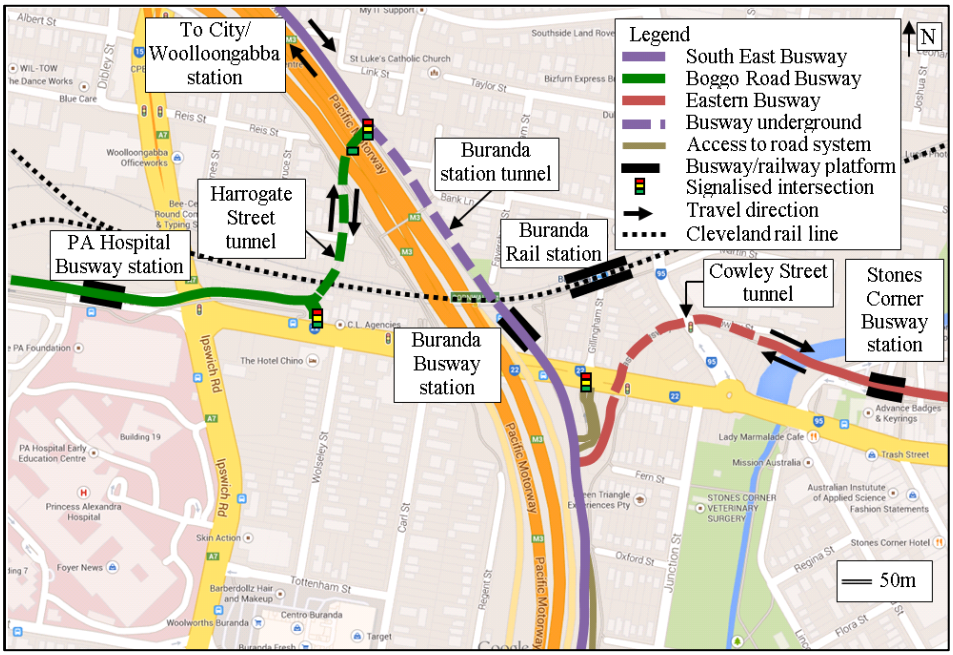

Figure 4-9: Buranda busway station
(base: google map)

4.3.8 SEB / Cornwall and Juliette Street Ramps to SEB / Barnsadle Place Intersection

This section consists of Greenslopes station (chainage 6 km) and the unsignalised SEB / Barnsdale Place access intersection. No regularly scheduled routes join the SEB using this access. Greenslopes Station provides an interchange to a connecting shuttle bus service to nearby Greenslopes Private Hospital. It also has a significant park and ride role, with 40 off-street and 120 on-street commuter spaces available. Most Rocket services, CityExpress and BUZ routes do not observe Greenslopes. Some SEB spine routes and some all stops routes do observe the station (see Section 4.4). This station operates satisfactorily.

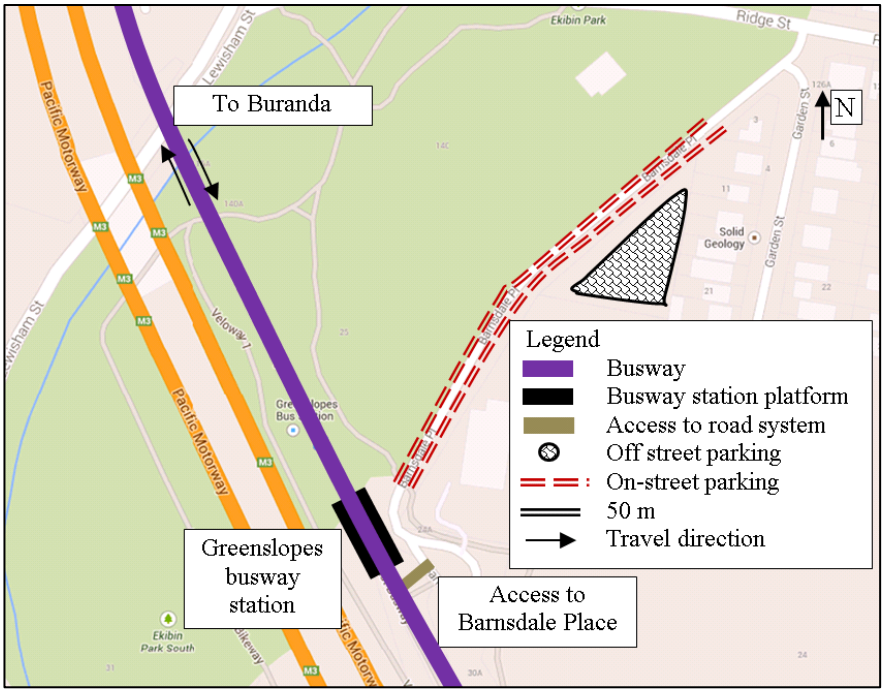

Figure 4-10: Greenslopes Busway Station
(base: google map)

4.3.9 SEB / Barnsadle Place Intersection to Holland Park West Busway Station

This section contains Holland Park West station (chainage 8.6 km) and the unsignalised SEB / Birdwood Road access intersection, which is located 1 km to the station's north. This access is used by a number of bus routes joining SEB from Holland Park and Mount Gravatt East suburbs (refer Figure 4-15, Figure 4-16 and Figure 4-17). Both the station and the intersection operate satisfactorily.

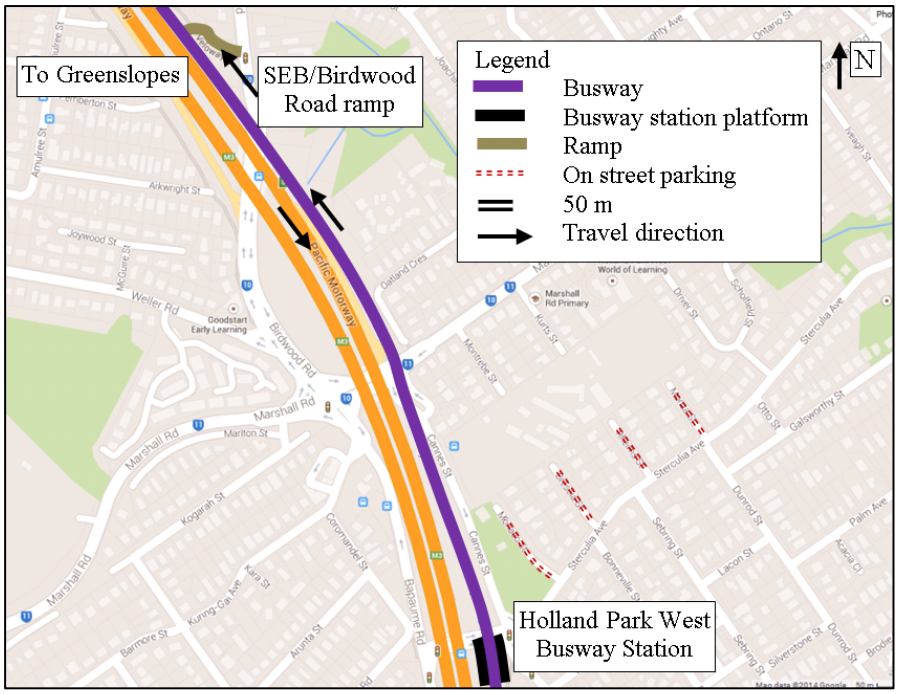

Figure 4-11: Holland Park West busway station
(base: nearmap)

4.3.10 Holland Park West Station to SEB / Klumpp Road Ramp

This section contains Griffith University station (chainage 10.8 km). The unsignalised SEB / Sports Road access intersection is located 50 m north of the station and provides access to Griffith University Mount Gravatt Campus. However, no regularly scheduled routes use this access to SEB.

The unsignalised SEB / Klumpp Road access intersection is located 300 m south of the station and provides access to the highest number of buses joining the SEB in outer suburban areas (refer Figure 4-15, Figure 4-16 and Figure 4-17). Furthermore, this intersection allows buses to access Griffith University Nathan Campus to the west.

Griffith University station is a high demand station due to its proximity to Griffith University, which has one campus to the station's east and another to its west. A shuttle bus service (non TransLink) connects both of Griffith University's adjacent campuses, with passengers interchanging to SEB services at the station.

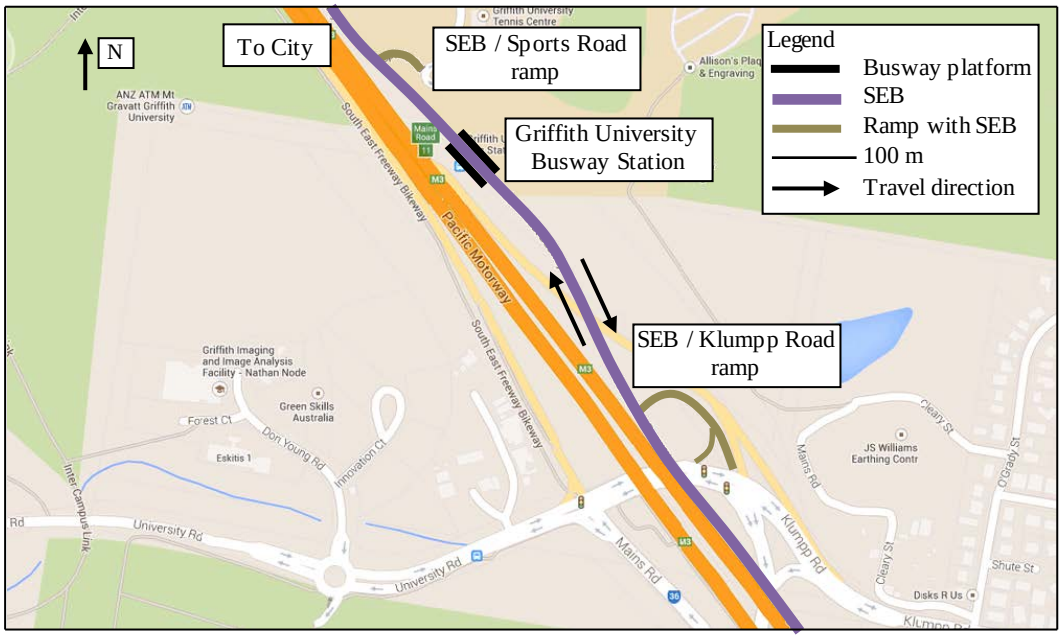

Figure 4-12: Griffith University Busway Station
(base: google map)

4.3.11 SEB / Klumpp Road Ramp to SEB / Macgregor Street Ramp

This section comprises Upper Mount Gravatt station (chainage 13.4 km) and the unsignalised intersection of SEB / Macgregor Street access.

Upper Mount Gravatt station (Figure 4-13) is a two level interchange. The lower level is a normal template station on the SEB proper. The upper level is a suburban bus interchange adjacent to the Garden City regional commercial hub and shopping centre. This station operates similarly to a traditional bus / rapid transit interchange, with most suburban bus routes terminating at the station's upper level and passengers transferring to access SEB services on the lower level. Consequently this station is one of the most significant passenger transfer stations on SEB outside of its inner core. It also serves a significant role for transit access to the commercial hub and shopping centre.

A substantial number of bus routes join the SEB at the SEB / Macgregor Street access intersection, which is located 270 m to the south of the station (refer

Figure 4-15, Figure 4-16 and Figure 4-17). Moreover, this intersection provides direct access to the SEB from the Upper Mount Gravatt bus depot. Both the busway station and the intersection operate satisfactorily.

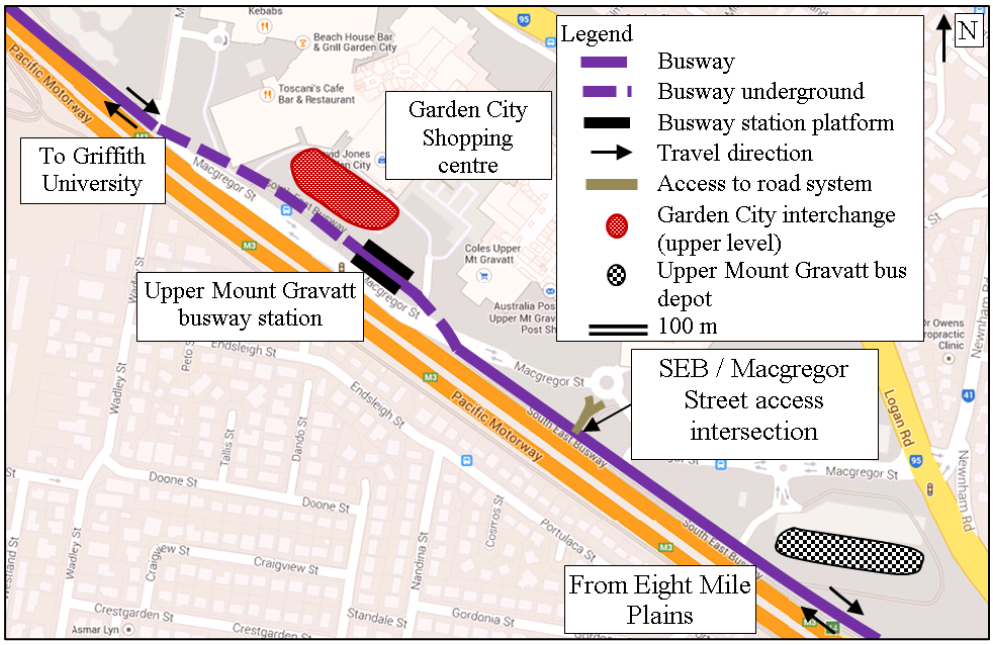

Figure 4-13: Upper Mount Gravatt Busway Station
(base: google map)

4.3.12 SEB / Macgregor Street Access Intersection to SEB / Gateway Motorway Ramp

This section includes Eight Mile Plains station (chainage 16 km) and three intersections; SEB / Miles Platting Road access intersection, SEB / Pacific Motorway southbound ramp, and SEB / Gateway Motorway northbound ramps (Figure 4-14).

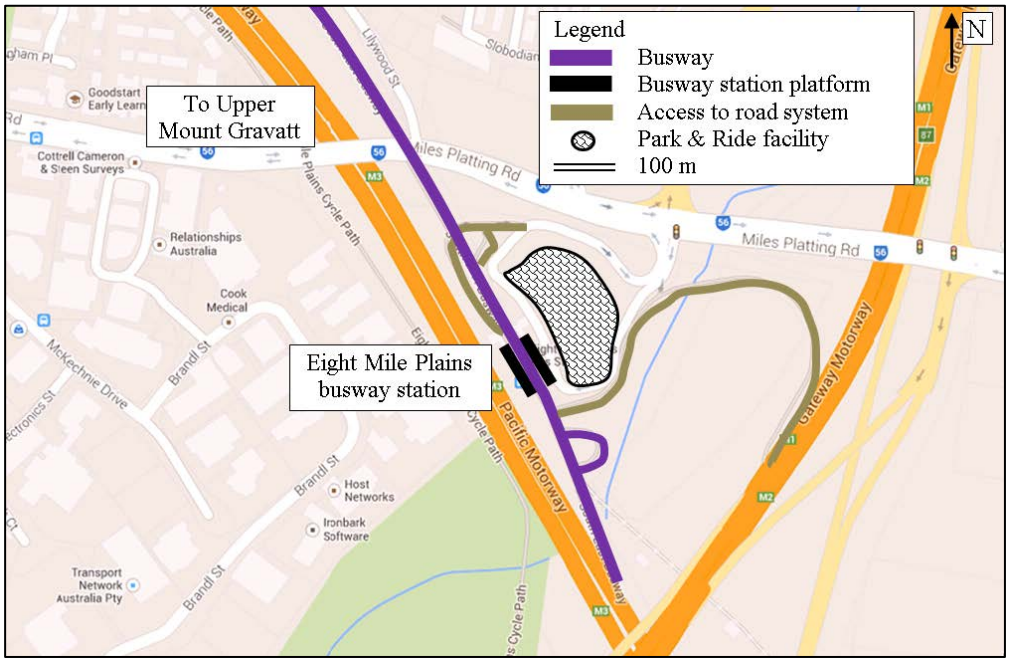

Figure 4-14: Eight Mile Plains Busway Station
(base: google map)

Eight Mile Plains station is the southern terminus of SEB proper, although the southbound SEB / Pacific Motorway ramp and northbound SEB / Gateway Motorway ramp provide for routes that extend south and west into Logan City. These ramps generally operate satisfactorily although congestion on either or both motorways can cause delays to buses entering / exiting SEB during motorway peak periods.

The signalised SEB / Miles Platting Road access intersection provides for routes that extend to the south east suburbs of Brisbane and Redland City (refer Figure 4-15, Figure 4-16 and Figure 4-17). This intersection operates satisfactorily.

The station is the dominant Park and Ride facility on SEB with up to 400 parking spaces. This facility was developed to attract commuter traffic from the immediate area and both the Pacific and Gateway Motorways. The station itself operates satisfactorily.

4.3.13 Daily and Peak Hours' Bus Movements Accessing SEB

Bus access movements were derived from TransLink's published timetable (access date: 10/04/2014). The inbound peak hour is between 07:30 and 08:30 while the outbound peak hour is between 16:30 and 17:30. Peak bus movements at each access to the SEB are depicted in Figure 4-15. Figure 4-16 shows the daily bus movements of SEB while Figure 4-17 illustrates the daily bus movements of SEB.

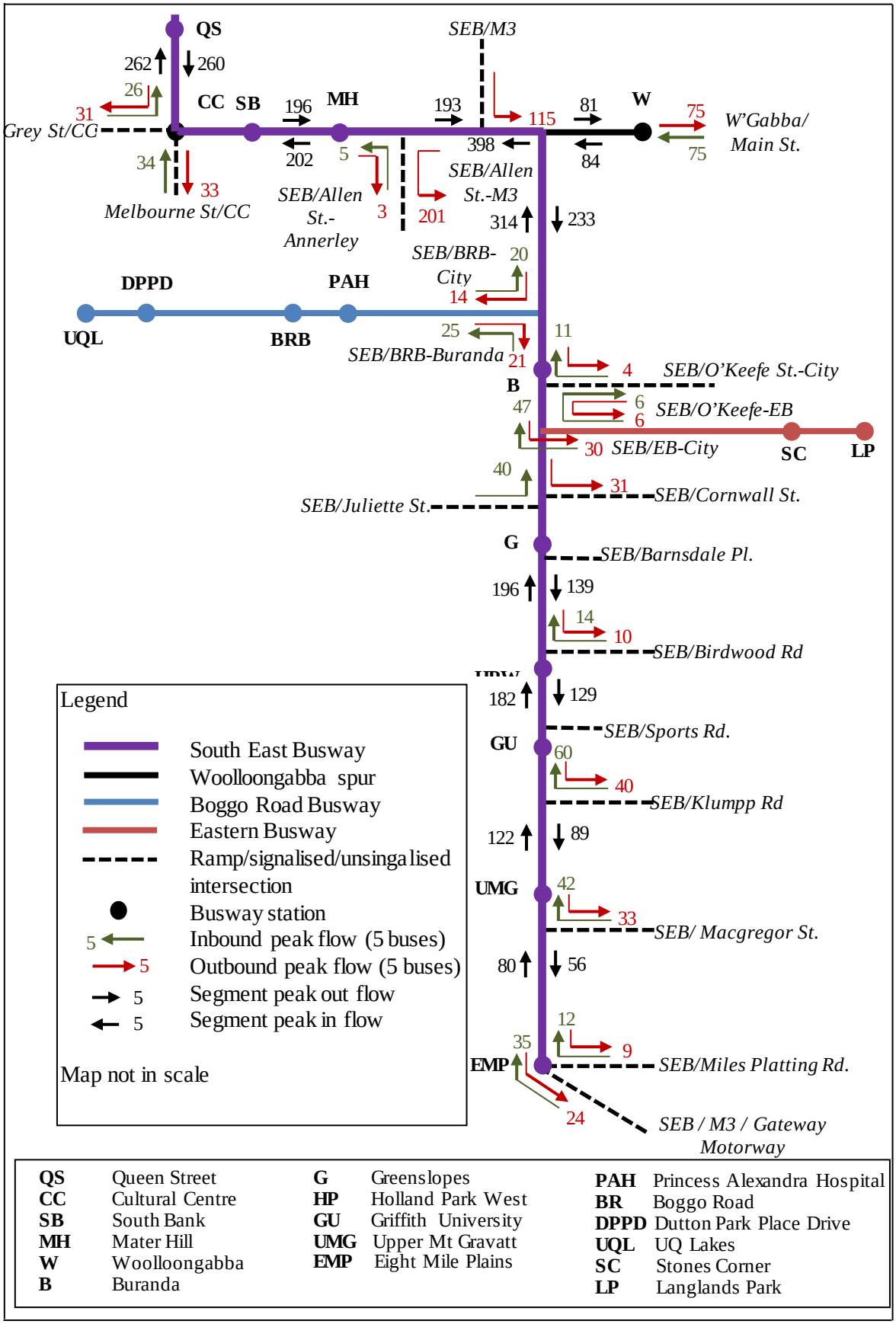

note: SEB/BRB-City indicates buses travelling towards city using BRB and SEB. SEB/BRB-Buranda indicates buses travelling towards Buranda using BRB and SEB.

Figure 4-15: South East Busway Network Showing Access Movements for peak periods

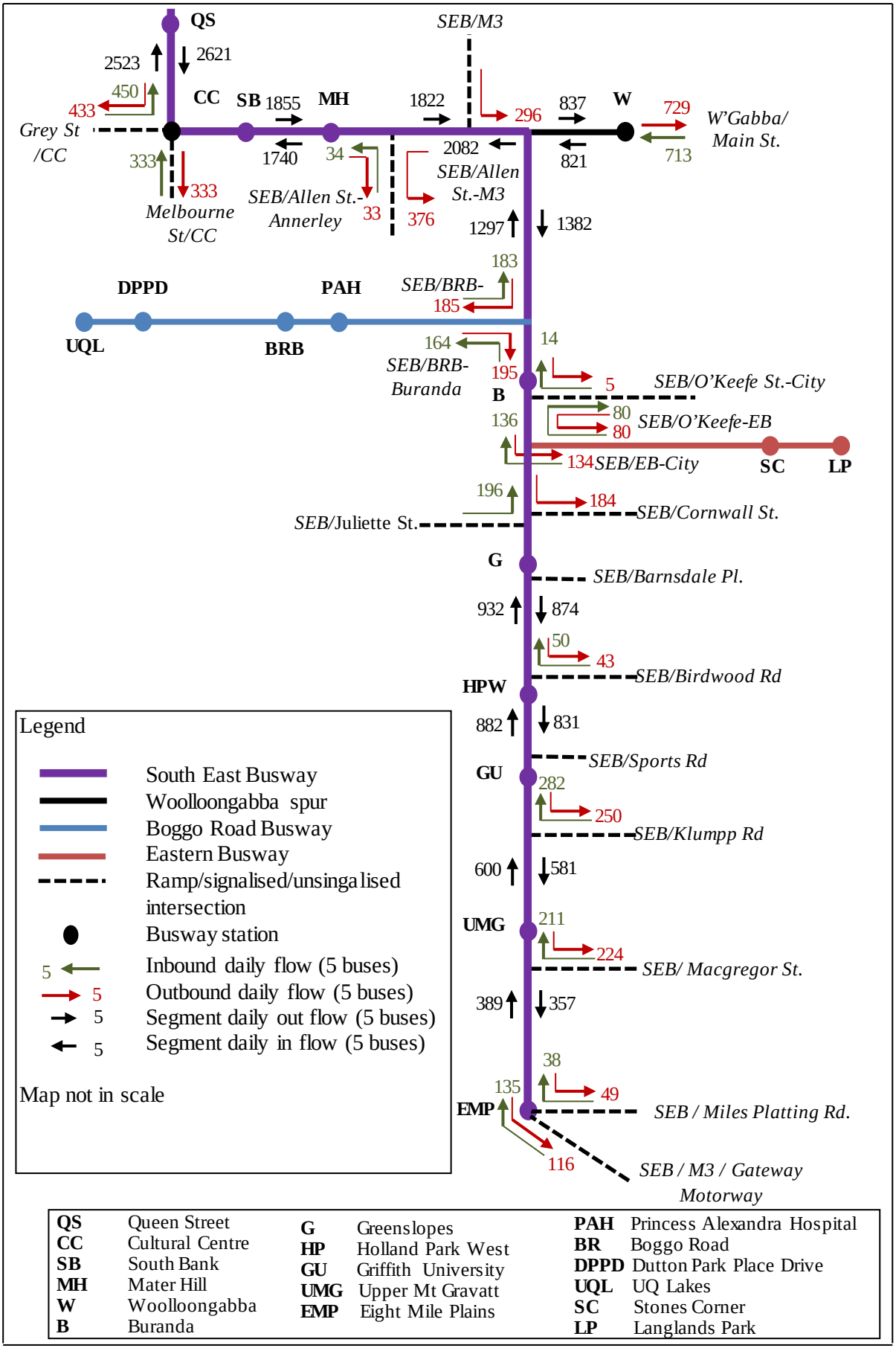

Figure 4-16: Daily South East Busway Network Showing Access

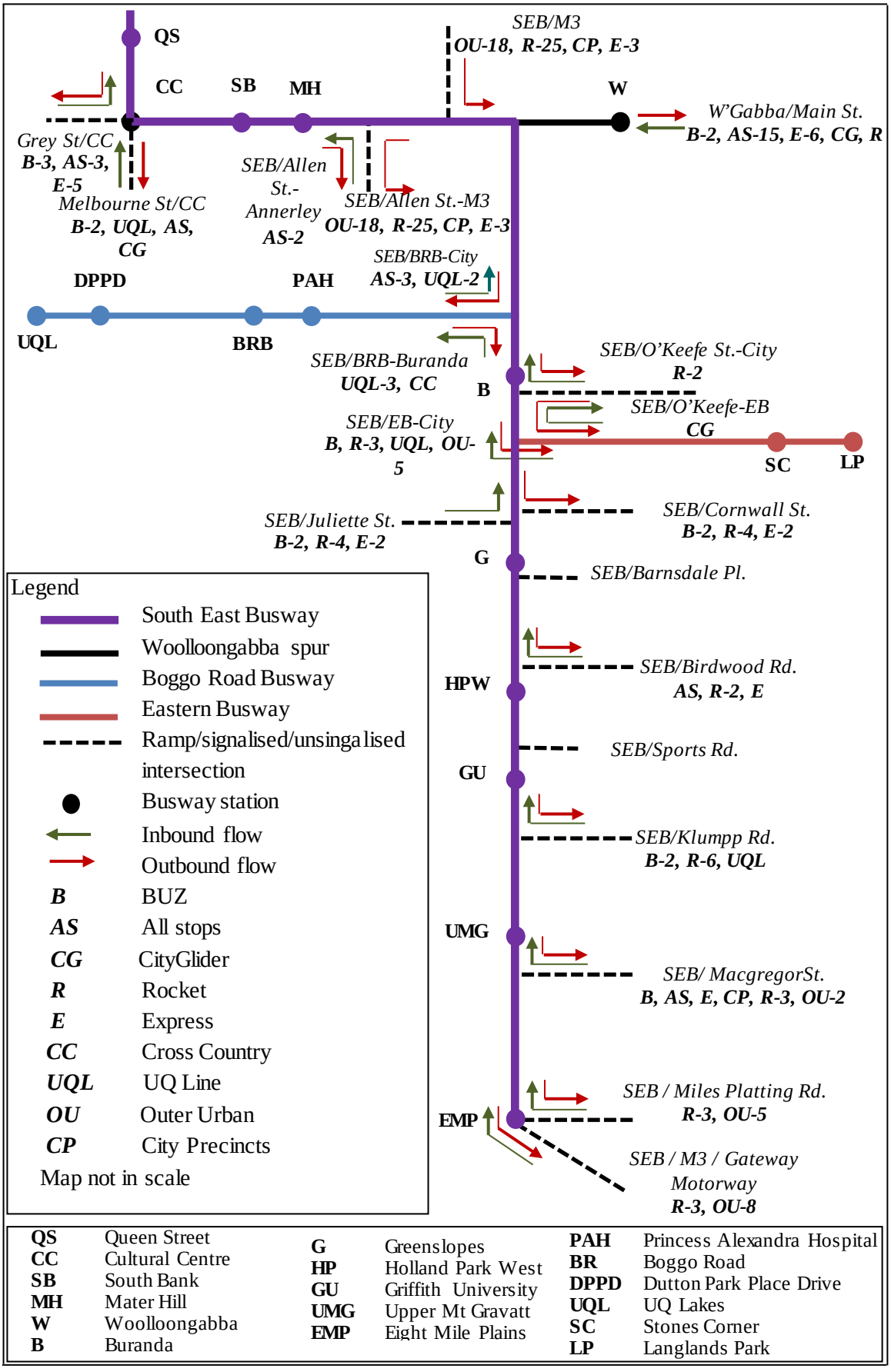

note: Please refer section 4.4 for bus service patterns

Figure 4-17: Bus route types accessing South East Busway network

4.4 Bus Route Types Operating on SEB

The existing route categories operating on SEB are described as follow:

- All-stops routes normally observe all stops both on their on-street component as well as all stations on their SEB component. Their frequencies and spans of service can vary significantly depending on overall route characteristics and their markets.
- Bus Upgrade Zone (BUZ) routes normally observe a restricted stopping pattern on their on-street component to facilitate higher speeds, and commonly observe all stations on their SEB component, where spacings are higher than on-street. Some variation in these route design principles does exist between BUZ routes. Their service frequencies are high, typically 10 minutes in peak periods and 15 minutes in off-peak periods, seven days per week. Their spans of service are also high, typically between 05:00 and 0:00.
- CityGlider services (Maroon CityGlider and Blue CityGlider) operate similarly to BUZ routes, but within corridors focused on inner suburbs and stops and stations with very high passenger demand. They operate 18 hours per day from Sunday to Thursday and 24 hours per day on Friday and Saturday. Frequencies are 10 minutes during peak periods and 15 minutes during off-peak periods. On weekend nights they operate at 30 minute frequencies after midnight. These routes use some inner sections of the SEB.
- CityExpress services generally operate similar to BUZ services, but typically with lesser frequencies and spans of service.
- Rocket routes normally observe a restricted stopping pattern on their on-street component, and observe a restricted stopping pattern on the SEB component – typically only the station adjacent to their road system access point. SEB Rocket routes commonly bypass the core SEB stations, instead crossing the Brisbane River using the Captain Cook Bridge of the Pacific Motorway (M3) and observing a restricted stopping pattern within the CBD. Rocket services' spans are generally limited to inbound during the

weekday three hour morning peak period and outbound during the weekday three hour evening peak period. Their frequencies are typically 10 to 15 minutes.

- City Precincts Express routes are very similar to Rocket routes. However, their CBD stops are dispersed to the flanks of the CBD.
- Outer urban routes vary considerably. Some operate similarly to BUZ, others similarly to CityExpress, and others similar to Rocket. Because of their longer distances and travel times, they generally observe more restricted stopping patterns to maintain reasonable speeds. Lower demand routes may have very low frequencies and/or spans of service.

4.5 Bus Equipment Operated on SEB

Table 4-1shows the attributes of buses used on the SEB.

Table 4-1: comparison of bus attributes

Bus type	Length /(m)	Number of doors	Number of channels		Capacity/(passengers)		Floor type
			Boarding	Alighting	Seated	MSL	
Standard two axle	12.5	2	2	1 or 2	44	66	Low
	12	1	2	1	55	55	High
Three axle	14.5	2	2	2 or 3	55	75	Low
Articulated	18.5	2	2	1 or 2	65	95	Low
	18.5	3	2	2 or 3	62	90	Low

note: MSL: Maximum Schedule Load Vehicle Capacity

Standard buses

The length of standard buses used in Brisbane is 12.5 m. Most of Brisbane's standard buses have two doors (Figure 4-18(a)), while some coaches are equipped with a single door (Figure 4-18 (b)) (Otto, 2008).

(a) (b)

Figure 4-18: Two door bus (a) and single door coach (b)
(base:http://busaustralia.com)

High Capacity Buses

Some transit agencies choose High Capacity Buses (HCBs) to increase seating capacity which increase operator productivity (saving labour costs) and reduce peak vehicle requirements (Dockendorf et al., 2001). While capital cost of the HCB may be significant, HCBs can potentially be more attractive when considered on a capacity-per-vehicle basis.

There are some improvements emerging in HC vehicle technologies such as introduction of bi-articulated buses (Figure 4-19), which can carry more than 200 passengers. Accordingly, Curitiba's bi-articulated buses can carry 270 passengers (TRB, 2003a). However, Curitiba's they are mainly designed to carry standing passengers (57 seated and 213 standing). Therefore, passengers per linear metre of these buses is far higher than normal bi-articulated buses (TRB, 2003b). Most of these high capacity bus systems use trunk and feeder system to gain more efficiency (FTA, 2004).

Figure 4-19: Bi-articulated buses in Bogota's TransMilenio busway system
(base:http://buswatchnz.blogspot.com.au)

Articulated and bi-articulated buses have some operational limitations compared to standard 12.5 m rigid buses. Articulated buses tend to have lesser vehicle performance (acceleration gradeability and manoeuvrability) than standard rigid buses. However, articulated buses with hybrid technology significantly improve acceleration, gradeability and fuel economy (Bragdon, 2010 ; TRB, 2008). Newly introduced 14.5 m length diesel buses in Brisbane have more gradeability than standard 12.5 m natural powered gas buses.

Reducing dwell time to take full advantage of HCBs remains a significant challenge. For articulated buses, the ability to use all doors for simultaneous boarding and exiting is a key proposition to reduce dwell times, because more and wider doors facilitate quicker passenger flow when an off-board fare collection system is in use (TRB, 2008).

HCBs have been introduced into operation on SEB in recent years to meet growing passenger demand without needing to add services during peak periods. Most HCBs are operated on high frequency bus routes. They include 14.5 m three axle and 18.5 m articulated buses (Widanapathiranage et al., 2013a).

14.5 m three axle buses

14.5 m three axle buses operating on SEB have essentially the same level of manoeuvrability as a standard bus, because a steerable tag axle is utilized.

Figure 4-20: 14.5m three axle bus used in Brisbane
(base: http://busaustralia.com)

Articulated (18.5 m) buses

Two types of articulated buses are operated on some SEB mainline routes. Two door articulated buses that are powered by natural gas have lower gradeability than diesel powered three door articulated buses. This is not problematic when these buses

are used on SEB spine routes due to the generous geometry and control features of the facility compared with on-street operation.

(a) (b)

Figure 4-21: Articulated Rigid Buses (two door (a) and three door (b)) in Brisbane (Otto, 2008)

4.6 Fare Collection System used on SEB

The fare collection system used in South East Queensland, including all SEB services, uses two media; paper ticketing and smart card.

4.6.1 Paper Ticketing

Passengers can use paper tickets to travel on most routes aside from prepaid routes, which tend to be Rocket and some City Express routes. Passengers may purchase a paper ticket from the driver (who in most cases is able to provide change) or buy a valid ticket from a vending machine located on a busway station platform. Passengers are required to show their paper ticket to driver while boarding but not while alighting. A 30 percent cost premium applies to paper ticket fares over smart card fares, which aims to deter passengers from using this legacy ticketing product (Widanapathiranage, et al., 2013b).

A prepaid platform policy was introduced in 2009 for inner busway stations during peak periods. However, it was abandoned after smart card became popular among passengers.

4.6.2 Smart Card

South East Queensland's (SEQ) transit agency, TransLink Division, introduced a touch contact smart card called "go card" in 2008 (Jaiswal et al., 2009). According

to TransLink, during 2011 more than 85 percent of public transport trips were made using go card (TransLink, 2011).

The current passenger flow operational strategy in Brisbane mostly restricts passengers to boarding through the front door after any passengers who have chosen to exit through the front door have done so. However, all doors boarding is being trialled on selected high frequency inner urban routes.

Passengers are required to "touch on" using one of two smart card readers in the front door vestibule area, and "touch off" using either the same card readers in the front door vestibule, or two smart card readers located in the rear door vestibule.

The use of smart card reduces the vehicle dwell time significantly. According to TransLink, smart card use reduces individual boarding time from 11 s or higher, down to 3 s, which translates to a time saving of up to seven minutes on an average bus trip (TransLink, 2011). The other advantage of smart card is richness of transaction data. This provides much larger volumes of personal travel data than it is possible to obtain from other data sources. In addition, smart transaction data shows continuous trip data covering longer period of time which was not possible using legacy fare technology (Widanapathiranage, et al., 2013b).

4.7 Busway Station Selection

As mentioned in Chapter 2, to construct a dwell time model and loading area efficiency model this research required selection of a suitable study busway station. Further, a busway station characteristics need to be considered in order to validate the proposed bus traffic simulation model.

Most busway stations situated at the edge of SEB conflict with general traffic. These stations could not be selected due to possible disturbance to bus and general traffic operation.

The selected station needed to have higher passenger exchange and high bus throughput in order to develop models reflecting high range conditions as mentioned above. Passenger interchange at stations varies due to bus-bus interchange and bus-other (rail / ferry / car) interchange. Bus throughput capacity depends on station's connection with other busways, access (ramp, signalised or unsignalised intersection)

to the road system. Table 4-2 lists the characteristics of every station on SEB, which were required in order to choose the best station for study.

Table 4-2: Busway station selection for loading area efficiency, dwell time and simulation model development

Busway station	not conflict with general traffic	connect with suburban bus routes	connect with other busways	bus-bus interchange	bus-rail interchange	access to the road system	distance from CBD (km)	passenger interchange (H/M/L)	Bus throughput (H/M/L)
Cultural Centre		✓		✓		✓	0.7	H	H
South Bank	✓				✓		1.7	M	H
Mater Hill	✓	✓					2.5	M	H
Woolloongabba		✓		✓		✓	3.2	M	H
Buranda	✓	✓	✓	✓	✓	✓	**4.4**	**H**	**H**
Greenslopes	✓	✓				✓	6.0	L	H
Holland Park West	✓						8.6	L	H
Griffith University	✓	✓				✓	10.8	M	H
Upper Mount Gravatt	✓	✓		✓			13.4	H	H
Eight Mile Plains		✓		✓		✓	16.0	H	M

note: H/M/L indicate High / Moderate / Low

Cultural Centre station could not be selected because it experiences high conflict with general traffic. South Bank and Mater Hill busway were generally considered to be possible candidates for study. Upper Mount Gravatt busway station has higher passenger interchange due to its interchange station.

Overall, when considering all of the factors addressed in Table 4-2, Buranda was selected as the optimal study station due to its high throughput, separation from general traffic, high passenger exchange, proximity to the Brisbane CBD, connection with general traffic via ramps and connection with nearby busway systems.

Knowledge gaps found in Chapter 2 and busway station selection in Chapter 3 lead to Research Design in the following chapter.

Chapter 5: A Case Study of Buranda Busway Station Operational Analysis

5.1 Overview

This chapter provides detailed analysis of the components that affect busway station capacity, which were first identified in Chapter 2. Based on Chapter 4, Buranda station on Brisbane's South East Busway (SEB) is used as the case study. The chapter first describes Buranda station's bus operation over the research period between 2011 and early 2014. Factors affecting Buranda station's operation and a methodological approach of analysis are discussed in Section 5.3. Section 5.4 presents the data collection procedure. This is followed by data analysis in section 5.5. The chapter summary is then provided.

5.2 Variation in Buranda Busway Station Bus Traffic during Study Period

We have identified that, during the course of the research between 2011 and 2014, Buranda station has experienced three distinct bus traffic loading conditions. Prior to August 2011, connections adjacent to Buranda station were Boggo Road Busway (BRB) at SEB / BRB Harrogate Tunnel portal intersection to its north end, and SEB / O'Keeffe Street access and the Cornwall Street / Juliette Street couplet its south end (refer Figure 4-9).

Operating characteristics of Buranda station changed considerably when the Eastern Busway (EB) opened in August 2011, whose connection to the SEB is located to the south of the station, between the O'Keeffe St access intersection and the Cornwall St / Juliet St ramps access junction. Many additional routes were introduced to the SEB via Buranda station when EB opened, due to that busway being fed by routes from the Old Cleveland Road corridor, which is the dominant eastern bus corridor in Brisbane. At that time, some SEB services were also added (Widanapathiranage et al. 2014). We established that these changes resulted in a 25 percent increase in the number of buses stopping at Buranda station in the inbound direction during morning peak period.

More recently, in December 2013 TransLink Division restructured SEB bus routes and timetables by reducing bus frequencies on certain lower demand routes to improve network efficiency. This has reduced the number of buses observing Buranda station by 12 percent.

Table 5-1 lists the bus route type the numbers of buses observing Buranda station inbound on a daily basis as per the current published timetable (https//:translink.com.au accessed 20/04/2014).

Table 5-1: Bus movements and characteristics at Buranda in April 2014

Route Type	Number of stopping routes	Inbound peak (07:00-09:00) stopping buses	Inbound daily stopping buses	Operation duration (daily/peak)
all stop	2	16	62	daily
BUZ	5	97	414	daily
cross country	1	8	30	daily
Express	4	19	60	daily and peak
outer urban	17	97	161	daily and peak
prepaid or rocket	11	100	104	peak
Total	40	337	831	

note: refer Section 3.4 for bus route types

5.3 Effect of *Temporary* Loading Area on Busway Station Capacity

Chapter 2 identified the factors affecting capacity for a typical busway station like Buranda include dwell time, dwell time variability, clearance time and loading area efficiency. During the morning peak period bus queuing is recurrent at Buranda due to large number of dwelling buses plus higher passenger exchange, which leads to drivers occasionally creating a fourth, *temporary* loading area at the rear of the platform.

A bus dwelling on the *temporary* loading area can offer passenger exchange only via its front door, because its rear door is positioned upstream of the platform due to overhang. The *temporary* loading area is associated with the following:

- It may only occur when the third loading area (LA3) is occupied.

- A standard 12.5 m bus can generally occupy a fourth *temporary* loading area without encroaching onto the passing lane.
- The longer, 14.5 m three axle buses and 18.5 m articulated buses each generally encroach on the passing lane when occupying the *temporary* loading area. This causes blockage of the whole busway upstream of the platform. Some drivers operating long buses avoid using the *temporary* loading area to avoid blocking the busway while dwelling.

Usually, average dwell time at *temporary* loading area is higher than other loading areas due to passenger processing only through the front door, and higher boarding lost time (Section 2.3.5).

A new method is required to estimate loading area efficiency on the basis of the role of the *temporary* loading area. Therefore, this chapter provides an improved method to estimate the number of effective loading areas and the efficiency of each loading area for use in capacity estimation. Field surveys were conducted to estimate parameters mentioned above.

5.4 Data Collection

Data collection process was conducted in April 2013 and February 2014. Here, we used one surveyor additional to the standard data collection procedure described in Section 3.4. Figure 5-1 shows surveyors' positioning at Buranda station. The surveyor of each loading area (LA1, LA2, LA3 and LA4) collected bus arrival time, first door open time, last door closed time, departure time and clearance time. Additionally, they recorded whether the bus was in queue (yes or no) along with bus route number.

At times, multiple surveyors recorded the same bus in queue, not knowing its final loading area. LA1 surveyors also sometimes faced difficulty in observing whether a bus arrived after being in queue, due to occlusion caused by high passenger density on the platform. To mitigate these challenges, the fifth surveyor recorded bus route number, arrival time at platform entry (ie: A-A in Figure 5-1) and any waiting time in queue. This procedure enables each queued bus's correct final loading area to be established.

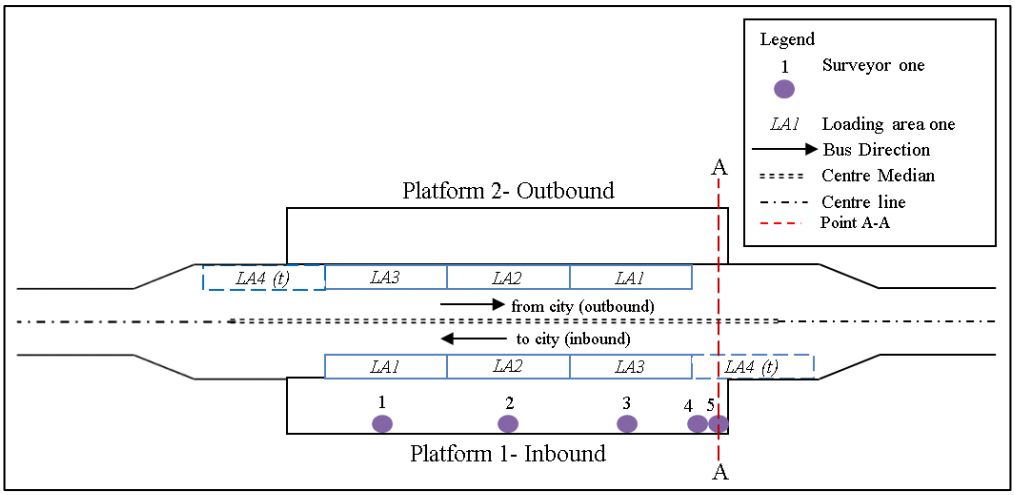

Figure 5-1: Surveyors' positioning at Buranda station

5.5 Data Analysis

Data was analysed to estimate the components that affect busway station capacity. Dwell time, clearance time and loading area efficiencies were estimated using measured data. This is now discussed.

5.5.1 Dwell Time and Clearance Time

Figure 5-2 shows a survey data snapshot for LA1, which was obtained from the smartphone application developed for this survey. Detail overview of the smart phone application is provided in Section 3.4. Here bus arrival time is the timestamp of when the bus had come to a stop at the platform, while departure time is the timestamp when the bus had commenced its departure from the platform. Moving out time is the timestamp when the bus had completely moved out of the loading area into the adjacent passing lane. Section 5.5.2 provides a detailed description of the queuing bus departure procedure.

The dwell time of each bus is equal to the difference in timestamp between when the last door closed and the timestamp when the first door opened. Figure 5-2 highlights for the route 133 bus in red a dwell time equal to 12 s (07:34:20 - 07:34:08).

Clearance time here is considered as the amount of time required for a stopped bus to completely clear the loading area, by moving out to the adjacent passing lane plus the time for a queued bus to replace it in the loading area. The clearance time includes the time spent waiting for a gap of sufficient length in the adjacent traffic for the

buses stopping in a loading area.the TCQSM 2013 identified this component of waiting time as re-entry delay (TRB, 2013).

Figure 5-2 shows a screen shot of actual data collection sheet and illustrates examples of clearance time estimation. Consider the route 133 bus, whose re-entry delay was 4 s (07:34:24 - 07:34:20). Once this route 133 bus found a sufficient gap, the bus cleared the loading area, which took 3 s (07:34:27 - 07:34:24). The next bus, route 178 was in queue, took 4 s (07:34:36 - 07:34:32) to come to a stop into that same the loading area. Therefore, the clearance time for this particular case was 11 s.

route	platform entry time A-A (t_{ent})	arrival time (t_{arr})	first door open time (t_{opn})	last door closed time (t_{clo})	departure time (t_{dep})	moving out time (t_{out})	queue (Y/N)
209	7:30:10	7:30:15	7:30:17	7:30:29	7:30:33	7:30:38	
581	7:30:39	7:30:42	7:31:08	7:31:08	7:31:10	7:31:12	Y
111	7:31:30	7:31:35	7:31:39	7:32:04	7:32:08	7:32:15	N
179	7:32:18	7:32:24	7:32:27	7:32:38	7:32:41	7:32:46	Y
222	7:33:13	7:33:16	7:33:19	7:33:33	7:33:36	7:33:42	N
133	7:34:01	7:34:05	7:34:08	7:34:20	7:34:24	7:34:27	N
178	7:34:32	7:34:36	7:34:38	7:34:46	7:34:48	7:34:51	Y
250	7:34:55	7:34:58	7:35:00	7:35:06	7:35:06	7:35:11	N
573	7:35:36	7:35:43	7:35:49	7:36:02	7:36:05	7:36:10	N
176	7:36:35	7:36:40	7:36:43	7:36:54	7:36:56	7:37:02	N
120	7:37:13	7:37:16	7:37:17	7:37:52	7:37:57	7:38:04	Y
119	7:38:07	7:38:11	7:38:12	7:38:44	7:38:52	7:38:57	Y
243	7:39:00	7:39:06	7:39:09	7:39:27	7:39:28	7:39:35	Y
133	7:40:23	7:40:27	7:40:32	7:40:40	7:40:44	7:40:49	N
201	7:41:15	7:41:18	7:41:21	7:41:32	7:41:35	7:41:40	N
171	7:42:00	7:42:04	7:42:05	7:42:17	7:42:20	7:42:25	N
579	7:42:31	7:42:35	7:42:40	7:42:56	7:42:57	7:43:01	Y
77	7:43:40	7:43:45	7:43:49	7:44:12	7:44:16	7:44:20	

Figure 5-2: Sample data set snapshot of LA1

Average Dwell Time

Table 5-2 summarizes the average dwell time estimated for each loading area. Average dwell time varies between 16 s and 19 s with a coefficient variation of dwell time varying between 0.45 and 0.60. Coefficient variation of dwell time lies in between values suggested by the TCQSM 2013 (0.40-0.60).

Average dwell time of the *temporary* loading area is higher than the rest of loading areas, which we attribute to two reasons:

- Buses serve passenger exchange (alighting then boarding) using only the front door, and

- Boarding passengers require additional time to walk from their original position on the platform to reach this loading area (higher boarding lost time).

Table 5-2: Measured average dwell time

Date (07:30-08:30)	Average dwell time (s)				Average dwell time per stop (s)	Coefficient variation of dwell time
	LA1	LA2	LA3	LA4 *(t)*		
19/02/2014	19	20	14	22	19	0.45
18/04/2013	21	17	14	22	18	0.59
17/04/2013	18	16	15	18	17	0.59
16/04/2013	19	16	16	16	17	0.60

The average dwell time was highest on 19/02/2014. Table 5-3 shows the number of stopping buses at Buranda during each study period. A reduction in buses observing Buranda station occurred under the new timetable that was introduced in December 2013. With similar passenger demands, each bus is expected to carry more passengers, and incur greater passenger exchange at stops/stations, resulting in greater average dwell time.

Table 5-3: Number of stopping buses at Buranda during each study period

Date (07:30-08:30)	Number of stop buses				
	LA1	LA2	LA3	LA4 *(t)*	total
19/02/2014	63	56	45	12	176
18/04/2013	72	59	49	17	197
17/04/2013	65	58	57	22	202
16/04/2013	65	59	51	25	200

Table 5-4 presents the statistical analysis of dwell time and Figure 5-3 illustrates their distributions on each survey date.

Table 5-4: Statistical analysis of dwell time distribution

	μ	σ	Mean (s)	Variance	Skewness	Kurtosis
19/02/2014	2.8	0.49	19	86	1.71	5.30
18/04/2013	2.7	0.61	18	106	1.21	1.84
17/04/2013	2.7	0.54	17	95	1.72	4.07
16/04/2013	2.6	0.62	17	97	1.52	3.07

By analysis of the distribution of the dwell time, it is apparent that the dwell time distribution follows a log normal distribution. This observation is consistent with Li et al. (2012). Figure 5-3 shows dwell time distribution plots.

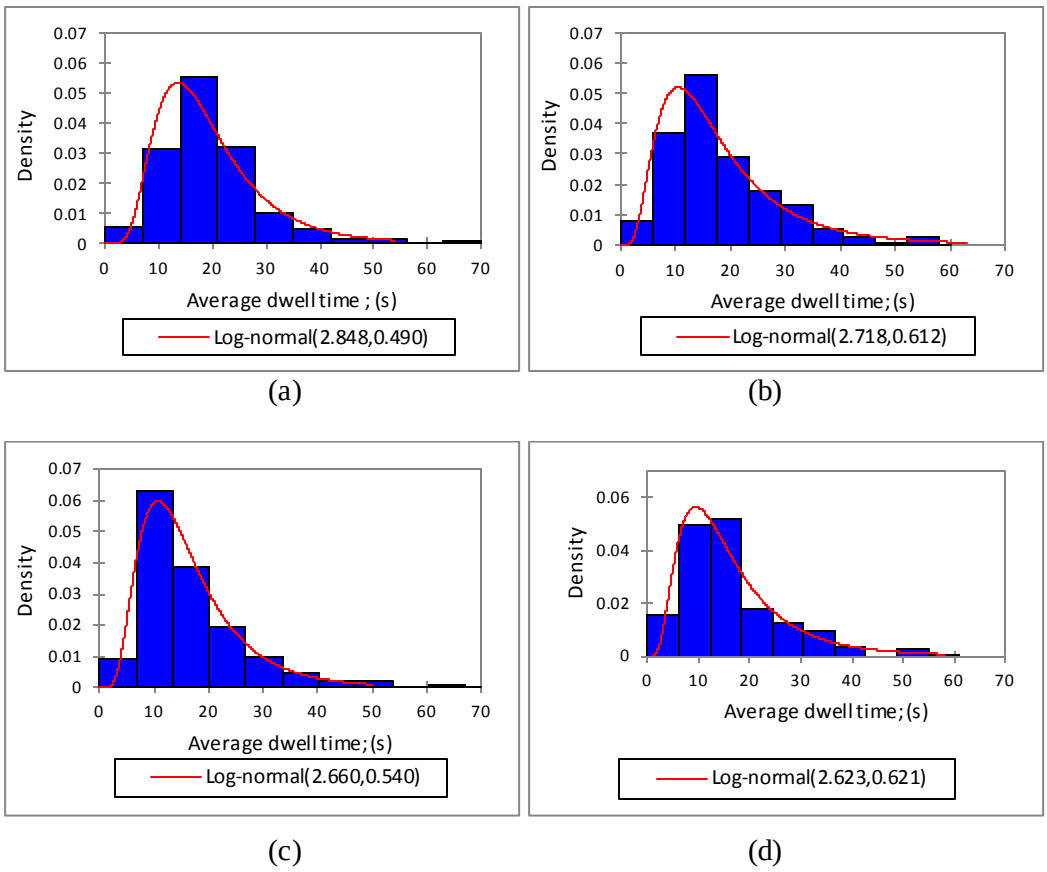

Figure 5-3: Dwell time distributions for 19/02/14 (a), 18/04/13 (b), 17/04/13 (c) and 16/04/13 (d)

Average Clearance Time

Table 5-5 presents the average clearance time estimated for each loading area on each survey date. The average clearance time for the stop varies around 12 s, which is in the range of 10 s to 20 s reported by the TCQSM 2013. Table 5-5 shows that average clearance time increases from the rear loading area to the front loading

area. This is attributed to buses take longer time to travel from the queue departure point at A-A to LA1 and LA2 (Figure 5-1).

Table 5-5: Measured average clearance time

Date (07:30-8:30)	Average clearance time (s)				Average clearance time per stop (s)
	LA1	LA2	LA3	LA4 *(t)*	
19/02/2014	12	11	11	10	11
18/04/2013	14	13	12	10	13
17/04/2013	13	12	10	7	12
16/04/2013	12	11	9	9	11

The average clearance time measured here also follows a log normal distribution. Table 5-7 shows the statistical analysis of clearance time and Figure 5-4 shows their distributions.

Table 5-6: Statistical analysis of clearance time distribution

Date (07:30-8:30)	Clearance time (s)					
	μ	σ	Mean	Variance	Skewness	Kurtosis
19/02/2014	2.3	0.29	11	12	1.62	5.99
18/04/2013	2.5	0.40	13	37	2.26	6.77
17/04/2013	2.3	0.35	11	17	1.76	7.27
16/04/2013	2.3	0.41	11	19	1.92	7.44

Figure 5-4 shows the clearance time distribution during the study period.

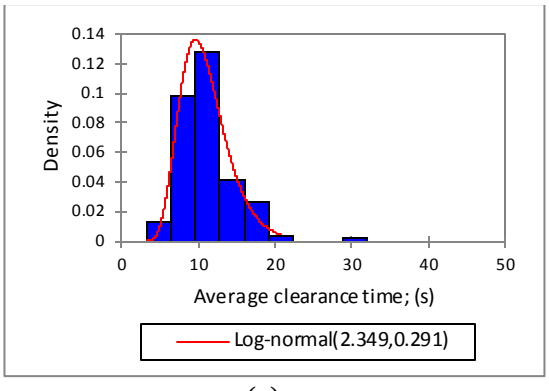

(a)

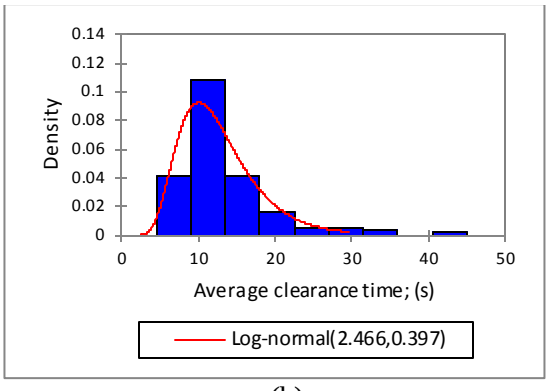

(b)

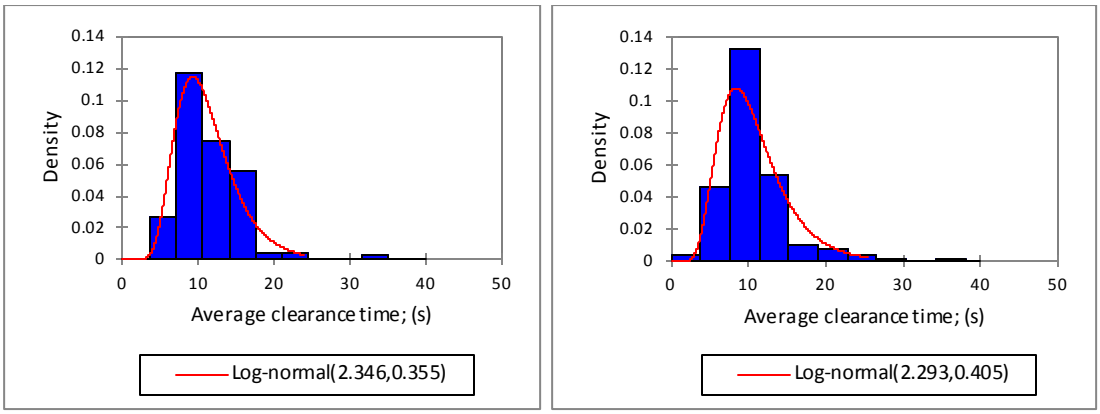

(c) (d)

Figure 5-4: Clearance time distributions for 19/02/14 (a), 18/04/13 (b), 17/04/13 (c) and 16/04/13 (d)

5.5.2 Loading Area Efficiency

The efficiency of a given loading area depends on occupancy of preceding loading area/s (Section 2.3.3). Occupied time of loading area consists of three time periods. First is dwell time of the stopped bus $(t_{clo} - t_{\text{opn}})$. Second is time taken by a bus to moving out from loading area once the doors have closed $(t_{out} - t_{\text{clo}})$. Finally, time taken by next bus to arrive to the platform and to open its doors $(t_{arr} - t_{\text{ent}})$. However, estimation of second time period differs when a bus waited in a queue. Figure 5-5 illustrates this particular scenario with different cases. Figure 5-5 (a) shows queued bus (LA3-2) which starts to enter the platform as soon as a stopped bus (LA3-1) starting to move out while Figure 5-5 (b) demonstrates that queued bus (LA3-2) waited till stopped bus (LA3-1) completely move out from loading area. Figure 5-5 (c) illustrates queued bus (LA3-2) which enters to platform during stopped bus (LA3-1) moving out. Finally, Figure 5-5 (d) shows non-queued bus (LA3-2) entering to platform.

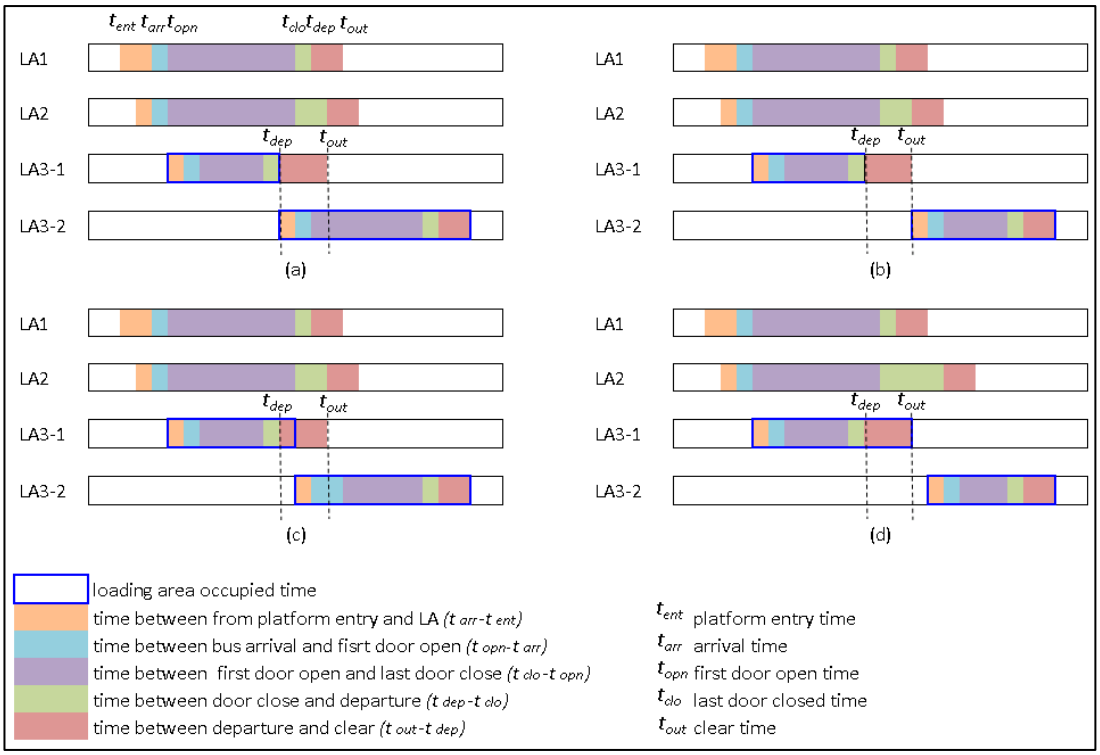

Figure 5-5: A typical example of a bus occupying at LA3

When a *temporary* loading area manifests at a busway station it is convenient to consider that the station acts as a four loading area station during a certain amount of time ($\sum_{i=3}^{5} t_i$) during the study period (Figure 5-6 (b)), while during the remainder of the study period ($\sum_{2} t_i + \sum_{i=7}^{10} t_i$) the station acts as a three loading area station (Figure 5-6 (a)). Figure 5-6 demonstrates this platform separation procedure with three loading areas and four loading areas.

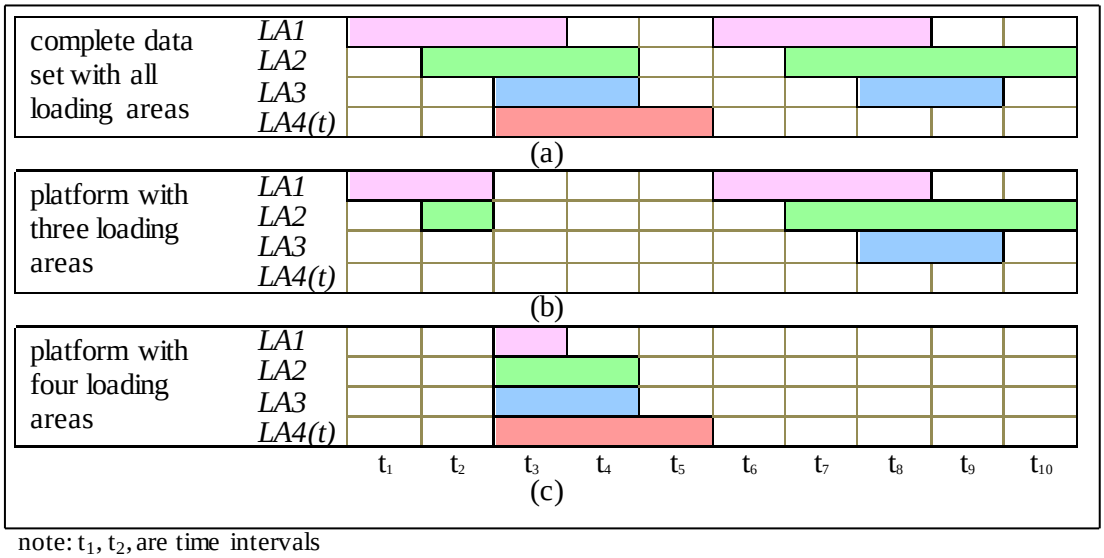

note: t_1, t_2, are time intervals

Figure 5-6: Platform separation with and without *temporary* loading area

The following equations estimate the loading area efficiencies accordingly.

The efficiency of loading area 1 is given as;

$$\eta_{LA1} = \left(1 - \frac{\sum_{h=1}^{q} t_{h,4}}{T}\right)\left(\frac{\sum_{i=1}^{m} t_{i,(2\vee3\vee(2\wedge3))\bar{\wedge}4} - \sum_{j=1}^{n} t_{j,(2\vee3\vee(2\wedge3))\bar{\wedge}1\bar{\wedge}4}}{\sum_{i=1}^{m} t_{i,(2\vee3\vee(2\wedge3))\bar{\wedge}4}}\right) \quad \text{Equation 5-1}$$

$$+ \frac{\sum_{h=1}^{q} t_{h,4}}{T}\left(\frac{\sum_{k=1}^{o} t_{k,(2\vee3\vee(2\wedge3))\wedge4} - \sum_{l=1}^{p} t_{l,(2\vee3\vee(2\wedge3))\bar{\wedge}1}}{\sum_{k=1}^{o} t_{k,(2\vee3\vee(2\wedge3))\wedge4}}\right.$$

where,

η_{LA1} = Efficiency of loading area 1

T = Study period duration (3600 s)

q = Number of time intervals during study period when loading area 4 was occupied.

$t_{h,4}$ = Duration of the h^{th} time interval when loading area 4 was occupied.

m = Number of time intervals during study period when loading area 2 OR loading area 3 OR loading areas 2 and 3 were occupied AND loading area 4 was not occupied.

$t_{i,(2\vee3\vee(2\wedge3))\bar{\wedge}4}$ = Duration of the i^{th} time interval when loading area 2 OR loading area 3 OR loading areas 2 and 3 were occupied AND loading area 4 was not occupied.

n = Number of time intervals during study period when loading area 2 OR loading area 3 OR loading areas 2 and 3 were occupied AND loading area 1 was not occupied AND loading area 4 was not occupied (from Figure 5-6; $\sum_{i=2} t_i + \sum_{i=7}^{10} t_i$).

$t_{j,(2\vee3\vee(2\wedge3))\bar{\wedge}1\bar{\wedge}4}$ = Duration of the j^{th} time interval when loading area 2 OR loading area 3 OR loading areas 2 and 3 were occupied AND loading area 1 was not occupied AND loading area 4 was not occupied (from Figure 5-6; $\sum_{i=9}^{10} t_i$).

o = Number of time intervals during study period when loading area 2 OR loading area 3 OR loading areas 2 and 3 were occupied AND loading area 4 was occupied.

$t_{k,(2\vee3\vee(2\wedge3))\wedge4}$ = Duration of the k^{th} time interval when loading area 2 OR loading area 3 OR loading areas 2 and 3 were occupied AND loading area 4 was occupied (from Figure 5-6; $\sum_{i=3}^{5} t_i$).

p = Number of time intervals during study period when loading area 2 OR loading area 3 OR loading areas 2 and 3 were occupied AND loading area 1 was not occupied AND loading area 4 was occupied.

$t_{l,(2\vee3\vee(2\wedge3))\bar{\wedge}1\wedge4}$ = Duration of the l^{th} time interval when loading area 2 OR loading area 3 OR loading areas 2 and 3 were occupied AND loading area 1 was not occupied AND loading area 4 was occupied (from Figure 5-6; $\sum_{i=4}^{5} t_i$).

Efficiency of loading area 2 is given as;

$$\eta_{LA2} = \left(1 - \frac{\sum_{h=1}^{q} t_{h,4}}{T}\right)\left(\frac{\sum_{i=1}^{m} t_{i,3\bar{\wedge}4} - \sum_{j=1}^{n} t_{j,3\bar{\wedge}1\bar{\wedge}4}}{\sum_{i=1}^{m} t_{i,(3\vee)\bar{\wedge}4}}\right) + \frac{\sum_{h=1}^{q} t_{h,4}}{T}\left(\frac{\sum_{k=1}^{o} t_{k,3\wedge4} - \sum_{l=1}^{p} t_{l,3\bar{\wedge}1\wedge4}}{\sum_{k=1}^{o} t_{k,3\wedge4}}\right) \quad \text{Equation 5-2}$$

where,

η_{LA2} = Efficiency of loading area 2

$t_{i,3\bar{\wedge}4}$ = Duration of the i^{th} time interval when loading area 3 was occupied AND loading area 4 was not occupied.

$t_{j,3\bar{\wedge}1\bar{\wedge}4}$ = Duration of the j^{th} time interval when loading area 3 was occupied AND loading area 1 was not occupied AND loading area 4 was not occupied.

$t_{k,3\wedge4}$ = Duration of the k^{th} time interval when loading area 3 was occupied AND loading area 4 was occupied.

$t_{l,3\bar{\wedge}1\wedge4}$ = Duration of the l^{th} time interval when loading area 3 was occupied AND loading area 1 was not occupied AND loading area 4 was occupied.

Efficiency of loading area 3 is given as;

$$\eta_{LA3} = \left(1 - \frac{\sum_{h=1}^{q} t_{h,4}}{T}\right) + \frac{T_4}{T}\left(\frac{\sum_{h=1}^{q} t_{h,4} - \sum_{l=1}^{p} t_{l,1\bar{\wedge}4}}{\sum_{h=1}^{q} t_{h,4}}\right)$$ Equation 5-3

where,

η_{LA3} = Efficiency of loading area 3

$t_{l,\bar{\wedge}4}$ = Duration of the l^{th} time interval when loading area 4 was occupied AND loading area 3 was not occupied.

Efficiency of the fourth, *temporary* loading area is given by,

$$\eta_{LA4\,(t)} = \frac{\sum_{h=1}^{q} t_{h,4}}{3600}$$ Equation 5-4

where,

$\eta_{LA4\,(t)}$ = Efficiency of fourth *(temporary)* loading area

Therefore, the number of effective loading areas is given as;

$$N_{el} = \eta_{LA1} + \eta_{LA2} + \eta_{LA3} + \eta_{LA4}$$ Equation 5-5

Figure 5-7 illustrates some important scenarios that affect busway station efficiency;

a) only a single bus is occupied at LA1

b) LA1 and LA2 both are occupied

c) all three loading areas are occupied

d) LA2 or LA3 or both LA2 and LA3 occupied multiple times while LA1 occupied once

e) Four buses occupied the platform including the *temporary* loading area

LA2, LA2 and LA4 *(t)* can be occupied multiple time when LA1 occupied once;

f) LA1, LA2 and LA3 occupied once while LA4 *(t)* occupied twice

g) LA1 and LA2 occupied once whereas LA3 and LA4 (t) occupied twice

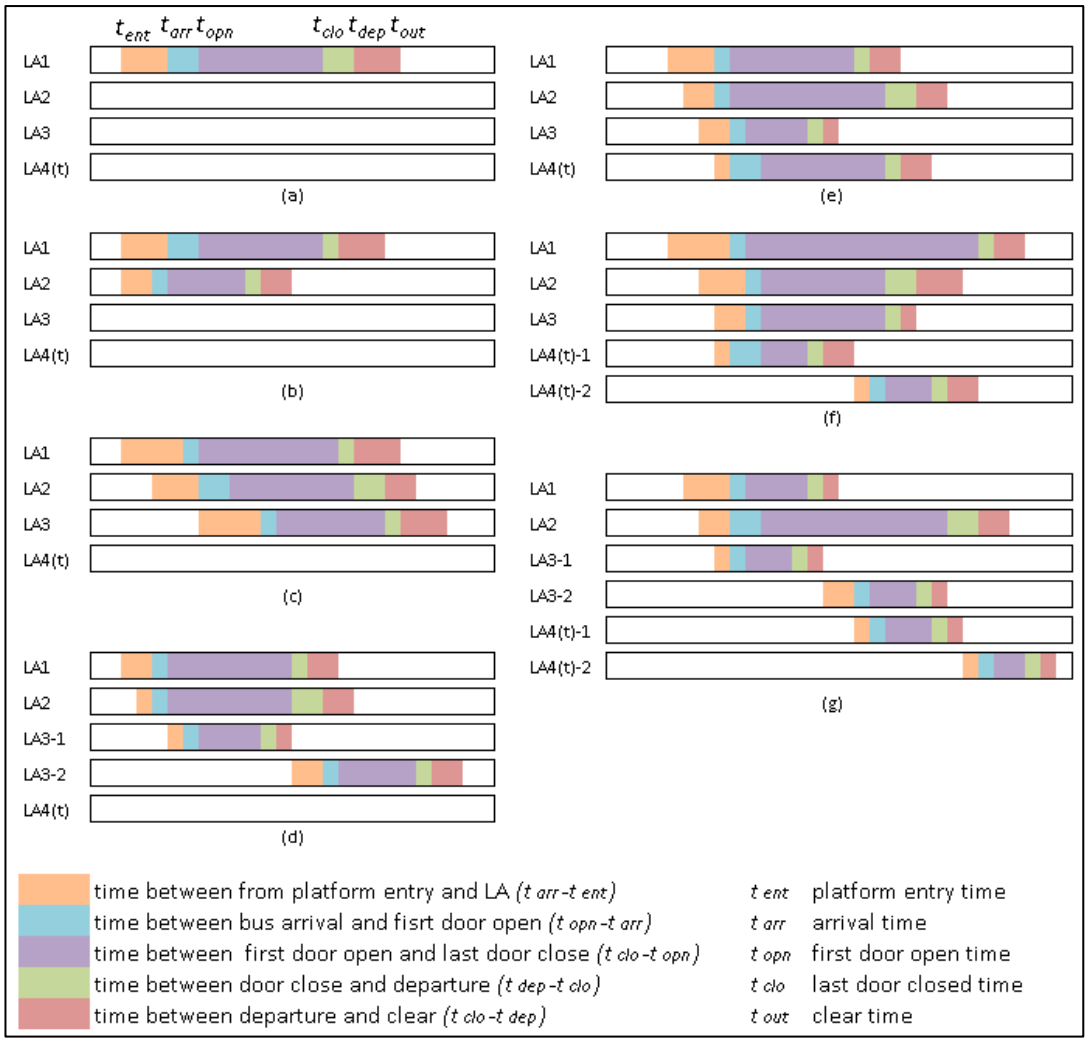

Figure 5-7: Possible bus occupancy scenarios

Table 5-7 shows the preceding loading area/s occupied time and loading area blocked time while preceding loading area/s occupied for a one hour study period.

Table 5-7: Preceding loading area/s occupied time and loading area blocked time while preceding loading area/s occupied

Date	Description	$LA1$		$LA2$		$LA3$
		$(LA1)_3$	$(LA1)_4$	$(LA2)_3$	$(LA2)_4$	$(LA3)_4$
19/02/2014	Preceding LA's occupied time (s)	1601	341	903	341	341
	LA blocked time (s)	343	266	163	158	71
18/03/2013	Preceding LA's occupied time (s)	1701	537	946	517	537
	LA blocked time (s)	481	396	176	289	200
17/03/2013	Preceding LA's occupied time (s)	1632	610	970	494	610
	LA blocked time (s)	442	483	191	293	189
16/03/2013	Preceding LA's occupied time (s)	1590	724	984	625	724
	LA blocked time (s)	436	564	197	387	225

note: $(LA1)_3$ is the preceding loading areas occupied time for three LA platform and
$(LA1)_4$ is the preceding loading areas occupied time for four LA platform

As expected LA1 is the busiest loading area then followed by LA2 and LA3. The total occupied time on 19/02/2014 is lower than other days because, number of stopping buses at Buranda is lesser than that in April 2013. Table 5-8 shows the loading area efficiency estimation for each loading areas.

Table 5-8: Loading Area Efficiency at Buranda station

Date (07:30-08:30)	Loading area efficiency (η)							N_{el}
	η_{LA1}		η_{LA2}		η_{LA3}		$\eta_{LA4(t)}$	
	$(\eta_{LA1})_3$	$(\eta_{LA1})_4$	$(\eta_{LA2})_3$	$(\eta_{LA2})_4$	$(\eta_{LA3})_3$	$(\eta_{LA3})_4$		
19/02/2014	0.71	0.02	0.74	0.05	0.91	0.08	0.09	2.6
18/04/2013	0.61	0.06	0.69	0.07	0.85	0.1	0.15	2.53
17/04/2013	0.61	0.04	0.67	0.07	0.83	0.12	0.17	2.51
16/04/2013	0.58	0.05	0.64	0.08	0.79	0.13	0.2	2.47

note: $(\eta_{LA1})_3$ = LA1 efficiency with three loading areas active on platform during study period

$(\eta_{LA1})_4$ = LA1 efficiency with four loading areas active on platform during study period

N_{el} = Number of effective loading areas during study period

The results show that when the *temporary* loading area efficiency increases, the efficiency of other loading areas decreases along with number of effective loading areas. The TCQSM 2013 gives the standard value of N_{el} for the busway station with three off-line loading areas as 2.60 (TRB, 2013).

However, these results showed that N_{el} is lower than the standard values when a *temporary* loading area is occupied. The risk of front loading area/s blocked becomes higher and higher when *temporary* loading increases. Therefore, N_{el} value reduced despite *temporary* loading efficiency increases.

5.6 Conclusion

Analysis of dwell time estimation showed that the average dwell time was typically 18 s and the coefficient variation of dwell time was between 0.45 and 0.6 during the study peak period. The dwell time distribution was determined to follow a lognormal distribution. These results are consistent with values reported in the TCQSM 2013 and the existing literature.

The average clearance time at Buranda is 12 s which lies within the 10 s to 20 s range reported by the TCQSM 2013. Clearance time showed a lognormal distribution. It will be useful to conduct further investigation of clearance time distributions at different busway stations under different demand conditions.

Temporary loading area plays an important role with respect to loading area efficiency. When the effect of *temporary* loading area is greater, the overall efficiency of the station decreases. Importantly, this investigation has established that the *temporary* loading area created by some drivers is a factor which actually reduces the overall station bus efficiency.

Chapter 6: Estimating Busway Station Bus Dwell Time Using Smart Card Data

6.1 Overview

The aim of this chapter is to seamlessly estimate bus dwell time using smart card data. An empirical model based on the smart card data and observed dwell time is proposed, in order to satisfy research objective 4, which was identified in Chapter 1.

This chapter first describes Brisbane's transit smart card operation in Section 6.2. The methodological approach to development of dwell time models using smart data is presented in Section 6.3. Section 6.4 discusses the data investigation procedure. Terminology for development of the smart card based dwell time models is described in Section 6.5. Development of Gross Dwell Time Model, Net Dwell Time Model and Queuing Transaction Time Models are presented in Section 6.6, Section 6.7 and Section 6.8, respectively. The chapter concludes in Section 6.9.

6.2 Smart Card Processing at SEB

South East Queensland's (SEQ) transit agency, TransLink Division, introduced a touch contact smart card called 'go card' in 2008 partly in an effort to reduce buses' dwell times across the network. According to TransLink, 85 percent of public transport trips in SEQ were made using smart cards in 2011, when this research commenced (TransLink, 2011). Chapter 2 discussed that the implementation of smart cards has significantly reduced bus dwell times at stops (Section 2.3.3).

Smart card data provides much larger volumes of personal travel data than is possible to obtain from other data sources. This includes detailed travel information of each smart card holder, such as boarding time, boarding stop, alighting time, alighting stop, public transport vehicle ID used, etc.

Estimating dwell time using smart card data is less simple than by using Automatic Vehicle Location (AVL) system data. Usually, AVL system data provides door opening timestamp and door closing timestamp and therefore precise dwell time of a

bus at a stop. In contrast, passengers using a smart card system such as Brisbane's can tag off as soon as the bus reaches their stop's geo-fence, which can generally occur prior to the time when the bus comes to rest at the stop. If this time component were ignored, dwell time using smart card transaction data might be overestimated. In this chapter we define this time component as queuing transaction time. Dwell time estimated including this queuing transaction time component is hence defined as gross dwell time, while dwell time estimated excluding queuing transaction time is defined as net dwell time.

6.3 Methodological Approach

For this study we again selected Buranda busway station (Chapter 4). Figure 6-1 illustrates the study process adopted, which consists of three phases. The first phase is used to develop dwell time models while last two phases are used to validate dwell time models under different conditions. The first phase of this research was conducted using morning peak survey data and smart card transaction data, while the second and third phases were used morning off-peak and afternoon off-peak survey data and smart card transaction data.

The first phase of this research was to develop a Gross Dwell Time Model and Net Dwell Time Model using peak transaction data (07:30-08:30). The second phase of this research was to determine whether the Net Dwell Time Model was valid given morning off-peak transaction data (10:00-11:00).

In the third phase, three hours (12:00-15:00) of afternoon off-peak transaction data and survey data (afternoon survey data) were used to validate both the Gross Dwell Time and Net Dwell Time Models (Figure 6-1). Finally, these two models are used to define a Bus Time in Queue Model (Figure 6-1).

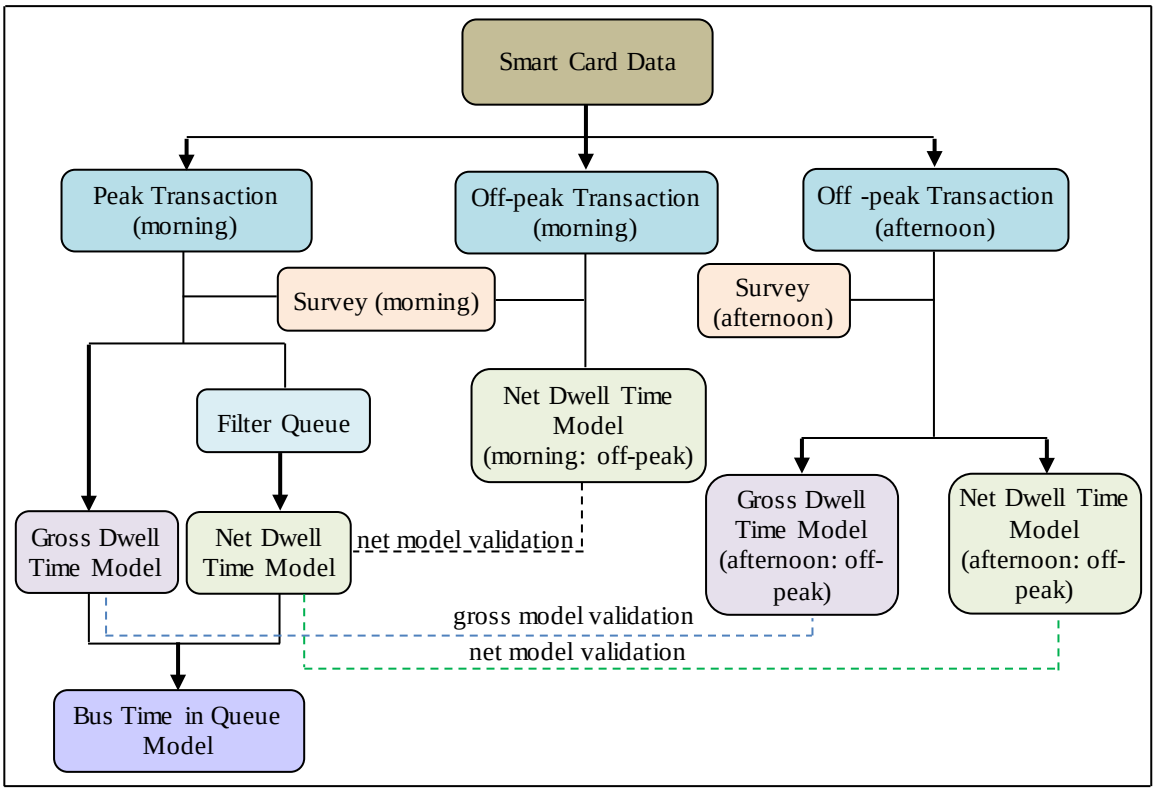

Figure 6-1: Dwell time model development framework

This research subsequently included data only pertaining to two-door buses on the basis that over 80 percent of TransLink buses had this configuration at the time of observation (Otto, 2008; TransLink, 2012; Widanapathiranage et al., 2013).

6.4 Data Investigation

Data investigation was carried out in two stages. The first was to collect field survey data and the second was to extract smart card data for the same survey periods.

6.4.1 Field Surveys

Survey procedures are described in Chapter 3 (Section 3.4).

6.4.2 Smart Card Data Extraction

Raw smart card transaction data obtained from Translink Division, coinciding with this study's field surveying dates, were first filtered in order to remove unwanted detail and determine transaction times. A MatLab code was developed to calculate the transaction time for a bus at the stop, being equal to the last passenger's (boarding or alighting) transaction timestamp minus the first passenger's (boarding

or alighting) transaction timestamp. The transaction times were scrutinized to eliminate any erroneous transaction values.

6.5 Smart Card Based Dwell Time Models

Figure 6-2 illustrates a generalised timeline of a bus observing a busway station. The solid time line (top) shows an example extent of actual passenger exchange timestamps, while the dashed timeline (bottom) shows the feasible, corresponding extents of smart card tag-off and tag-on transaction timestamps respectively.

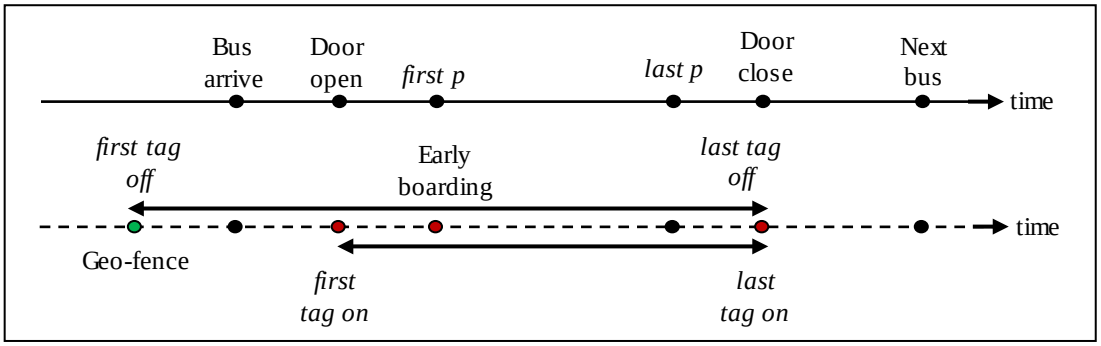

note: *first p* represents first passenger boarding or alighting, *last p* represents last passenger boarding or alighting

Figure 6-2: Normal passenger operation and smart card transaction at busway station

Once a bus arrives on the platform to serve passengers, the driver opens the door. Tag on activity can only occur between the door opening timestamp and the door closing timestamp. However, tag off activity can occur prior to the door opening timestamp. When the bus reaches the geo-fence (which is 50 m upstream of the busway station), the on-board smart card readers become activated for transactions. As a result, passengers can tag off between the timestamp when the bus reaches the geo-fence and the door closing timestamp (Figure 6-2).

This study has identified 16 combinations of transaction activity as a consequence of four tag-on and four tag-off scenarios (Table 6-1). Sometimes passengers can move very close to the approaching bus door and board early, defined as up to 1 s following the door opening timestamp (B1 and B3 cases in Table 6-1).

Table 6-1: Smart card transaction scenarios

Tag off scenario	Tag on Scenario			
	B1: commenced and concluded within 1 s of door opening timestamp	B2: commenced late (after 1 s of door opening timestamp) and concluded before door closing timestamp	B3: commenced within 1 s of door opening timestamp and concluded before door closing timestamp	B4: no tag-on occurred
A1: commenced and concluded before bus door opening timestamp	B1A1	B2A1	B3A1	B4A1
A2: commenced after bus door opening timestamp and concluded before bus door closing timestamp	B1A2	B2A2	B3A2	B4A2
A3: commenced before bus door opening timestamp and concluded before bus door closing timestamp	B1A3	B2A3	B3A3	B4A3
A4: no tag-off occurred	B1A4	B2A4	B3A4	B4A4

For instance, B3A1 represents the scenario where tag on commenced within 1 s of door opening timestamp and concluded before door closing timestamp, whereas tag off commenced and concluded before bus door opening timestamp (Figure 6-2).

6.6 Gross Dwell Time Model Development

The initial objective was to develop a Gross Dwell Time Model calibrated for the peak hours. This includes cases where buses spend time in queue before reaching an available loading area. Smart card transaction times (refer Section 6.4.2) were

obtained and for each bus classified into one of the 16 cases described in Table 6-1. As mentioned in Chapter 5, the dwell time of each bus is equal to the difference in timestamp between when the last door closed and the timestamp when the first door opened (Section 5.5.1), which were measured manually on the station platform during the survey. These timestamps were cross-matched with the smart card transaction times for each bus. The icons in Figure 6-3 represent the smart card transaction times (X-axis) and cross-matched dwell times (Y-axis) measured during surveys.

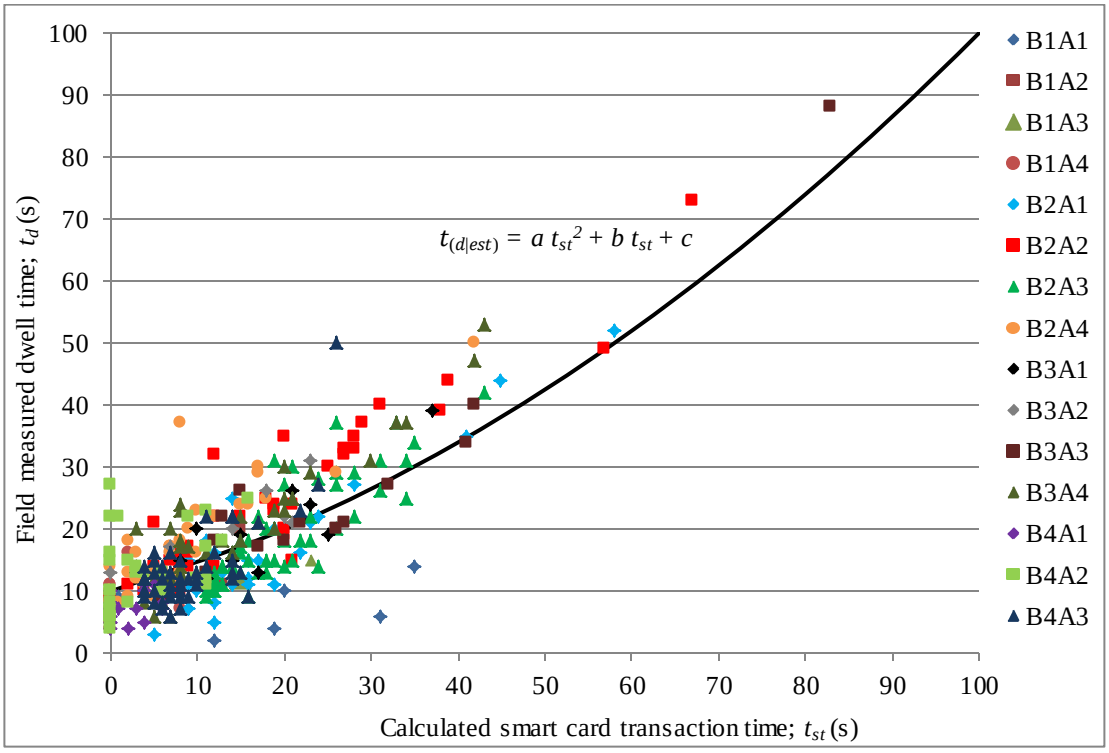

Figure 6-3: Peak hour gross smart card transaction versus field measured dwell time relationship

Figure 6-3 shows that smart card transaction time does not correspond precisely to survey dwell time. One key reason for this is that smart card transaction time maybe greater than dwell time due to an early tag off after the bus enters the geo-fence but before it stops to dwell on the available loading area. This may be exacerbated if the bus needs to wait in queue to enter an available loading area.

A second key reason is that a single transaction results in a zero transaction time, while a small number of transactions, such as a couple of tag off transactions in rapid succession, may result in very small transaction times. The actual dwell times would

still be expected to be larger due to the door opening and closing time component of dwell time, plus the physical processing time per passenger through the door(s).

A positive Y axis intercept on Figure 6-3 is to be expected, and is a measure of average minimum dwell time. By inspection of the data of Figure 6-3, a nonlinear polynomial equation of the form of (Equation 6-1) was determined to be most suitable for this Gross Dwell Time Model:

$$t_{d|est} = at_{st}^2 + bt_{st} + c \qquad \text{Equation 6-1}$$

where;

$t_{d|est}$ = Estimated dwell time; (s)

t_{st} = Smart card transaction time; (s)

a, b, c = Curve fitting constants; (s)

Note that constant c in Equation 6-1 represents the Y axis intercept, in this case an average minimum dwell time.

In order to determine suitable values of the curve fitting constants in Equation 6-1, it was necessary to reiterate the purpose of the model of Equation 6-1, which is to provide the best estimate of dwell time for a given smart card transaction time. More generally, we aim to provide the best estimate of the distribution of dwell times given a distribution of smart card transaction times. Chapter 5 has shown that dwell time tends to be distributed log-normally; which was also presumed here for model development.

Two objectives were therefore established to determine values of curve fitting constants in Equation 6-1 that provide the best estimates of:

1. average measured dwell time and coefficient of variation of measured dwell time, and
2. average of the logarithms of measured dwell time and coefficient of variation of the logarithms measured dwell time for distribution shape.

Numerical optimisation was applied to achieve both of the following objective functions together;

$$Obj\ I\ (a,b,c) = min\left(\left(\bar{t}_{d|meas} - \bar{t}_{d|est}\right)^2 + \left(cv\left(t_{d|meas}\right) - cv\left(t_{d|est}\right)\right)^2\right) \quad \text{Equation 6-2}$$

$$Obj\ II(a,b,c) = min\left(\left(\overline{ln\left(t_{d|meas}\right)} - \overline{ln\left(t_{d|est}\right)}\right)^2 + \left(cv\left(ln\left(t_{d|meas}\right)\right) - cv\left(ln\left(t_{d|est}\right)\right)\right)^2\right); \quad \text{Equation 6-3}$$

where

$\bar{t}_{d|meas}$ = Average measured dwell time; (s)

$\bar{t}_{d|est}$ = Average estimated dwell time using Equation 6-1; (s)

$cv\left(t_{d|meas}\right)$ = Coefficient of variation of measured dwell time

$cv\left(t_{d|est}\right)$ = Coefficient of variation of estimated dwell time using Equation 6-1

The results of the numerical optimisation for the Gross Dwell Time Model using the morning peak hour data are provided in the first column of Table 6-2.

Figure 6-4 shows that for the values of curve fitting constants determined, objective functions are practically zero. Under objective function (I) there is negligible difference between average measured dwell time and average estimated dwell time, and also negligible difference between coefficient of variation of measured dwell time and coefficient of variation of estimated dwell time. These are both important quantities in transit capacity and quality of service analysis (TRB, 2013).

Figure 6-3 includes Equation 6-1 with the values of the curve fitting constants from Table 6-2. Although spread is apparent for reasons described above, the second order polynomial fits the data reasonably. Figure 6-4 illustrates the cumulative distributions of both measured dwell time, and estimated dwell time using Equation 6-1 with constants of Table 6-2. By visual inspection, for dwell times larger than 10 s, the estimated distribution aligns with the measured distribution very closely as is ensured by objective function (II). For small dwell times less than 10 s, the estimated dwell time distribution differs from the measured distribution due to the average minimum dwell time of 5.7 s.

Traditional capacity analysis relies on average dwell time while QoS analysis relies on coefficient of variation of dwell time, and this difference for small dwell times is not critical for these purposes. However, should future study require the dwell time distribution for purposes such as microscopic simulation, the model should be further scrutinised in this small dwell time range.

The Kolmogorov-Smirnov statistic for the two distributions of Figure 6-4 was determined to be equal to 0.075, which is less than the critical value of 0.093 for a five percent confidence level. Thus, the null hypothesis that the samples are drawn from the same distribution was not rejected.

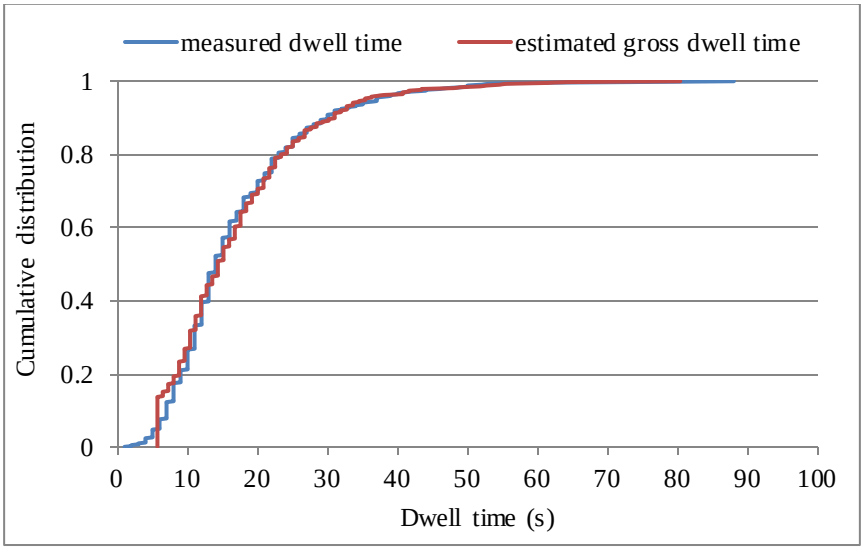

Figure 6-4: Cumulative distributions of peak hour measured dwell time and estimated using Gross Dwell Time Model of Equation 6-1 with Table 6-2 constants

Figure 6-5 illustrates for the calibration peak hour, each measured dwell time versus value estimated using the Gross Dwell Time Model of Equation 6-1 with Table 6-2 constants for the corresponding measured gross transaction time. While spread is evident, the R^2 was determined on a line of equality comparison to be equal to 0.58, indicating that this estimation method can provide for a particular bus a reasonable estimate of its actual dwell time if its gross transaction time is known.

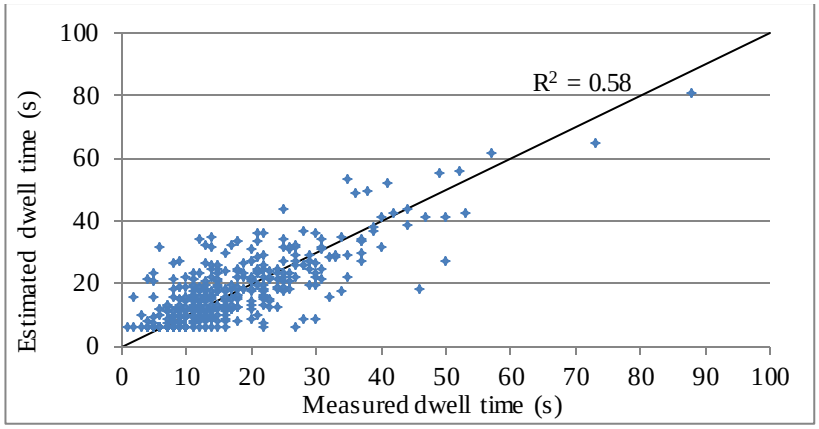

Figure 6-5: Peak hour measured dwell time versus estimated dwell time using Equation 6-1 and Table 6-2 constants

6.6.1 Gross Dwell Time Model Validation

The Gross Dwell Time Model of Equation 6-1 with coefficients calibrated for the morning peak hour was validated using afternoon off-peak data from survey data set 2 as identified in Figure 6-1. Table 6-2 also shows the results for each of three afternoon off-peak hours. Even though the surveying period for second data set is six hours, we selected the first three hours data because after 15:00 the numbers of journeys are subsequently less (due to inbound lower passenger demand) than during the 12:00 to 15:00 period.

Table 6-2: Gross Dwell Time Model calibration and validation

	Calibration Hour	Validation Hours (off-peak)		
	07:30-08:30	12:00-13:00	13:00-14:00	14:00-15:00
a	0.0016			
b	0.7665			
c	5.5			
$\bar{t}_{d\|meas}$; (s)	16.9	11.9	10.4	11.1
$\bar{t}_{d\|est}$; (s)	16.7	11.9	10.4	11.1
$cv(t_{d\|meas})$	0.62	0.66	0.56	0.79
$cv(t_{d\|est})$	0.63	0.62	0.55	0.74
Objective function (I)	4.00E-02	2.28E-02	1.39E-03	8.57E-02
Objective function (II)	3.48E-04	1.61E-03	1.23E-03	7.53E-03
R^2	0.58	0.65	0.66	0.63
Critical value (α =0.05)	0.093	0.184	0.176	0.176
K-S statistic	0.075	0.156	0.175	0.167
Reject Hypothesis?	no	no	no	no

The estimated average gross dwell time and coefficient variation of dwell time closely match the observed values under each study hour within 100 percent and 94 percent during respectively (Table 6-2).

Objective functions are very close to zero for all three off-peak validation hours. The Kolmogorov-Smirnov statistic for the distributions of each hour was calculated and null hypothesis of all samples was not rejected with a five percent confidence level. Under objective function (I) there is negligible difference between average measured dwell time and average estimated dwell time, and negligible difference between coefficient of variation of measured dwell time and coefficient of variation of estimated dwell time, for all three off-peak hours.

Figure 6-6 shows the gross dwell time distributions and cumulative distributions between 12:00-13:00 (a and b), between 13:00-14:00 (c and d), and between 14:00-15:00 (e and f) using Equation 6-1 and Table 6-2 constants. By visual inspection, for dwell times larger than 10 s, the estimated distributions align with the measured distributions very closely, as is ensured by objective function (II).

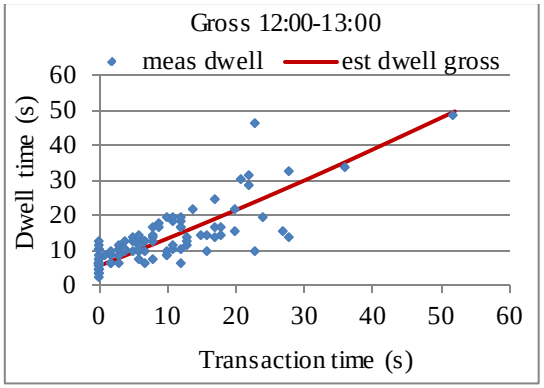

(a)

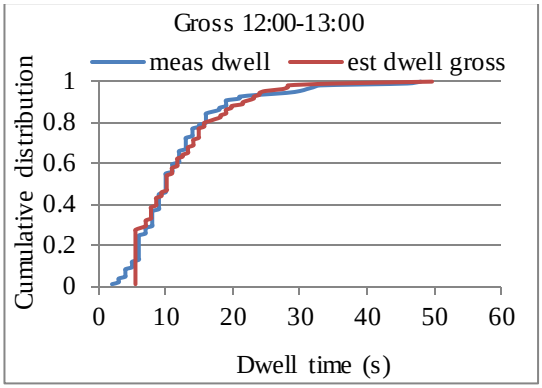

(b)

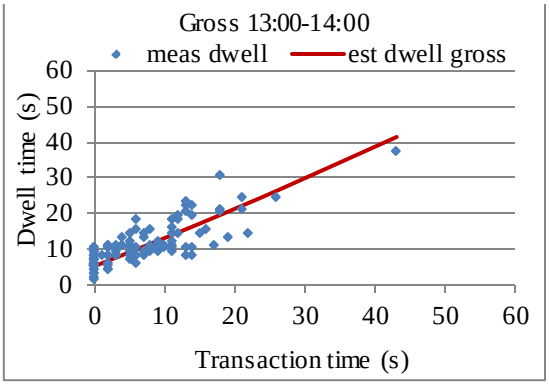

(c)

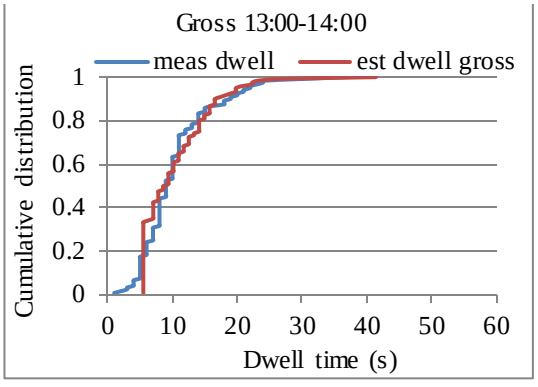

(d)

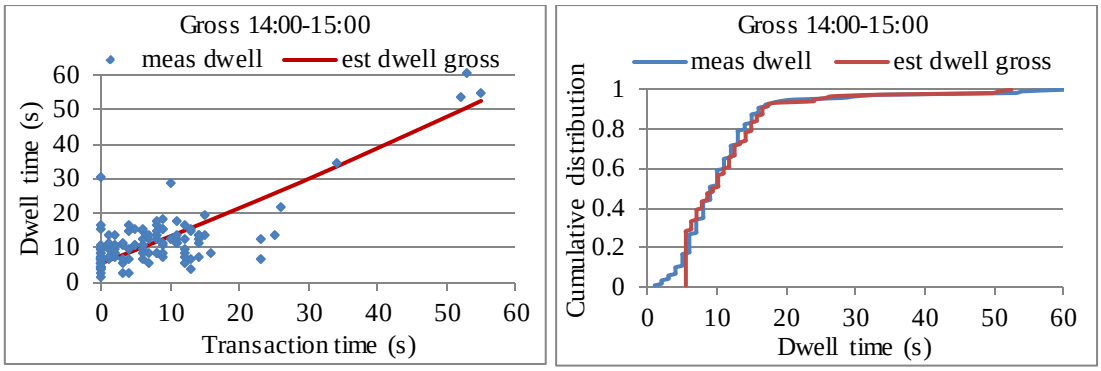

(e) (f)

Figure 6-6: Off-peak hour with gross dwell time model: Measured dwell time vs measured gross transaction time (a, c, e); gross cumulative distributions of measured dwell time and estimated dwell time (b, d, f)

Comparing results in Table 6-2, the Gross Dwell Time Model yields higher R^2 for the off-peak hours than the calibration peak hour, to which it was fitted. This can be explained by the peak hour having more transactions exceeding 20 s than in off-peak hours.

It is concluded that the Gross Dwell Time Model can be used to generate reasonable estimates of actual dwell times for known gross transaction times both under peak and off-peak conditions.

6.7 Net Dwell Time Model Development

While Equation 6-1 calibrated using the constants of Table 6-2 is useful for gross conditions which include bus time in queue, the data needed to be further investigated to establish a dwell time model for net conditions which exclude any effect of bus time in queue.

The on-board smart card transaction readers are activated once a bus reaches the geo-fence. Therefore a passenger can touch their smart card any time from the geo-fence arrival. Any transactions under Tag off scenarios A1 and A3 may overestimate the transaction time more than dwell time (Figure 6-2 and Table 6-1). This means time between door opening timestamp and first tag off becomes larger under cases A1 and A3.

Some significantly larger transaction times than actual dwell times were observed during the peak hour analysis. We reasoned that on these occasions the bus must be in queue awaiting an available loading area. A threshold time needed to be

established for identification of these occasions. With the distance between busway station and geo-fence being 50 m and for an unimpeded, a comfortable bus deceleration rate of 1 m/s^2, and average speed of bus upon reaching the geo-fence of 18 km/h, the resultant time threshold is 10 s.

The selection of 10 s buffer period was further investigated from the cumulative distribution for A1 and A3 cases. Figure 6-7 shows the cumulative plot for the A1 cases (B1A1, B2A1, B3A1 and B4A1). Fewer than 30 percent of buses under A1 cases have time difference between the first tag off and the door opening greater than 10 s. This was also evident for the A3 cases.

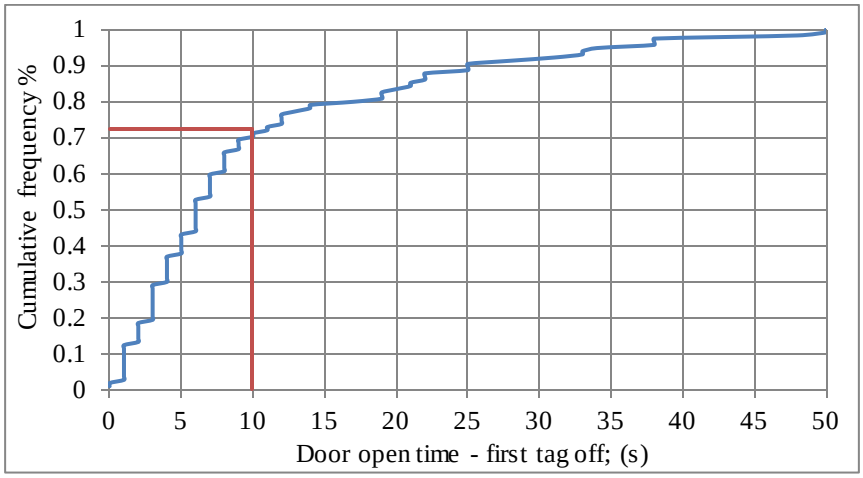

Figure 6-7: Cumulative distribution of transactions under A1 cases

Figure 6-8 illustrates the relationships between smart card transaction time and survey dwell time for four selected cases from A1 and A3 (Table 6-1). Plots (a), (b), (c) and (d) represent B2A1, B2A3, B3A1 and B2A3 cases respectively. In each plot blue diamonds represent occasions where buses arrived at the geo-fence within 10 s of the door opening timestamp while red squares represent where buses arrived at the geo-fence greater than 10 s of the door opening timestamp.

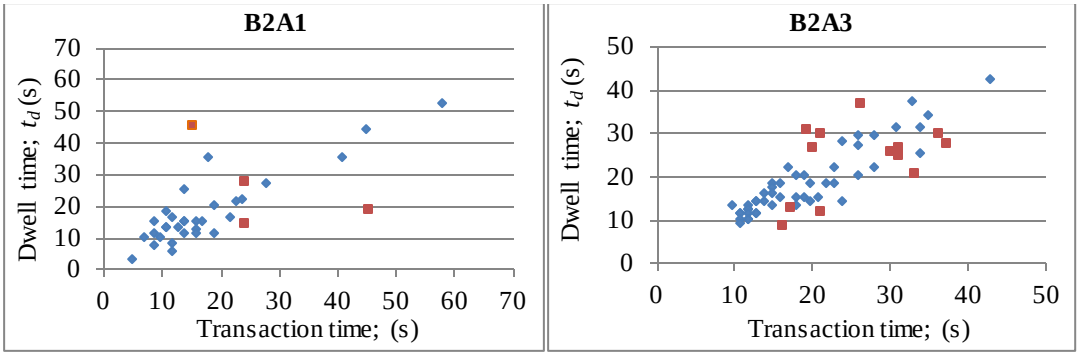

(a) (b)

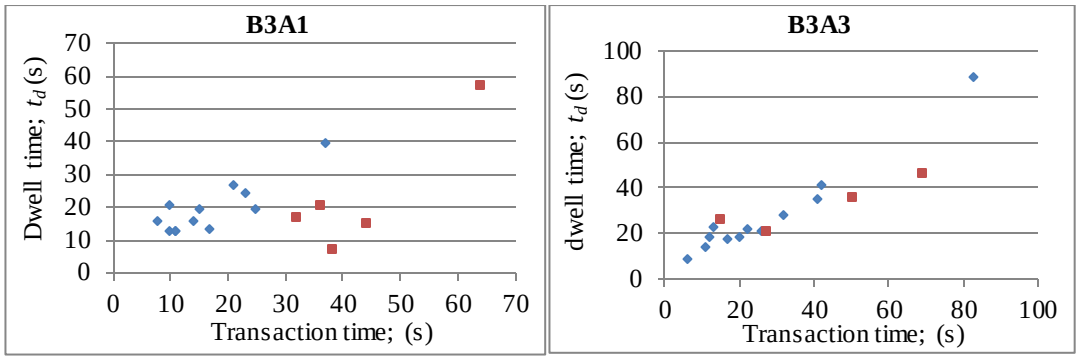

(c) (d)

Figure 6-8: Transaction time versus survey dwell time for B2A1, B2A3, B3A1 and B3A3 cases

Cases B2A1, B2A3, B3A1 and B2A3 include 11 percent, 25 percent, 29 percent and 23 percent of occasions respectively, where buses arrived at the geo-fence more than 10 s before their door opening timestamps.

To appreciate the improvement in dwell time estimation using the net model we compared R^2 for each of these cases. For case B2A1, R^2 improved from 0.52 to 0.70. For case B2A3, R^2 improved from 0.70 to 0.83. For case B3A1, R^2 improved from 0.44 to 0.75. For case B3A3, R^2 improved from 0.87 to 0.93. For these example cases it is evident that a stronger distribution exists between measured dwell time and transaction time when the data that is presumed to reflect bus queuing conditions is excluded.

As a consequence of similar investigation across all cases, the data displayed in Figure 6-3 was filtered to exclude occasions where the bus arrived at the geo-fence more than 10 s before its door opening timestamp on the available loading area, hence excluding queuing transactions. Figure 6-9 illustrates the remaining 84 percent of data and the optimal second order polynomial equation for a Net Dwell Time Model determined using the numerical optimization method described above.

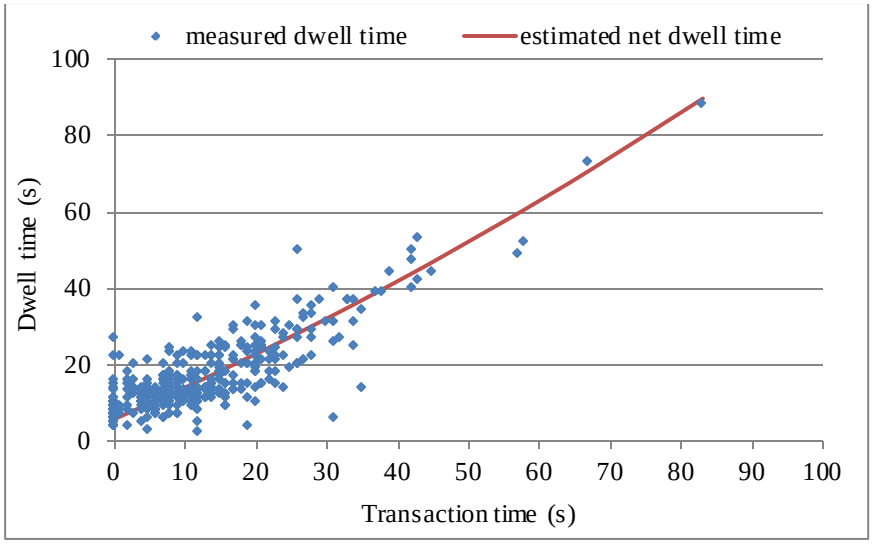

Figure 6-9: Peak hour net smart card transaction versus survey dwell time relationships

The results of the numerical optimisation for the Net Dwell Time Model are provided in Table 6-3.

Table 6-3 shows that for the values of curve fitting constants determined by objective function (I) and (II) is again close to zero showing negligible difference between average measured dwell time and average estimated dwell time, and also negligible difference between coefficient of variation of measured dwell time and coefficient of variation of estimated dwell time. Comparison of these values with those of Table 6-2 shows average estimated dwell time to be almost identical, and coefficient of variation of estimated dwell time to be identical, which suggests that using this model with net smart card transaction data can reliably synthesise the measured dwell time distribution.

Figure 6-9 includes Equation 6-1 with the values of the curve fitting constants from Table 6-3. It can be seen that the second order polynomial fits the data very well. The Kolmogorov-Smirnov statistic for the two distributions of Figure 6-10 was determined to be equal to 0.085, which is less than the critical value of 0.101 for a five percent confidence level. Thus, the null hypothesis that the samples are drawn from the same distribution was not rejected.

Figure 6-10 illustrates the cumulative distributions of both measured dwell time, and estimated dwell time using Equation 6-1 and the constants from Table 6-3. By visual inspection, for dwell times larger than 10 s, the estimated distribution aligns with the measured distribution very closely as is ensured by objective function (II). Again,

for dwell times less than 10 s the estimated dwell time distribution differs from the measured distribution due to the average minimum dwell time of 5.6 s (Table 6-3).

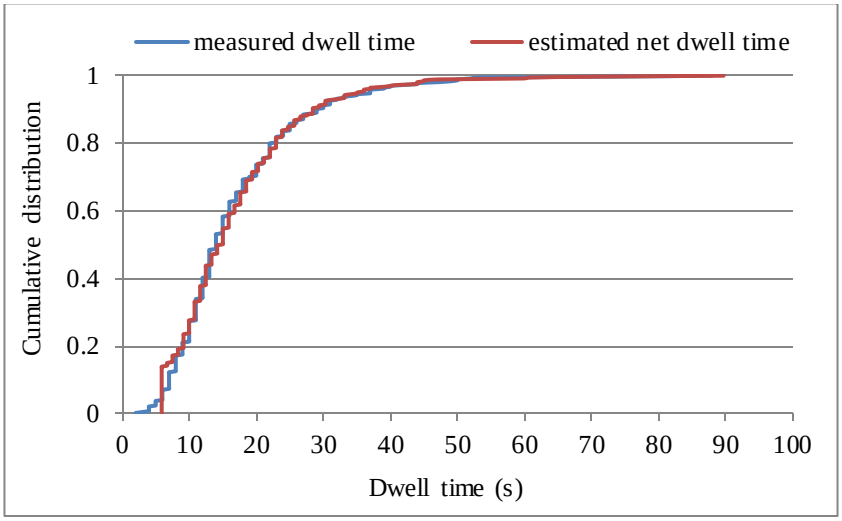

Figure 6-10: Cumulative distributions of peak hour measured dwell time and estimated dwell time using Equation 6-1 and Table 6-3 constants

Figure 6-11 illustrates for the peak hour each measured dwell time versus value estimated using the net peak hour dwell time model of Equation 6-1 with Table 6-3 constants for the corresponding measured net transaction time. While spread is evident, the R^2 was determined on a line of equality comparison to be equal to 0.71, indicating that this estimation method can provide for a particular bus a good estimate of its actual dwell time if its net transaction time is known.

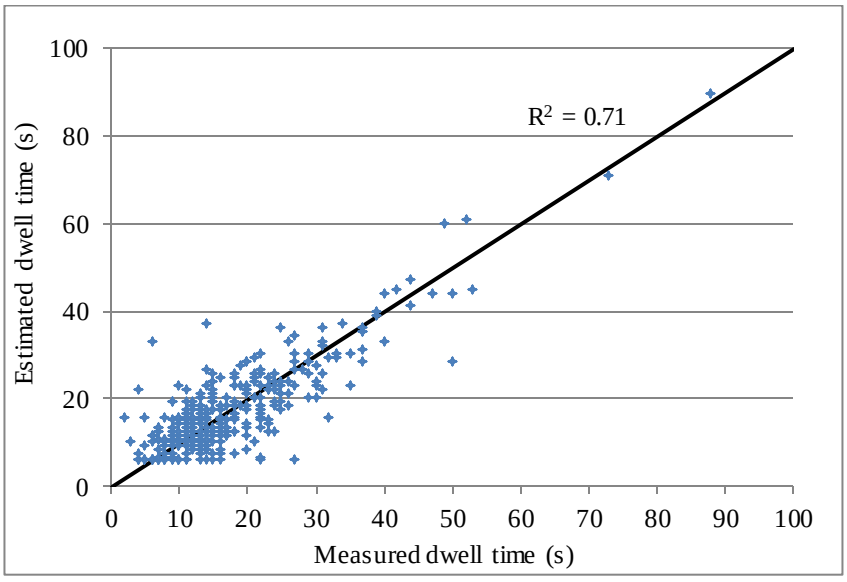

Figure 6-11: Peak hour net measured dwell time versus estimated dwell time using Equation 6-1 and Table 6-3 constants

6.7.1 Net Dwell Time Model Validation

The Net Dwell Time Model of Equation 6-1 with constants calibrated for the morning peak hour was validated using morning off-peak and afternoon off-peak data from survey data set 1 and data set 2 as identified in Figure 6-1.

The off-peak morning time hour between 10:00 to 11:00 was chosen to validate the Net Dwell Time Model. Three study hours (12:00 - 15:00) were chosen to further validate the Net Dwell Time Model. These hours were selected to account different demand conditions. The off-peak passenger demand at Buranda predominantly changes on passenger demand to UQ since most of eastern and southern suburb passengers use Buranda as their interchange station (Section 4.3). During 10:00 - 11:00, we observed the largest off-peak passenger interchange to UQ and then followed by 12:00 - 14:00 and 12:00 - 15:00 hours.

The number of buses during these hours was considerably less than during the peak hour. During the survey periods, loading areas 1 and 2 were used by buses, apart from some rare occasions. We observed bus queuing on very few occasions especially during 10:00 - 11:00 hour. Bus queuing was observed to be negligible during each of the three hours between 12:00 - 15:00. Between each study hour commencing 10:00, 12:00, 13:00 and 14:00, there were ten, nine, eight and four transactions having dwell time greater than 20 s respectively. Although, rare instances where tag off transactions commenced within 10 s of the bus door opening timestamp were again excluded.

Table 6-3 also shows the results for each of three afternoon off-peak hours as well as morning off-peak hour between 10:00 and 11:00.

Table 6-3: Net Dwell Time Model calibration and validation

	Calibration Hour	Validation Hours (off-peak)			
		Morning	Afternoon		
	07:30-08:30	10:00-11:00	12:00-13:00	13:00-14:00	14:00-15:00
a	0.0025				
b	0.8027				
c	5.6				
$\bar{t}_{d\|meas}$; (s)	16.4	13.4	12.0	10.4	10.9
$\bar{t}_{d\|est}$; (s)	16.4	13.4	11.9	10.5	10.6
$cv(t_{d\|meas})$	0.63	0.73	0.65	0.57	0.72
$cv(t_{d\|est})$	0.63	0.73	0.66	0.59	0.74
Objective function (I)	8.98E-02	4.97E-02	3.50E-03	1.83E-02	7.48E-02
Objective function (II)	6.67E-04	8.85E-04	7.99E-04	5.04E-04	5.90E-03
R^2	0.71	0.78	0.72	0.74	0.71
Critical value(α =0.05)	0.101	0.196	0.19	0.183	0.183
K-S statistic	0.085	0.125	0.176	0.18	0.164
Reject Hypothesis?	no	no	no	no	no

The estimated average net dwell times and coefficients of variation of dwell time for each validation period match the observed values very well. This indicated very good model fit. The accuracy in the estimation of average net dwell time is 98 percent and in coefficient of variation of dwell time 96 percent during these off-peak hours.

Objective functions are very close to zero for all four off-peak validation hours. The Kolmogorov-Smirnov statistic for the distributions of each hour was calculated and null hypothesis of all samples was not rejected with a five percent confidence level. Under objective function (I) there is negligible difference between average measured dwell time and average estimated dwell time, and negligible difference between coefficient of variation of measured dwell time and coefficient of variation of estimated dwell time, for all three off-peak hours.

Figure 6-12 shows the net dwell time distributions and cumulative distributions between 10:00 - 11:00 (a and b), between 12:00 - 13:00 (c and d), between 13:00 -

14:00 (e and f), and between 14:00 - 15:00 (g and h) using Equation 6-1 and Table 6-3 constants. By visual inspection, for dwell times larger than 10 s, the estimated distributions align with the measured distributions very closely, as is ensured by objective function (*II*).

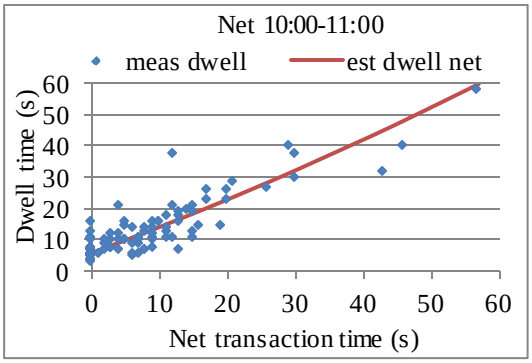

(a)

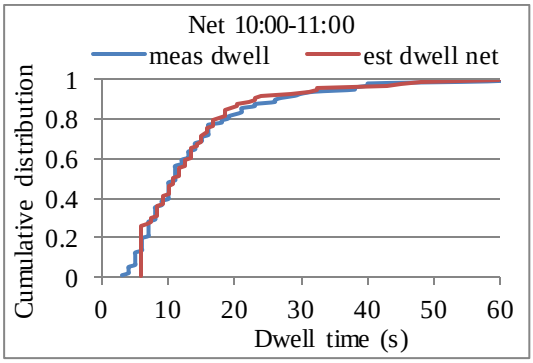

(b)

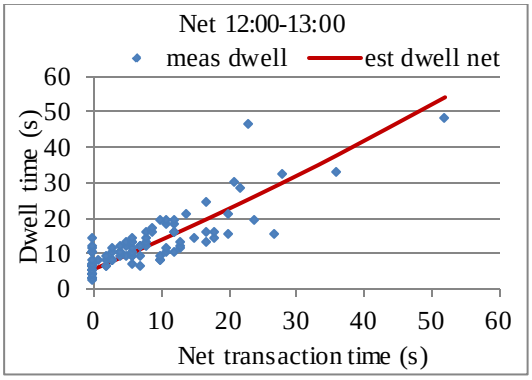

(c)

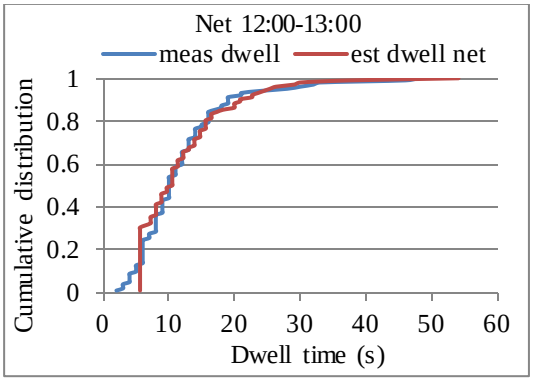

(d)

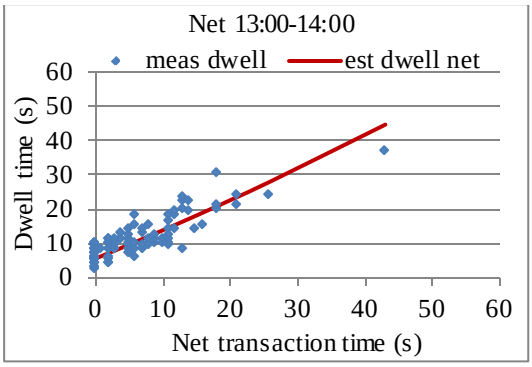

(e)

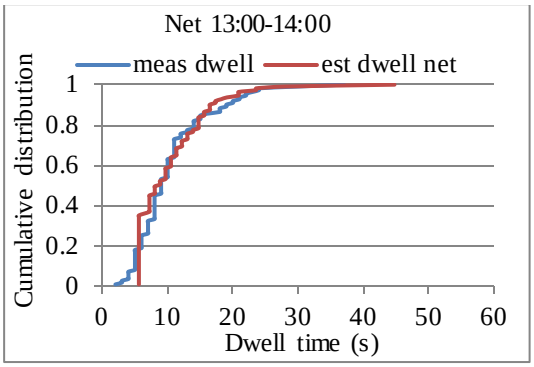

(f)

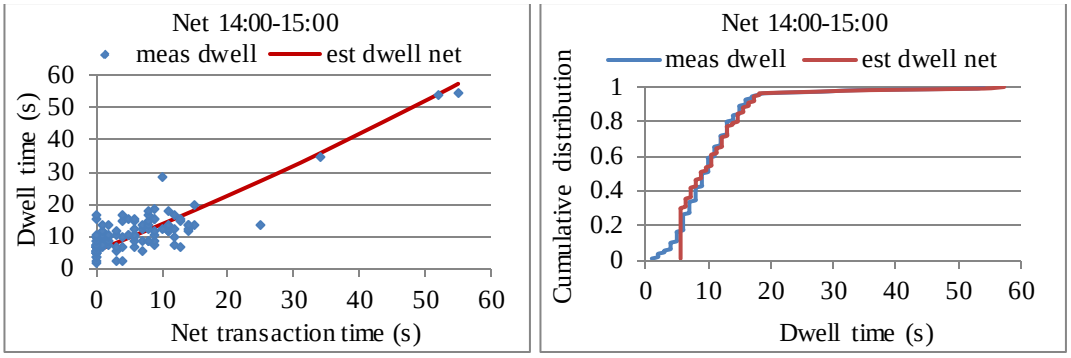

(g) (h)

Figure 6-12: Off-peak hour with net dwell time model: Measured dwell time vs measured net transaction time (a, c, e); net cumulative distributions of measured dwell time and estimated dwell time (b, d, f)

The R^2 values for the off-peak validation hours are equal or greater than the value of 0.71 for the calibration peak hour, because each off-peak hour has fewer data points. However, dwell time estimation beyond 30 s would require additional data samples.

It is concluded that the Net Dwell Time Model can be used to generate reasonable estimates of actual dwell times for known net transaction times both under both peak and off-peak conditions.

6.8 Queuing Transaction Time

Comparing the polynomial constants of Table 6-2 and Table 6-3, for all transaction times the dwell time estimated by the net model is greater than that estimated by the gross model. For a given dwell time the corresponding transaction time from the net model will be less than the corresponding transaction time from the gross model, as illustrated in Figure 6-13. The difference between the two transaction times represents the effect of excluding transactions corresponding to bus queuing conditions, and thus provides an estimate of bus time in queue as a function of dwell time, given by;

$$t_q = t_{sg}(t_d) - t_{sn}(t_d) \qquad \text{Equation 6-4}$$

where:

t_q = Bus queuing transaction time; (s)

t_d = Bus dwell time; (s)

$t_{sg}(t_d)$ = Gross smart card transaction time corresponding to t_d; (s)

$t_{sn}(t_d)$ = Net smart card transaction time corresponding to t_d; (s)

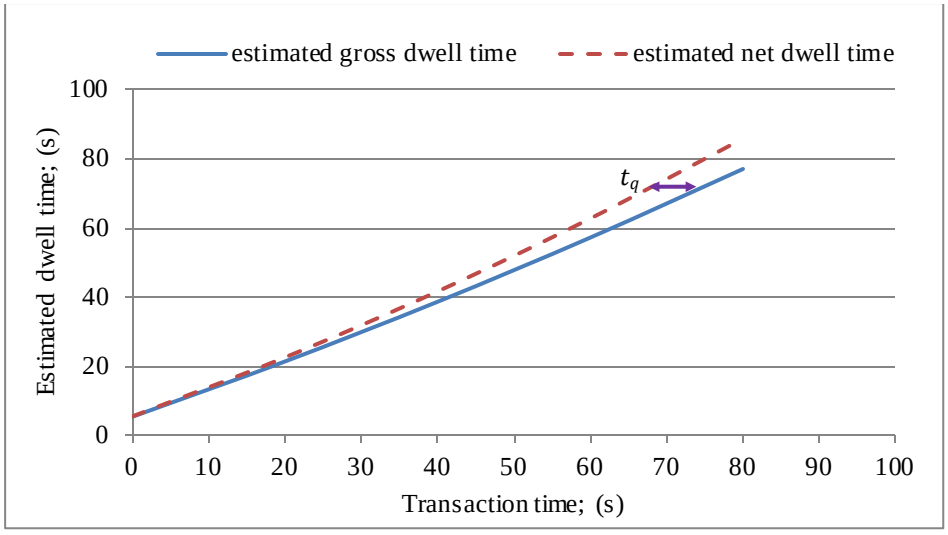

Figure 6-13: Estimated dwell time vs transaction time for Gross and Net Dwell Time models, and time in queue component

If the analyst wishes to estimate dwell times given transaction times under the conditions calibrated here for a peak hour at Buranda station, the gross model of Equation 6-1 with Table 6-2 constants is appropriate. Equation 6-4 can then be used to estimate the effect of bus time in queue (with in geo-fence), which may be useful for other purposes.

The ideal model should enable the analyst to estimate dwell times given transaction times where there is no bus queuing. The net model of Equation 6-1 with Table 6-3 constants is best to use here. We have established that for Buranda station, Equation 6-1 with Table 6-3 constants is an appropriate model under conditions without bus queuing, such as off peak hours.

6.9 Conclusion

This chapter demonstrated that smart card transaction data can be used to effectively estimate dwell time at a busway station. The Gross Dwell Time Model developed in this research for peak hour conditions can provide for a particular bus a reasonable estimate of its actual dwell time when the gross transaction time is known. Across all buses during the peak time period, this model can provide a strong estimate of the distribution of actual dwell times greater than 10 s from all measured transaction times. For dwell times less than 10 s the model is limited by its minimum average dwell time. Particularly pertinent to transit capacity and quality of service analysis, the model can provide precise estimates of average dwell time and

coefficient of variation of dwell time. The applicability of the Gross Dwell Time Model was examined for off-peak hours. Results showed the Gross Dwell Time Model can provide good estimates of actual off-peak dwell times.

The Net Dwell Time Model proposed in this chapter provides a more precise model to estimate the dwell time distribution from available smart card transaction data when situations where buses arriving in queue during the peak hour are excluded. Further, use of the Gross Dwell Time Model and Net Dwell Time Model together can enable bus time in queue to be estimated, which provides useful additional operational information.

Off-peak conditions were also studied in order to validate the Net Dwell Time Model. Although the net peak model does not estimate off-peak average dwell time or coefficient of variation of dwell time identically, its estimates are within five present of the measured values, and the model is validated by statistical inference. Moreover, the Net Dwell Time Model was further validated by using afternoon off-peak transactions. The Net Dwell Time Model can provide good estimates of actual dwell time for both peak and off-peak conditions.

Chapter 7: A Microscopic Simulation Modelling of Busway Station Bus Capacity

7.1 Overview

The aim of this chapter is to present the development of a microscopic simulation model of Buranda station on Brisbane's South East Busway (SEB) in order to understand busway station operation with stopping and non-stopping buses, and queue formation upstream of the station. This fulfils research objectives 4, 5 and 6 identified in Chapter 1.

This chapter first describes the microscopic simulation approach used in this research to model a busway station. Section 7.3 presents the methodological approach of this chapter. Simulation model development is explained in section 7.4. Section 7.5 presents the simulation model tuning with deterministic busway station capacity model. Thereafter two simulation models are developed;

1. All buses stopping (All-Stopping Buses, or ASB) at station
2. Some buses not stopping (Mixed-Stopping Buses, or MSB) at station

Section 7.6 and Section 7.7 present the estimation of potential capacity and average upstream queue respectively, under ASB operation. Subsequently, Section 7.8 and Section 7.9 present the estimation of potential capacity and average upstream queue respectively, under MSB operation. This is followed by chapter conclusion.

7.2 Busway Station Microscopic Simulation Modelling Approach and Definitions

Traffic simulation can efficiently represent a real world situation and reproduce its behaviour under a controlled environment and hence has widespread use in developing and testing scenarios (Fernández, 2010). The model proposed in this research is based on simulation, where for realistic representation of the network and reproduction of the network behaviour, the parameters of the simulation model are tuned with the real data collected via field survey and compared against standard

values given in the TCQSM (TRB, 2013). A detailed description of field survey procedures was given in Section 3.5.

A base scenario where all buses pass through the subject station stop to serve passenger exchange was defined as ASB operation. However, of the buses that pass through the study busway station of Buranda, some stop to serve passenger exchange, while others do not due to express operation. Therefore, we defined a second scenario for simulation model development defined above as MSB operation.

Maximum potential capacity achievable under ASB operation is defined as ASB potential capacity and maximum capacity under MSB operation defined as MSB potential capacity.

7.3 Methodological Approach

The methodology of this chapter is shown in Figure 7-1. The chapter consists of three specific sections. The first section (light green dotted line in Figure 7-1) develops a microscopic simulation model of the study station. Field surveys were conducted to identify capacity related measures that are relevant to microscopic simulation model development. The simulation model is tuned against the deterministic capacity model of the TCQSM (2013) assuming the case of constant dwell time, whereby coefficient of variation (c_v) of dwell times is equal to zero.

During the second phase, the ASB potential capacity from microscopic simulation model is compared with TCQSM theory for different coefficients of dwell time (0.4, 0.5 and 0.6). Again, additional relevant parameters were collected using field surveys. Then ASB potential capacity model is used to estimate ASB potential capacity and average time spent in the system by incorporating average upstream queue length of the system.

The third section (purple dotted line in Figure 7-1) is focused on developing the empirical equation on estimating MSB potential capacity model by including some non-stopping buses. Finally, average time spent in the system by incorporating average upstream queue length of the system under MSB operation is simulated.

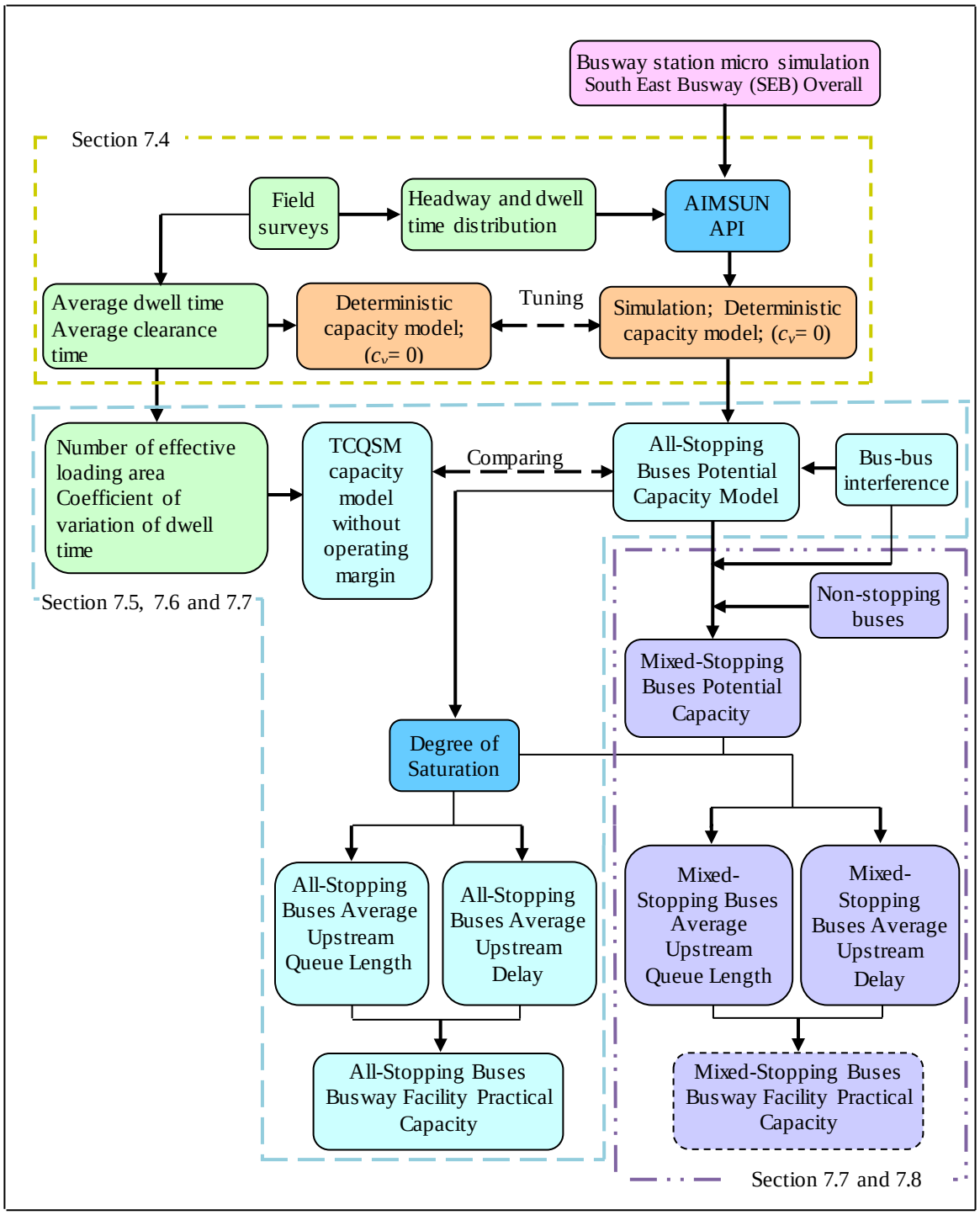

Figure 7-1: Microscopic simulation model development framework

7.4 Busway Station Simulation Model Development

Busway station microscopic simulation model development was carried out by first selecting a study busway station, then introducing variation in input parameters, and finally extraction of data that enabled estimation of capacity and average upstream queue length.

7.4.1 Selection of Busway Station

For this study we selected Buranda station as was justified in Chapter 4. Relevant data required for development of the microscopic simulation model was obtained using field surveys (refer Section 3.4).

7.4.2 Parameters Input and Model Development

A microscopic busway simulation model was developed using AIMSUN 6.1.6, which is a proprietary traffic microscopic simulation platform (TSS, 2010). The test bed station has three linear off line loading areas reflective of Buranda station (Figure 7-2). The simulated buses follow a car-following model, and during the bus merging manoeuvre, AIMSUN applies gap acceptance logic (TSS, 2010).

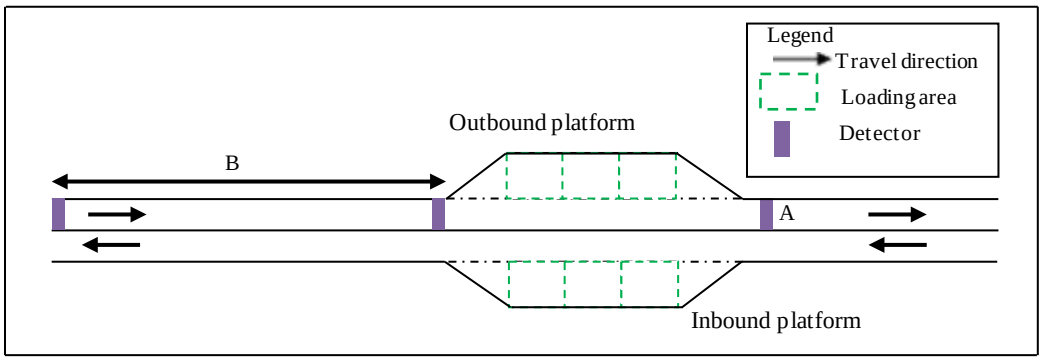

Figure 7-2: Cross section of the busway station model

AIMSUN in its standard manner stochastically generates public transport vehicles (buses) according to a normal distribution defined by mean headway and standard deviation of headway.

Figure 7-3 shows the headway distributions measured during field surveys at Buranda station during April 2013 and February 2014. These figures indicate that the headway distribution is actually best described using the negative exponential distribution, with a flow rate parameter (λ) varying between 0.045 - 0.055 bus/h.

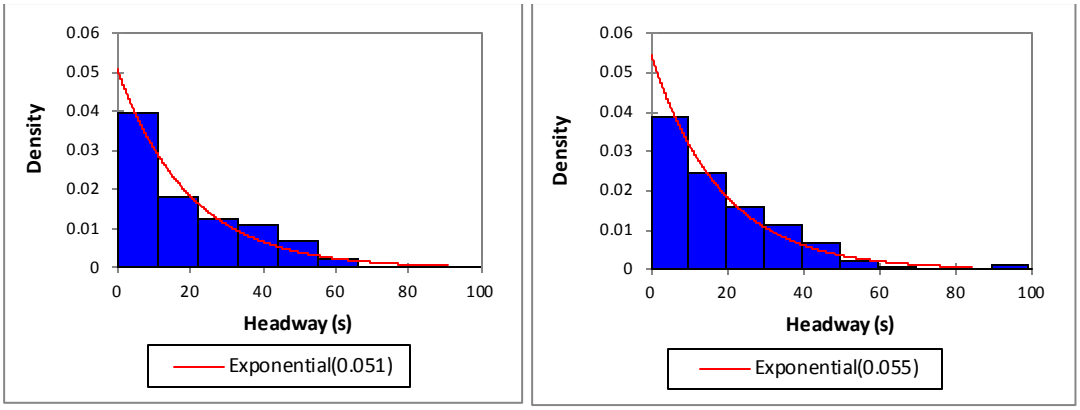

(a) (b)

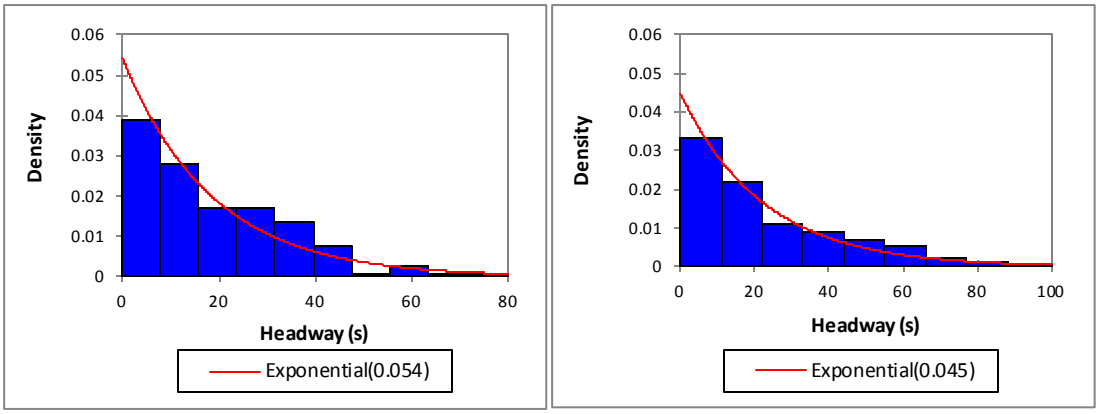

(c) (d)

Figure 7-3: Headway distribution at Buranda on 16/04/2013 (a), 17/04/2013 (b), 18/04/2013 (c) and 19/02/2014 (d)

AIMSUN in its standard manner also stochastically generates dwell time at a stop using a normal distribution. However, as was discussed in Section 5.5, analysis of real data obtained from the Buranda field surveys indicates that bus dwell time follows lognormal distribution.

As a consequence of the observed distributions differing from the AIMSUN assumptions of normal distributions, we elected to use an AIMSUN *Application Programme Interface (*API) to generate bus arrivals onto the test bed according to a negative exponential distribution, and bus dwell times on the loading areas according to a lognormal distribution. Even though dwell time follows a lognormal distribution, we still maintained the required average dwell times and coefficient of variation of dwell times (c_v) during model development phase.

AIMSUN requires estimation of the driver's performance characteristic of reaction time. Summala (2000) identified that driver reaction time varies between 0.75 s and

1.5 s. Therefore the reaction time during vehicle movement was assigned to be 0.75 s and from stationary position was assigned to be 1.35 s.

Simulation was performed using a simulation time step of 0.15 s to ensure accurate discretization of each driver's behaviour (TSS, 2010), therefore reaction time during vehicle movement equals five time steps while that from a stationary position equals nine time steps. For this study a basic system of operation was prescribed in order to develop fundamental empirical relationships.

7.4.3 Capacity and Average Queue Length Estimation

Potential capacity of buses was measured as outflow from the test bed just downstream of the station platform merging taper (detector marked as A - Figure 7-2). Queue length just upstream of the platform (see section B - Figure 7-2) was measured using two upstream detectors. The upstream section was extended 13 km to avoid any virtual queue being created beyond the test bed.

7.5 Simulation Model and Deterministic Model with No Dwell Time Variation

The potential capacity of a busway station, presuming no variation in dwell time, can be quantified deterministically according to Equation 7-1:

$$B = \frac{3{,}600}{(t_d + t_c)} N \qquad \text{Equation 7-1}$$

where:

B = Design bus capacity (bus/h)

t_d = Average bus dwell time

t_c = Average clearance time

N = Number of loading areas, equal to 3 in the case of Buranda

Equation 7-1 is a simplified form of the TCQSM (2013) capacity equation, where an empirical term for number of effective loading areas is replaced by the actual number of loading areas. Widanapathiranage, et al., (2014) argued that the number of effective loading areas, which is ordinarily less than the actual number of loading areas, implies effects of variation in dwell time that leads to asynchronous operation

of buses between loading area/s, and therefore less efficiency of the front loading areas due to intermittent blockages by buses dwelling on the rear loading area/s.

Table 7-1 shows the experiment scenarios considered in this chapter. Scenario 1 in Table 7-1 displays the details of the simulation model development with zero coefficient of variation of dwell time. All scenarios were performed with 100 replications each of one hour duration.

Table 7-1: Description simulation model development scenarios

Simulation model developed	Experimental Values			average dwell time
	c_v	NS (%)	DoS	
1) All-Stopping Buses Deterministic Capacity	0	0	1.0	5 s, 10 s, 15 s, 20 s, 30 s, 45 s, 60 s, 90 s
2) All-Stopping Buses Potential Capacity	0.4, 0.5, 0.6	0	1.0	5 s, 10 s, 15 s, 20 s, 30 s, 45 s, 60 s, 90 s
3) All-Stopping Buses Average Upstream Queue Length	0.5	0	0.0-1.0	10 s, 15 s, 20 s, 30 s, 45 s, 60 s,
4) Mixed-Stopping Buses Potential Capacity	0.4, 0.5, 0.6	10, 20, 30, 40	1.0	10 s, 15 s, 20 s, 30 s, 45 s, 60 s,
5) Mixed-Stopping Buses Average Upstream Queue Length (To be developed in future research)	0.5	10, 20, 30, 40	0.0-1.0	10 s, 15 s, 20 s, 30 s, 45 s, 60 s,

note: c_v: coefficient of variation of dwell time
NS%:non-stopping bus percentage
DoS: Degree of saturation

Figure 7-4 illustrates the results of simulation by way of measured ASB potential capacity, as dwell time ranges between 5 s and 90 s (scenario 1: Table 7-1).

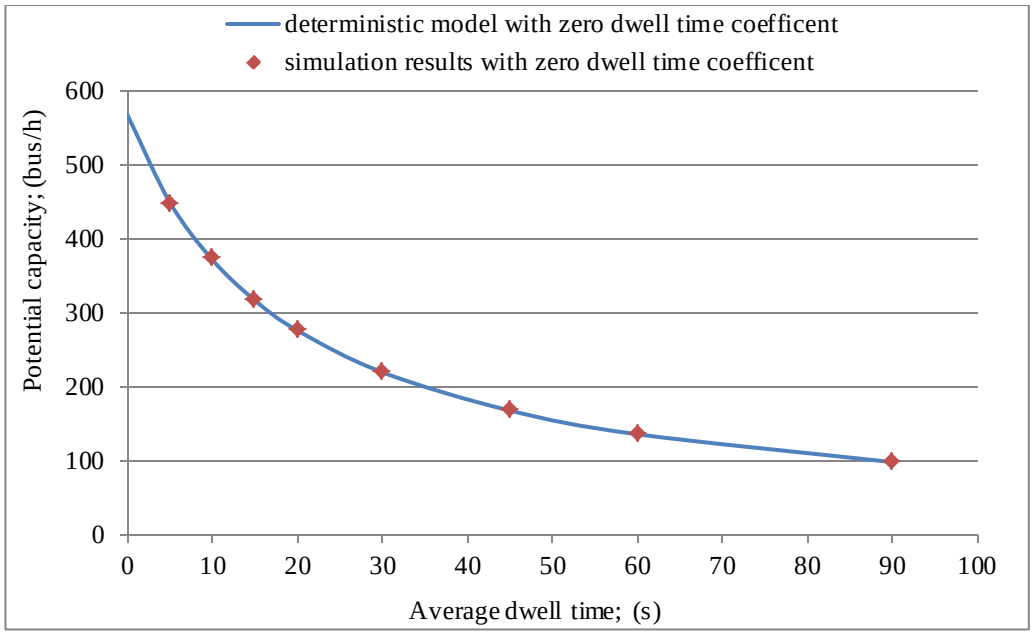

note: dwell time coefficient represents the coefficient of variation of dwell time

Figure 7-4: Bus station ASB potential capacity with no variation in dwell time, as dwell time varies

Figure 7-4 shows that the simulation provides identical results to the deterministic model of Equation 7-1. The coefficient of determination between the simulated data against the deterministic equation is equal to 0.99, which is a near perfect fit. These results are as expected and verify that the simulation model accurately models the most basic mode of operation of Scenario 1.

7.6 All-Stopping Buses (ASB) Potential Capacity Model Development

Busway station All-Stopping Buses (ASB) potential capacity $B_{asb|p}$ (bus/h) is defined here as the average maximum potential outflow of buses from the station area. This marks the region of the queue versus degree of saturation relationship where the queue length becomes unstable. Stable conditions occur when inflow to the station is less than the achievable outflow, conversely unstable condition occurs when the inflow to the station equals or exceeds the achievable outflow such that a queue of buses immediately upstream of the station area perpetuates.

The simulation model was used to model conditions of perpetual upstream bus queuing and therefore unstable conditions to empirically estimate $B_{asb|p}$ for a range of experiments mentioned in Table 7-1 under scenario 2.

In all cases, all buses stopped on the off-line linear platform lane of the test bed using one of three loading areas, such that there were no through buses in the passing lane. Average dwell time and coefficient of variation of dwell time were assigned as constants across all three loading areas (scenario 2: Table 7-1).

The smallest average dwell time simulated was 5 s, which may be just enough time for a bus to pull up, open and close its doors and depart. Although improbable on a real busway station, this value was used in order to estimate the highest feasible potential capacity. The largest average dwell time simulated was 90 s. In all field observations at Buranda station no dwell times of this size were observed (refer Figure 5-3). However, it was considered necessary to simulate this value to establish the lower magnitude of potential capacity under adverse conditions.

For each average dwell time, three values of coefficient of variation of dwell time were simulated; 0.4, 0.5 and 0.6. TCQSM specifies values in the absence of field data the upper value for on street bus operations and the lower value for light rail operations (TRB, 2013). Data collected on the outbound platform at Buranda station on April 2013 and February 2014 revealed a coefficient of variation of dwell time varying between 0.45 and 0.60 (Section 5.5). Figure 7-5 illustrates icons showing the $B_{asb|p}$ values determined from simulation across the ranges of average dwell time and coefficient of variation of dwell time. We excluded the operating margin in TCQSM capacity method in order to find the potential capacity and compare the potential capacity from simulation model (Figure 7-5).

As expected, ASB potential capacity decreases within creasing dwell time. It also decreases very marginally with increasing coefficient of variation of dwell time, which is attributed to the asynchronous conditions generated between buses as their dwell times vary. Capacities differ only marginally, as coefficient of variation of dwell time varies, with increasing average dwell time.

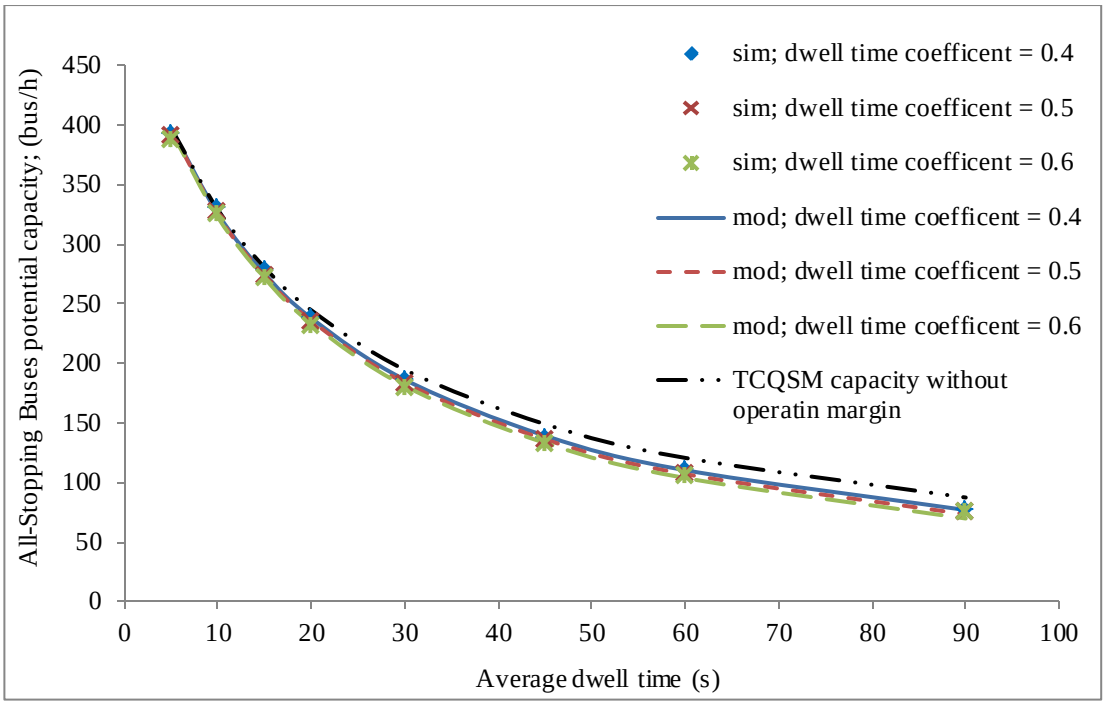

note: dwell time coefficient represents the coefficient of variation of dwell time

Figure 7-5: Busway station All-Stopping Buses potential capacity versus average dwell time with coefficient of variation of dwell time

Busway station capacity can be estimated using Equation 7-2 when dwell time is variable. The original TCQSM equation includes an operating margin term in the denominator; however, this term is excluded here because that parameter is intended as a buffer added to the original equation for purposes of determining a design capacity, rather than the maximum potential value.

$$B = \frac{3{,}600}{(t_d + t_c)} N_{EL} \qquad \text{Equation 7-2}$$

where:

B = Design bus capacity (bus/h)

t_d = Average bus dwell time on a loading area (s)

t_c = Average clearance time between buses using a loading area(s)

N_{EL} = Empirical factor reflecting number of effective loading areas

The off-line loading area efficiency factors given in the TCQSM and factors used to determine N_{EL} are based on observed experience at facilities in New York and New Jersey (TRB, 2013). The value of N_{EL} prescribed for a three loading area, off-line busway station in the TCQSM is 2.65. Figure 7-5 illustrates for this value the ASB potential bus capacity calculated using Equation 7-2 as a function of dwell time. The

TCQSM equation closely follows the simulation data results. However, slightly lower capacities result according to the simulation model, which is attributed to pronounced variation in dwell time.

An enhancement to Equation 7-1 to incorporate dwell time variation, as evident from simulation icons in Figure 7-5, was sought. The empirical equation determined in this study that best estimates potential capacity is given by:

$$B_{asb|p} = \frac{3{,}600}{(t_d + t_c)} N_{la} f_{bbi} \qquad \text{Equation 7-3}$$

where:

$B_{asb|p}$ = All-stopping-buses potential capacity (bus/h)

t_d = Average bus dwell time on a loading area (s)

t_c = Average clearance time between buses using a loading area(s)

N_{la} = Actual number of loading areas on platform, equal to 3 for study station

f_{bbi} = Empirical capacity reduction factor due to bus-bus interference within station area

Equation 7-3 was fitted with R^2 equal to 0.99. Comparison of Equation 7-2 and Equation 7-3 shows that the effect of variation in dwell time on potential capacity is more explicit by including a bus-bus interference factor than by presumed overall loading area effectiveness.

Subsequently, the simulation data were scrutinized to establish a model to estimate bus-bus interference factor (f_{bbi}) as a function of average dwell time (t_d) and coefficient of variation of dwell time (c_v). The best empirical equation was found to be of the following form; its coefficients determined with the average loading area bus clearance time t_c using ordinary least squares regression optimization:

$$f_{bbi} = 0.90 - 0.004\, c_v t_d \qquad \text{Equation 7-4}$$

where:

c_v = Coefficient of variation of dwell time (0.4, 0.5, 0.6)

t_d = Average bus dwell time (s) ($5 \text{ s} \leq t_d \leq 90 \text{ s}$)

As shown in Figure 7-6, f_{bbi} and therefore loading area efficiency decreases when either coefficient of variation of dwell time or average dwell time increases. This is intuitively reasonable because higher average dwell times relative to clearance times

should result in more blockages to the front and middle loading areas. However, more field data acquisition to measure f_{bbi} values is required to substantiate this position.

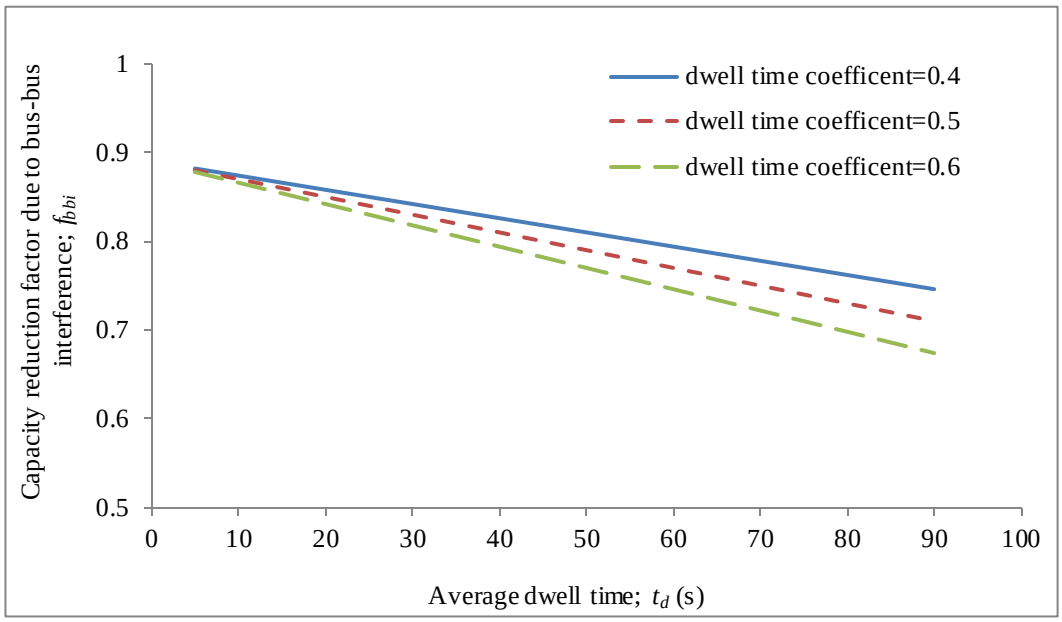

note: dwell time coefficient represents the coefficient of variation of dwell time

Figure 7-6: Bus-Bus interference factor vs. average dwell time and coefficient of variation of dwell time

The value of N_{EL} in Equation 7-2 equal to 2.65 under the conditions of this study implies a value of bus-bus interference factor (f_{bbi}) equal to 0.88. This value lies in the range of the refined empirical Equation 7-3.

The average clearance time determined from simulation model observations was 19 s, which corresponds to the observed values at the study station and lies within TCQSM's observed range of between 10 s and 20 s (TRB, 2013). Figure 7-5 also illustrates the use of Equation 7-3 and Equation 7-4 to estimate ASB potential capacity across the simulated ranges of average dwell time and coefficient of variation of dwell time listed above. The equations provide a very close fit with a Root Mean Square (RMS) error in potential capacity of between 2 and 3 bus/h, across the range of coefficient of variation of dwell time.

Equation 7-3 was developed using average dwell times of 5, 10, 15, 20, 30, 45, 60 and 90 s. The equation was tested further by comparing it with data obtained from simulations using 25, 50 and 75 s average dwell times and concluded that these values fit well with R^2 equal to 0.99 as presented in Figure 7-7.

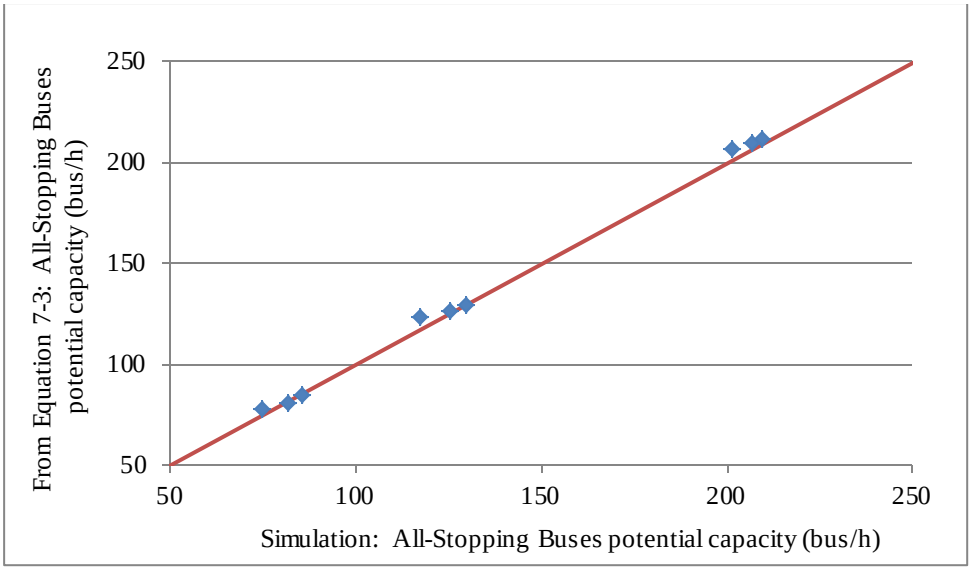

Figure 7-7: All-Stopping Buses potential capacity; simulation versus empirical equation

7.6.1 Parametric Considerations

The largest ASB potential capacity from Equation 7-3 and Equation 7-4 is 512 bus/h, which corresponds to a zero average dwell time, 19 s average clearance time and 0.9 bus-bus interference capacity reduction factor. In this case all buses come to a stop on a loading area and depart immediately. Despite this case being unrealistic, it is an important limiting parameter of the empirical equations.

Equation 7-3 and Equation 7-4 are asymptotic towards an ABS potential capacity of zero as average dwell time becomes very large, beyond the realm of the system. For the largest average dwell times of 90 s to which the equation was fitted, the potential capacity is very small, varying between 111 bus/h and 106 bus/h as coefficient of variation of dwell time varies between 0.4 and 0.6. In this case with each of the three loading areas occupied by successive buses each for an average of 90 s, the potential outflow is substantially less than the 137 bus/h which would be the case if these three loading areas were located in parallel with no bus-bus interference. Potential outflow with three parallel loading areas is calculated when the number of effective loading area becomes three, with 19 s clearance time and 60 s dwell time by using Equation 7-2.

7.7 Busway Station Queuing for All-Stopping Busway Operation

In this study we contend that busway station operation can be better understood through applying some features of traffic queuing theory. Specifically, the station is

analogous to a multi-channel server system, where each of the multiple off-line loading areas along the platform represents a server. These servers are only partially in parallel, as bus-bus interference prevents each of the loading areas from operating completely independently. Microscopic traffic simulation is ideal to model this bus-bus interference phenomenon.

7.7.1 An Improved Station Bus Queuing Theory

The TCQSM deterministic equation to estimate busway station bus service capacity considers that acceptable operation corresponds to a common desired failure rate for each loading area, which is equal to the probability of a bus in queue waiting for access to the loading area while another bus is dwelling (TRB, 2013). This implies that buses queue vertically on each loading area, such that loading area queues do not interfere with each other.

While we maintain that queuing as the best measure of acceptability of station operation, we contend that for a multiple loading area station an improved theory that reflects horizontal queuing is necessary, because it is undesirable for bus queues to extend back from the platform lane into the through lane on the mainline immediately upstream of the station. This may lead to adverse queue interaction with upstream control elements such as intersections, queue spillback to higher speed operating elements presenting a safety concern, and/or inconvenient delay to passengers who are on-board buses waiting for access to the station area.

The simulation model was used to model near steady state conditions under various bus inflow rates, B_{in}, between zero and potential capacity, for ranges of average dwell time and coefficient of variation of dwell time. Relationships could then be developed between upstream average bus queue length(Q_{av}), and station bus degree of saturation (X_{in}). The degree of saturation is equal to;

$$X_{in} = \frac{B_{in}}{B_{asb|p}} \qquad \text{Equation 7-5}$$

The average queue length was obtained from the simulation model for a given degree of saturation according to its corresponding inflow. The simulation model was developed according to the range and limitations mentioned in scenario 3 (Table 7-1).

Figure 7-8 shows for a 10 s average dwell time, the variation in upstream average queue length with coefficient of variation of dwell time between 0.4, 0.5, and 0.6. It is evident that this variation has very effect on upstream average queue. This is consistent with findings above regarding the effect of coefficient of variation of dwell time on potential capacity. Consequently, for subsequent investigation a coefficient of variation of dwell time of 0.5, which is consistent with survey results, was used.

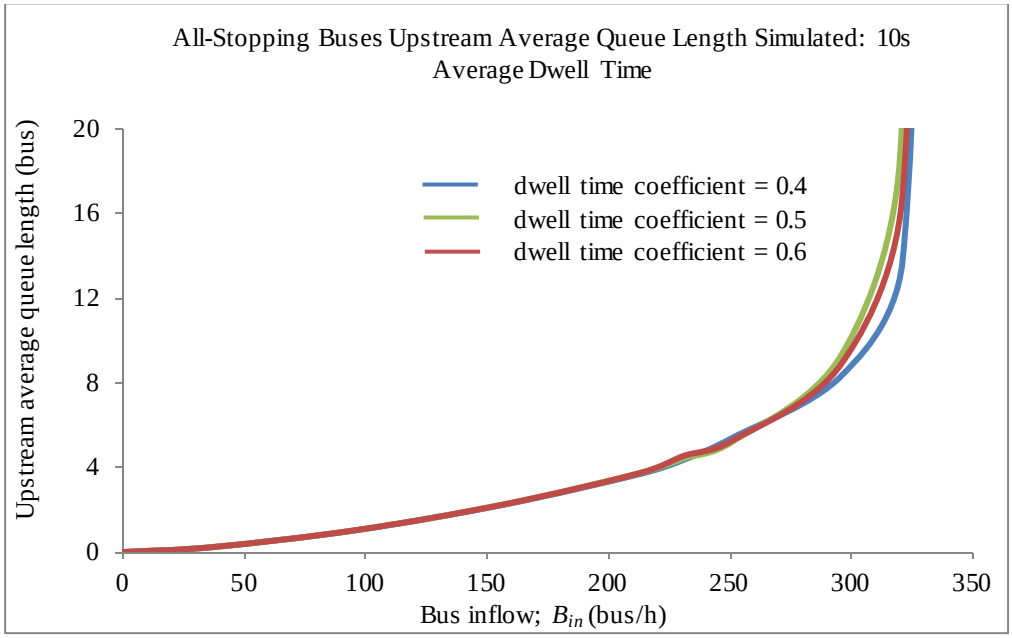

note: dwell time coefficient represents the coefficient of variation of dwell time

Figure 7-8: Upstream average bus queue length versus bus inflow under 10 s average dwell time and coefficient of variation of dwell time as 0.4, 0.5 and 0.6

Figure 7-9 illustrates an example of variation in upstream average queue length with the degree of saturation, for an experiment with loading area average dwell time of 10 s and coefficient of variation of dwell as 0.5.

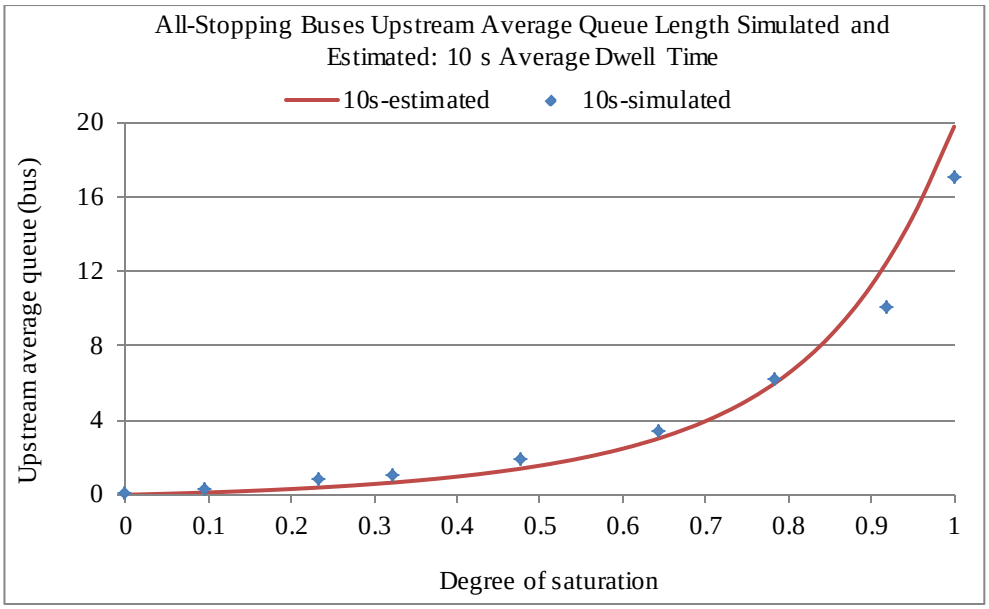

Figure 7-9: Busway station upstream average bus queue length versus degree of saturation

In order to quantify the average queue length of buses in the system, the platform area was regarded as a server, with a single queuing channel representing the upstream mainline through lane. It can be demonstrated that in such a system, average queue is equal to the product of the average time spent in the system and the arrival flow rate, according to:

$$Q_{av} = st_{av}\left(\frac{B_{in}}{3600}\right) \qquad \text{Equation 7-6}$$

where:

Q_{av} = Upstream average queue length (bus)

st_{av} = Average time spent in the system (s)

B_{in} = Bus inflow (bus/h)

In order to quantify the average time spent in the system, the system was considered to be analogous to an unsignalized intersection movement with respect to queuing. The Highway Capacity Manual's (TRB, 2000) estimating equation for average delay to such a movement was investigated for applicability using the simulation results. The empirical equation was modified as follows to reflect that multiple interfering channels are present within the server itself.

$$st_{av} = \frac{3600}{B_{asb|p}} + 900\,T\left((X_{in}-1)^2 + \sqrt{(X_{in}-1)^2 + \frac{(N_{LA}f_{bbi})^2 X_{in}}{150\,T}}\right)$$

Equation 7-7

where:

st_{av} = Average time spent in the system (s)

$B_{asb|p}$ = Potential capacity (bus/h)

X_{in} = Degree of saturation (demand/capacity)

N_{LA} = Number of loading areas (in this case 3 loading areas)

f_{bbi} = Bus-bus interference factor

T = System time, equal to 1h (3600s)

900 and 150 are empirical constants

It is important to note that Equation 7-7 does not quantify average bus delay. The first term in Equation 7-7 represents the average service time of the platform area as a combined server, and hence it is the inverse of its potential capacity. Average bus delay can be quantified by multiplying the first term in Equation 7-7 by the number of loading areas and adding that value to the second term.

Figure 7-9 illustrates the application of Equation 7-6 and Equation 7-7 for a particular case where simulation results fit the empirical equation very closely with R^2 equal to 0.98.

Figure 7-10 shows the upstream average queue length and bus inflow variation with average dwell time for simulation results and for mathematical model developed in Equation 7-6 and Equation 7-7. Simulated points here are the average of multiple simulations performed for 100 hours. For an instance, 10-est represents the estimated average upstream queue length from Equation 7-6 and Equation 7-7 while 10-sim represents simulated average upstream queue length.

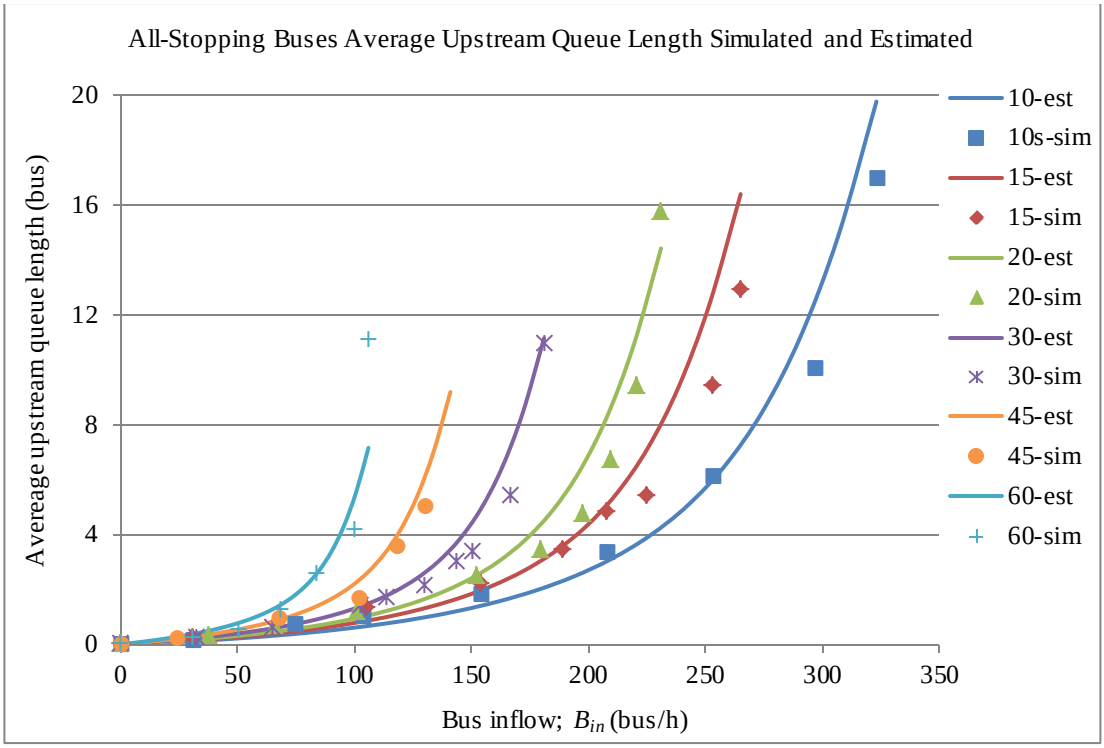

Figure 7-10: Upstream average queue length and bus inflow variation with average dwell time

The data pattern from the example of Figure 7-9, Figure 7-10 and form of Equation 7-6 are familiar to queuing systems as the Highway Capacity Manual (TRB, 2000) describes for unsignalized intersection queuing. However, it was necessary to check that the form is applicable across the simulated range of operations of the busway station.

Figure 7-11 illustrates a line of equality comparison between each upstream average bus queue length estimated using Equation 7-6 and the simulated value. In order to ensure stable model fitting queue lengths corresponding to the extremely volatile range of degree of saturation exceeding 0.96 were excluded. Icons above the line indicate that Equation 7-6 overestimates simulation average queue length while those below the line indicate that it underestimates.

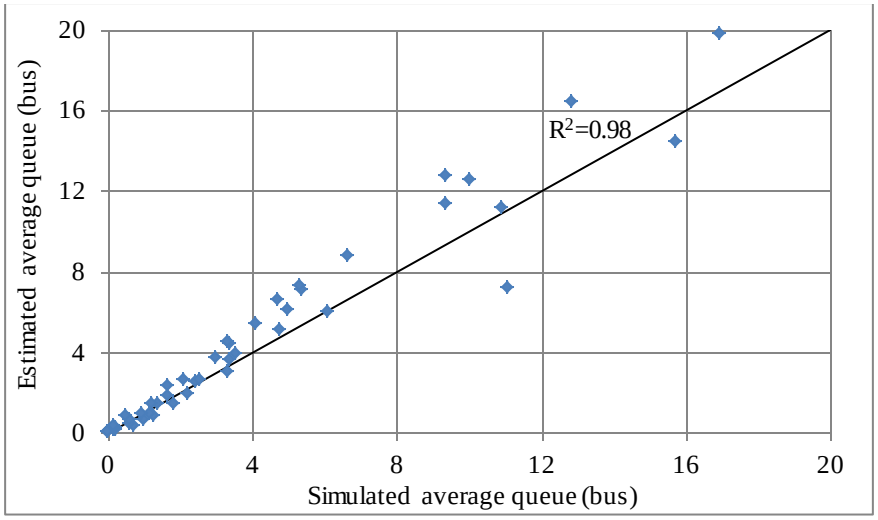

Figure 7-11: Busway station upstream average bus queue length estimated by model versus simulated

Figure 7-11 demonstrates that the Equation 7-6 model provides a good fit to upstream average queue length for queue lengths less than 6 buses, but does tend to conservatively overestimate queue length. Across all average dwell times, we consider average queue lengths of 6 buses or more to be excessive because they correspond to a volatile range of degree of saturation in excess of 0.95. The model is less accurate in estimating such queue lengths, because very small change in degree of saturation results in extremely large change in average queue length.

7.7.2 All-Stopping Buses Busway Facility Practical Capacity

Definition of a practical capacity under ASB operation with respect to degree of saturation, average upstream queue length and bus inflow can assist in the maintenance of reliable busway facility operation. Figure 7-12 presents the upstream average queue length variation according to Equation 7-6 and Equation 7-7, identifying three regions of operation.

For degree of saturation less than 0.6, average queue length varies between 0 and 2.5 buses. In this serene region, average queue length increases gradually with increase in the degree of saturation.

The second, more sensitive region lies between degrees of saturation of 0.6 and 0.8, where the rate of increase in average queue length is more sensitive to degree of saturation. Average queue length doubles across this region as degree of saturation increases by 20 percent, becoming more difficult to maintain reliable operation.

The third, highly volatile region includes degrees of saturation beyond 0.8. Average upstream queue can increase drastically with only incremental rise in degree of saturation. Operation in this region will be very unreliable and should be avoided.

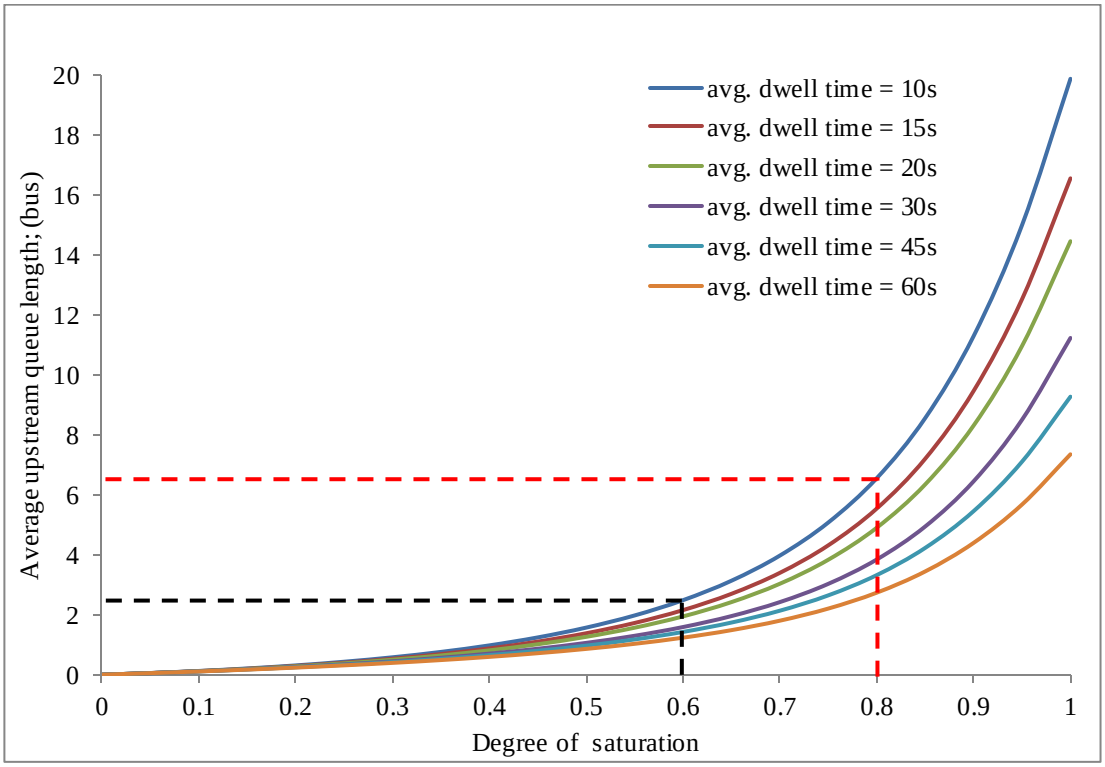

Figure 7-12: Average upstream queue length variation with degree of saturation estimated by using Equation 7-7 and Equation 7-8

This study recommends a practical degree of saturation of 0.8 corresponding to the boundary between the sensitive and highly volatile regions. This value is consistent with the unsignalised intersection practical degree of saturation (TRB, 2000).

Table 7-2 gives the design practical capacity and average bus queue upstream of the platform, for an off-line busway station platform with three loading areas, across the realistic range of average dwell time. It is recognised that the model proposed here will need to be further validated for different busway station configurations and different bus movement patterns.

Table 7-2: Test bed busway station practical capacity

Average dwell time (s)	Degree of Saturation = 1.0	Degree of Saturation = 0.8	
	ASB potential capacity (bus/h)	ASB facility practical capacity (bus/h)	Average upstream queue (bus)
10	328	262	6.5
15	276	221	5.5
20	238	190	4.9
30	185	148	3.8
45	139	111	3.3
60	106	85	2.7

7.8 Mixed-Stopping Bus Potential Capacity

As described earlier (Section 7.2), stations on busway lines may operate with a mixture of stopping and non-stopping buses. Mixed-Stopping Buses (MSB) potential capacity ($B_{msb|p}$), will be greater than ABS potential capacity under this operation. However, the TCQSM model of Equation 7-2 does not explicitly account for such operation. The analyst would need to apply the shared lane general traffic adjustment factor in the TCQSM methodology to attempt to account for non-stopping buses. No other methodology to explicitly account for non-stopping buses on busway facilities is evident in the literature.

In order to fill this knowledge gap in busway capacity estimation, this research enhanced the simulation model described above to incorporate non-stopping buses through the station to accurately estimate MSB potential capacity. Proportions of non-stopping buses equal to 0.1, 0.2, 0.3, and 0.4 were applied in this research (scenario 4: Table 7-1). It would be considered unusual for 50% (0.5) or more of all buses past a critical busway station to be either scheduled so as not to observe it, or not to receive stopping requests or flag-falls during a peak period. For reference, the proportion of non-stopping buses past Buranda station during the peak periods was measured to be 0.3.

As with the ASB simulation model, a range of average dwell time between 10 s and 60s was simulated, along with coefficient of variation of dwell times of 0.4, 0.5 and

0.6. Figure 7-13 illustrates the MSB potential capacity versus average dwell time for different proportions of non-stopping buses with 0.4 coefficient of variation of dwell time. For an instance, 10% (mod) indicates the MSB potential capacity from Equation 7-8 model and 10% (sim) indicates the MSB potential capacity from simulation model for 10% of non-stopping buses.

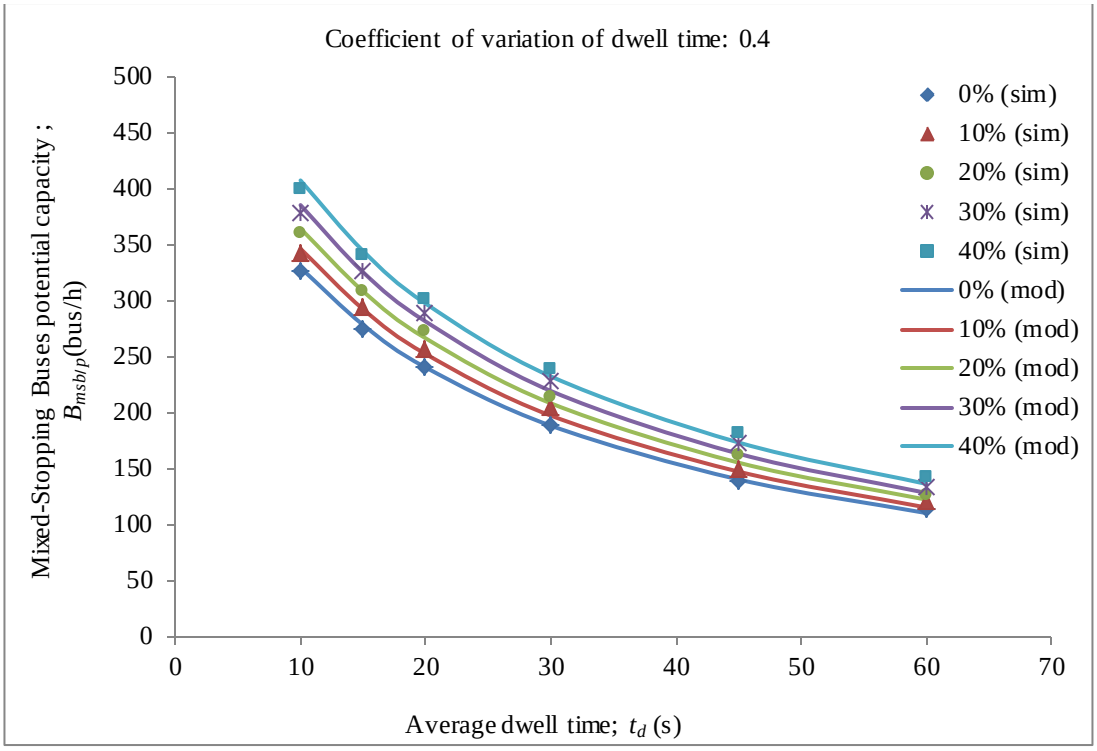

Figure 7-13: Busway station Mixed-Stopping Buses potential capacity versus average dwell time with 0.4 coefficient of variation of dwell time

The best model determined to estimate MSB potential capacity across the ranges of average dwell time, coefficient of variation of dwell time, and proportion of non-stopping buses was found to be:

$$B_{msb|p} = \frac{B_{asb|p}}{(1 - 0.48P_{nsb})} \qquad \text{Equation 7-8}$$

where:

$B_{asb|p}$ = ASB Buses potential capacity (bus/h)

P_{nsb} = Proportion of non-stopping buses

This model was fitted using Ordinary Least Squares regression with R^2 equal to 0.98. From Equation 7-8, under conditions with a mixture of stopping and non-stopping buses, the station's potential capacity of stopping buses is equal to:

$$B_{sb|p} = \frac{B_{asb|p}(1 - P_{nsb})}{(1 - 0.48P_{nsb})}$$ Equation 7-9

where:

$B_{sb|p}$ = Stopping Buses (SB) potential capacity under MSB operation (bus/h)

The presence of non-stopping buses therefore impedes the station's potential capacity for stopping buses by approximately 0.65 times the proportion of non-stopping buses.

From Equation 7-8, under conditions with a mixture of stopping and non-stopping buses, the station's potential capacity of non-stopping buses is equal to:

$$B_{nsb|p} = \frac{B_{asb|p}P_{nsb}}{(1 - 0.48P_{nsb})}$$ Equation 7-10

where:

$B_{nsb|p}$ = Non-stopping Buses (NSB) potential capacity under MSB operation (bus/h)

Figure 7-14 illustrates the variation in potential capacities based on Equation 7-8, Equation 7-9 and Equation 7-10 as proportion of non-stopping buses varies between 0 and 0.4, with a reference ASB potential capacity equal to 100 bus/h. It can be seen that despite a reduction in stopping bus capacity with increasing proportion of non-stopping buses, the MSB total capacity increases moderately.

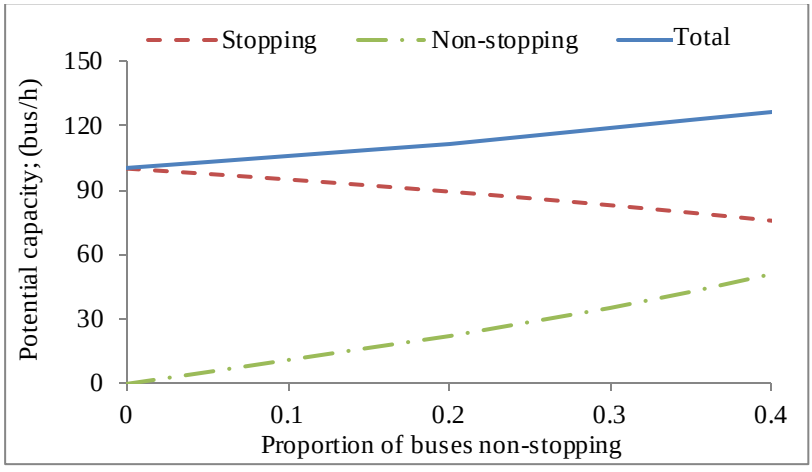

Figure 7-14: Mixed-Stopping Buses (MSB) capacity variation with non-stopping buses

7.9 Busway Station Upstream Queuing under Mixed-Stopping Buses Operation

For estimation of average upstream queue and delay we again used different non-stopping percentages as in Section 7.8. As an example, Figure 7-15 shows the Mixed-Stopping inflow variation versus average upstream queue length for 30 s average dwell time and 0.5 coefficient of variation of dwell time with different non-stopping percentage. Again multiple simulations were performed for 100 hours as per scenario 5 in Table 7-1.

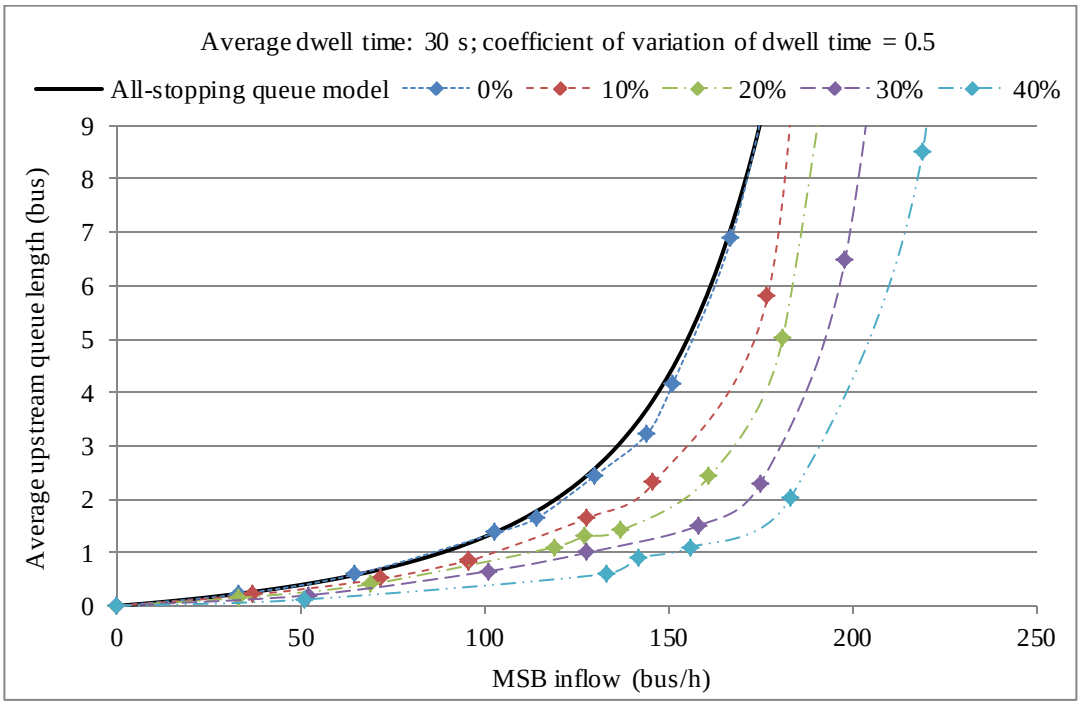

Figure 7-15: Average upstream queue length versus Mixed-Stopping Buses inflow

As expected, average queue length decreases with increasing non-stopping percentages. Further refinement is required with different average dwell times in order to develop an empirical equation to estimate average upstream queue length under MSB conditions.

7.10 Conclusion

This chapter demonstrated that microscopic simulation model can be used to study and analyse the operating characteristics of busway stations to determine potential capacity. A mathematical equation was proposed to estimate All-Stopping Bus (ASB) potential capacity using empirical data from simulation and found to

complement theory of the TCQSM (TRB, 2013). The difference between TCQSM and ASB potential capacities is attributed to the effect of bus-bus interference on the loading area efficiency. It is observed that bus-bus interference depends on average dwell time and coefficient of variation of dwell time.

We developed an empirical equation to estimate upstream average queue length with varying inflow using an analogy of traffic queuing similar to the HCM unsignalized intersection model. The equation was calibrated using simulation model output of queue length as bus inflow to the station varies. This is a significant enhancement to the current TCQSM methodology for estimating busway station capacity because it gives the capability to estimate design station capacity not only with respect to demand but also with respect to upstream queue length. The TCQSM methodology implies vertical storage of queues on each loading area, rather than the observed case where queues are stored horizontally on the mainline upstream of the station platform.

Existing theory does not explicitly model conditions when some buses pass through the busway station without stopping. Therefore, a model was proposed to estimate potential capacity under Mixed-Stopping Bus conditions as a function of proportion of non-stopping buses.

Empirical equations for Mixed-Stopping Buses Potential Capacity (MSB) and Non-Stopping Buses Capacity (NSB) were developed. These can be used to better understand facility capacity under various mixtures of stopping and non-stopping buses proportions at stations. This will be helpful to agencies in bus route and schedule planning as well as capacity analysis.

Estimates of both capacity and queuing are needed in traffic engineering analysis of busway facilities, particularly as some systems are now reaching capacity at certain stations and queue interaction between nodes arises to avoid additional delays of passenger travel time.

Chapter 8: Conclusion and Future Directions

8.1 Overview

This chapter summarizes the findings of this research and draws conclusions and future directions. First a summary of how each chapter has achieved the research objectives identified in Chapter 1 is presented. Second, contributions of this research are highlighted. Third, contributions relevant to practice are discussed. Thereafter, the conclusion of this research is presented. Finally, recommendations for future research on this topic are provided.

8.2 Summary of this Thesis

This thesis presented the analysis of busway station operation by using real data analysis and microscopic simulation modelling. A summary of each chapter is presented below in logical sequence.

Chapter 1 established research objectives to fulfil the research aim of "Improving existing methodologies of quantifying busway corridor performance particularly under the conditions unique to the busway system of Brisbane, Australia". Thereafter, the scope of the research was specified.

Chapter 2 provided an extensive literature review to reveal knowledge gaps in busway operation and busway corridor performance estimation to address research goals identified in Chapter 1. Classification of BRT facilities was discussed. Particular context was given with respect to the classification of Brisbane's busway system. This chapter identified that presently no methodology exists to estimate busway facility capacity under conditions where there is a mixture of stopping and non-stopping buses, which is an important operating characteristic of Brisbane's busway. It also identified that there is presently no methodology to empirically estimate a busway facility's practical capacity with respect to bus inflow, queue, and degree of saturation.

Chapter 3 formalised a comprehensive research methodology to study segregated busway operation, in response to the knowledge gaps identified in Chapter 2. In particular, this chapter considered busway station bus operation and identified

various parameters that impact on station capacity. It was identified that during peak hours at some stations, some bus drivers create an ad-hoc loading area (named here as the *temporary* loading area) at the rear of the station platform. This chapter also conceptualised a means of estimating busway station efficiency. In addition, the potential applicability of using smart card transaction data to estimate certain parameters of station operation was considered. Then the use of microscopic traffic simulation modelling of busway operation was addressed. Chapter 3 concluded by describing the process of data collection including ethical clearance requirements.

Chapter 4 discussed the selection of Brisbane's South East Busway (SEB) as the study facility for this research. A detailed investigation of the facility was conducted in order to select the best station for study, considering the overall performance of the strategic elements of SEB such as stations, ramps, intersections, transitway sections, busway stations and so forth. SEB bus movements under peak hour and daily conditions were assessed. Bus route and equipment types were discussed. Considering these aspects together, Chapter 4 concluded by identifying and selecting Buranda station as the case study station for the remainder of this research.

Chapter 5 examined the components that affect station capacity by studying the Buranda station. This chapter considered operational changes that have been imposed at Buranda during this study's research period between 2011 and 2014. A series of surveys were conducted over a three year span. From each survey data, was used to estimate the important operational parameters of dwell time, clearance time and station efficiency. A statistical analysis was conducted utilizing the data, which revealed that average dwell time and average clearance time closely follow a log normal distribution which is important as their variations have an significant impact on busway station capacity. Chapter 5 then introduced a comprehensively improved methodology to estimate station efficiency under conditions when a *temporary* loading area exists.

Chapter 6 presented a novel methodology to estimate bus dwell time on a loading area at a station platform using smart card transaction data. Empirical equations to estimate dwell time were proposed in this chapter, which were calibrated under peak hour conditions and validated under off-peak hour conditions by statistical analysis.

Chapter 7 described the development of a microscopic simulation model of Buranda station in order to understand queue formation upstream of the station, and operation

with a mixture of stopping and non-stopping buses, and. Empirical equations were developed for two modes of operation; when all buses stop at the station (All-Stopping Buses, or ASB), and when some buses pass express through the station (Mixed-Stopping Buses, or MSB). These equations were developed to estimate potential capacity, average bus delay in system, average upstream queue length. Considering the relationships observed between average upstream queue length and degree of saturation, a practical degree of saturation was identified, which enables estimation of a station practical capacity.

8.3 Contributions to the State of the Art

This research provides detailed understanding of SEB operation (Chapter 3) and addresses key knowledge gaps (as identified in Chapter 2) in determining the impact of mixed-stopping and non-stopping bus operation on the practical station capacity of a busway corridor.

The major original contributions of this research are identified below. They have theoretical and practical impact regarding how busways are planned, designed, operated and managed.

1. The average dwell times and average clearance times of buses at loading areas on the platform at the Buranda study station were found to follow a log-normal distribution. This is an important finding because the effect of variability found in dwell time and clearance times has a direct and significant impact on busway station capacity (Chapter 5).

2. This study found that some drivers create a *temporary* loading area at the rear of Buranda station platform during the peak hour, when the three formal loading areas are occupied. Passengers of a bus dwelling on the *temporary* loading area can only alight and board through the front door. We have discovered that the *temporary* loading area can adversely impact station bus capacity by actually reducing the overall combined efficiency across all loading areas. A method introduced here can be applied for any busway station with off-line loading areas and can be further developed for on-street bus stops (Chapter 5). Contributions 1 and 2 satisfy research objective 3.

3. A novel methodology was developed that facilitates the use of smart card transaction data to estimate bus dwell time empirically. The gross dwell time empirical equation proposed here provides reasonable estimation of actual dwell time for a particular bus when the gross transaction time is known. On the other hand, the net dwell time empirical equation also proposed here can more precisely estimate dwell time than gross dwell time estimation method, when the net smart card transaction time is known. In addition, queuing transaction time between the smart card system geo-fence and busway platform can be easily estimated using empirical equations suggested in Chapter 6. This satisfies research objective 4.

4. An empirical equation was developed in Chapter 7 to estimate potential capacity under a basic mode of operation where all buses stop on the platform, called ASB potential capacity, using analysis of microscopic simulation model data output to complement the empirical equation of the TCQSM (TRB, 2013). Rather than estimating loading area efficiency with conventional field survey measurements, a bus-bus interference factor was developed to provide a means of directly estimating impacts on busway station loading area efficiency, satisfying research objective 5.

5. Empirical equations were developed to estimate upstream average queue length and average upstream delay under an ASB mode of operation. A practical degree of saturation was established, which corresponds to an acceptable threshold average queue length. In turn, ASB practical capacity can be determined as the product of ASB potential capacity and practical degree of saturation (Chapter 7). This satisfies research objective 6.

6. Similar to contribution 5, an empirical equation was developed in this research to estimate potential capacity under a MSB mode of operation where some buses pass through the station without stopping, for instance while running express. This condition reflects Brisbane's SEB, thereby fulfilling the knowledge gaps identified regarding this mode of facility operation. The models proposed can be used to better understand busway corridor capacity due to various mixtures of stopping and non-stopping buses (Chapter 7). This should assist responsible agencies in preparing bus route and schedule planning as well as capacity and reliability analysis, satisfying research objective 5.

8.4 Contributions to Practice

Although this research was conducted using the one representive busway station of Buranda, its methodologies can be applied to any stations with multiple off-line loading areas on a busway similar to Brisbane's South East Busway. Considering research contributions mentioned above, practical implications are as follow:

1. A practical degree of saturation of 0.8 should not be exceeded in estimating busway station design capacity under ASB operation. Degree of saturation beyond 0.8 is a highly volatile region as average upstream queue can increase drastically with only incremental rise in degree of saturation. This recommendation is applicable for average dwell times between 10 and 60 seconds and coefficients of variation in dwell time between 0.4 and 0.6, as it is consistent with range observed during field surveys.
2. In order to satisfactorily operate a busway station under ASB operation, average upstream queue length should not exceed 6 buses for an average dwell time of 10 s, down to 3 buses for an average dwell time of 60 s, when coefficient of variation of dwell time ranges between 0.4 and 0.6.

3. Non-stopping buses through stations actually reduce capacity of buses which need to stop at the station to serve passengers, as shown in Table 8-1. If an operator needs to increase capacity for stopping buses at a station under MSB operation, Table 8-1 shows that it is necessary to divert some non-stopping buses. This is an important finding on bus route, busway station and busway facility design under MSB operation.

   Table 8-1: Total, stopping and non-stopping buses capacity variation from Figure 7-14

	Non-stopping percentage (%)				
	0	10	20	30	40
Total bus capacity (bus/h)	100	106	112	119	127
Stopping bus capacity (bus/h)	100	95	90	83	76
Non-stopping bus capacity (bus/h)	0	11	22	36	51

4. Transit agencies should consider restricting drivers from creating a *temporary* loading area at the rear of the busway station platform, as evidence herein (refer Chapter 5; Section 5.5.2) suggests that it reduces busway facility capacity.

8.5 Conclusions

This thesis found that understanding the variables governing the busway station capacity is absolutely essential to fully understand and analyse busway operation. The traditional approach to estimating busway station efficiency and capacity may not be reliable for a busway station with a *temporary* loading area in operation. This is because of *temporary* loading area blocks designated loading areas and ultimately reduces number of effective loading areas. Increasing occupancy of *temporary* loading area reduces number of effective loading areas. Therefore, new equations were proposed in this research to estimate busway station efficiency with *temporary* loading area.

Estimation of dwell time currently requires real field measurements or recommended standard values. This could be costly or may lead to human errors. However, estimating dwell time using fare collection data requires very limited cost. This research developed a robust methodology to estimate average dwell time and coefficient of variation of dwell time, which are necessary for bus capacity analysis.

Prior to this research no method was known to exist that can estimate busway corridor performance measures with a mixture of stopping and non-stopping buses. Therefore, this research developed empirical equations to estimate capacity and average queue calibrated using microscopic simulation modelling. Estimates of both capacity and queuing are needed for traffic engineering analysis of busway facilities, particularly as some systems are now reaching capacity at certain stations and queue interaction between nodes arises to avoid additional delays of passenger travel time.

8.6 Recommendations for Future Work

This research has identified numerous future research directions as follow:

1. Temporary loading area efficiency model requires more investigation with a range of different bus stop configurations and conditions.
2. An empirical equation to estimate average upstream queue length under MSB conditions should be developed by using simulation results shown in Section 7.9. This will then enable development of design practical capacity under MSB operation.
3. Further validation of proposed empirical equations on average queue length should be conducted using observed queues at selected busway stations on Brisbane's SEB.
4. This research will be continued to estimate 95^{th} percentile queue for both ASB and MSB conditions as degree of saturation is varied.
5. This research identified that the clearance time follows a log normal distribution. However, a further validation will be conducted at different stations to represent different demand conditions.
6. This research can be expanded further to develop a methodology to estimate dwell time for on-street bus stops using smart card transitions data.

References

1. AUSTROADS 2012. The Use of Microsimulation Traffic Models for On-road Public Transport.
2. BCC. (2007). Brisbane Mass Transit Investigation.
3. BRAGDON, D. (2010). Regional High Capacity transit system plan 2035 Summary report.
4. CHEN, X., CAI, P., ZHU, L., & YU, L. (2010, 19-22 Sept. 2010). Micro-simulation study of the effect of median bus lanes with midblock stop on capacity of urban signalized intersection. Paper presented at
5. CURRIE, G. 2006. Bus Rapid Transit in Australia: Performance, Lessons Learned and Futures.
6. DOCKENDORF, J., LEVINSON, H. S., FICHTER, D., HAGHANI, A., HUNDENSKI, R. J., & PRESTRUD, C. E. (2001). Bus Transportation: A Look Forward. 1-6.
7. FERNÁNDEZ, R. 2007. Results of the Microscopic Modelling of Traffic Interactions at Stops, Junctions and Roads for the Design of Bus Rapid Transit Facilities.
8. FERNÁNDEZ, R. 2010. Modelling Public Transport Stops by Microscopic Simulation. Transportation Research Part C.
9. FRICKER, J. D. 2011. Bus dwell time analysis using on-board video. TRB 2011 Annual Meeting.
10. FTA 2007. Report on South American Bus Rapid Transit Field Visits: Tracking the Evolution of the TransMilenio Model. FTA-FL-26-7104.2007.03.
11. FTA 2008. Advanced Network Planning for Bus Rapid Transit: The "Quickway Model" as a Modal Alternative to "Light Rail Lite".
12. FTA. (2004). Institutional and Regulatory Options for Delhi's High Capacity Bus System: Lessons from International Experience.
13. GOLOTTA, K., & HENSHER, D. A. (2008). Why is the Brisbane Bus Rapid Transit System Deemed a Success? Road and Transport Research, 17(4), 14.

14. GUENTHNER, R. P. & SINHA, K. C. 1983. Modeling Bus Delays Due to Passenger Boardings and Alightings. Transportation Research Record, 915, 7-13.
15. HIDALGO, D., LLERAS, G. & HERNÁNDEZ, E. 2013. Methodology for calculating passenger capacity in bus rapid transit systems: Application to the TransMilenio system in Bogotá, Colombia. Research in Transport
16. HIDAS, P., AITKEN, S., SHARMA, S. & XU, M. 2009. Evaluation of Bus Operations by microsimulation in a Sydney CBD corridor. ATRF. Auckland.
17. JAISWAL, S., BUNKER, J. & FERREIRA, L. 2009. Modelling the relationships between passenger demand and bus delays at busway stations. 88th Annual Meeting of Transportation Research Board. Transportation Re
18. JAISWAL, S., BUNKER, J. & FERREIRA, L. 2010. Influence of Platform Walking on BRT Station Dwell Time Estimation: Australian Analysis. Journal of Transportation Engineering, 136, 1173-1179.
19. JAISWAL, S., BUNKER, J. & LUIS FERREIRA, F. 2007. Operating Characteristics and Performance of a Busway Transit Station. Australasian Transport Research Forum (ATRF). Melbourne, Australia.
20. KWAMI, A. V., KUAN, Y. X. & ZHI, X. 2009. Effect of Bus Bays on Capacity of Curb Lanes. Journal of American Science, 117-118.
21. LEVINSON, H. S. & JACQUES, K. R. 1998. Bus Lane Capacity Revisited. Transportation Research Record, 1618, 11.
22. LEVINSON, H. S. 1983. Analyzing Transit Travel Time Performance. Transportation Research Record 915, 1-6.
23. LI, F., DUAN, Z. & YANG, D. 2012. Dwell Time Estimation Models for Bus Rapid Transit Stations. Journal of Modern Transportation, 20, 10.
24. LIN, J., WANG, P. & BARNUM, D. T. 2008. A quality control framework for bus schedule reliability. Transportation Research Part E: Logistics and Transportation Review, 44, 1086-1098.
25. LIU, R. & SINHA, S. 2006. Modelling Urban Bus Service and Passenger Reliability.
26. LUCAS, S. (2009). What in the World? Australian Bus Rapid Transit – The Brisbane Busways. Paper presented at the APTA BRT Conference, Seattle,

Washington.

27. LUKE, S., & GRODUM, S. (2000). Busway Operational Issues and Impact on Busway Station Capacity. Paper presented at the Smart Urban Transport Conference.
28. MILKOVITS, M. N. 2008. Modeling the Factors Affecting Bus Stop Dwell Time. Transportation Research Record: Journal of the Transportation Research Board, 6.
29. NBRTI. Retrieved 06.01.2014, from http://www.nbrti.org/
30. OTTO, P. (2008). Brisbane Transport Fleet Facts. Retrieved from http://www.btbuses.info/downloads/btfleetfacts.pdf
31. PUONG, A. 2000. Dwell Time Model and Analysis for the MBTA Red Line.
32. RATHWELL, S., & SCHIJNS, S. (2002). Ottawa and Brisbane: Comparing a Mature Busway System with Its State-of-the-Art Progeny. Journal of Public Transportation, 5(163-182), 20.
33. SIDDIQUE, A. J., & KHAN, A. M. (2006). Microscopic Simulation Approach to Capacity Analysis of BRT Corridors. Journal of Public Transportation, BRT Special Edition.
34. SUN, Y. & XU, R. 2012. Rail Transit Travel Time Reliability and Estimation of Passenger Route Choice Behavior. Transportation Research Record: Journal of the Transportation Research Board.
35. TCRP-90. (2003). Curitiba, Brazil BRT Case Study. Volume 1.
36. TIAN, L., & HUANG, H. (2010). Simulation of Two-lane Traffic Flow Considering the Combined Effect of Intersection and Bus Stop. Paper presented at the Third International Joint Conference on Computational
37. TransLink. (2007). Public Transport Infrastructure Manual.
38. TransLink. (2010). TransLink Transit Authority Strategic Plan 2010–2015.
39. TransLink. (2011). Draft Connecting SEQ 2031.
40. TransLink. (2012a). Public Transport Infrastructure Manual.
41. Translink. (2012b). Translink Network Information. 2012, from http://translink.com.au/travel-information/network-information/maps
42. TRB 1999. Transit Capacity and Quality Service Manual (1st edition).
43. TRB 2000. Highway Capacity Manual (3rd edition).

44. TRB 2003a. Bus Rapid Transit Cooperative Research Program Report 90, Volume 1: Case Studies in Bus Rapid Transit, 1-62.
45. TRB 2003b. Transit Capacity and Quality of Service Manual, 2nd Edition. Washington, D.C.
46. TRB 2013. Transit Capacity and Quality Service Manual (3rd edition).
47. TRB. 2003c. Curitiba, Brazil BRT Case Study.
48. TRB. 2008. Uses of Higher Capacity Buses in Transit Service. Synthesis 75, 1-81.
49. TSS 2010. AIMSUN 6.1 Microsimulator and Mesosimulator User‘s Manual.
50. UNHSP. 2013. Planning and Design For Sustainable Urban Mobility.
51. VUCHIC, V. R. (ed.) 2005. Urban Transit Operations, Planning and Economics.
52. WIDANAPATHIRANAGE, R., BUNKER, J. M. & BHASKAR, A. 2013a. A Microscopic Simulation Model to Estimate Bus Rapid Transit (BRT) Station Service Capacity with Mixed Stopping and Non-stopping Bus Operation. OP
53. WIDANAPATHIRANAGE, R., BUNKER, J. M. & BHASKAR, A. 2013b. A Microscopic Simulation Model to Estimate Bus Rapid Transit Station Bus Capacity Australasian Transport Research Forum 2013 Proceedings. Queensland
54. WIDANAPATHIRANAGE, R., BUNKER, J. M. & BHASKAR, A. 2013c. Modelling Busway Station Dwell Time Using Smart Cards. Australasian Transport Research Forum 2013 Proceedings
55. WIDANAPATHIRANAGE, R., BUNKER, J. M. & BHASKAR, A. 2014. Modeling Bus Rapid Transit Station Bus Queuing for Bus Rapid Transit Station Bus Operation Analysis. In: TRB Annual Meeting, 2014 Washington DC.
56. WU, C. & MURRAY, A. T. 2005. Optimizing Public Transit Quality and System Access: The Multiple-Route, Maximal Covering/Shortest-Path Problem. Environment and Planning B: Planning and Design, 32(2), 16.

Appendix

Appendix A: Notations

a, b, c	= curve fitting constants; (s)
B	= design bus capacity; (bus/h)
$B_{asb\|p}$	= all-stopping-buses potential capacity; (bus/h)
B_{in}	= bus inflow; (bus/h)
B_l	= loading area bus capacity; (bus/h)
$B_{LA1}, B_{LA2}, B_{LA3}$	= loading area one, two and three bus capacities, respectively
$B_{nsb\|p}$	= Non-Stopping Buses (NSB) potential capacity under MSB operation; (bus/h)
B_s	= bus stop bus capacity; (bus/h)
$B_{sb\|p}$	= Stopping Buses (SB) potential capacity under MSB operation; (bus/h)
c_v	= coefficient of variation of dwell times
C_{vh}	= coefficient of variation of headways
$cv(t_{d\|meas})$	= coefficient of variation of measured dwell time
$cv(t_{d\|est})$	= coefficient of variation of estimated dwell time using Equation 6-1
DT_n	= n^{th} loading area dwell time; (s)
E_{LA1}	= efficiency of loading area 1 with only three nominated loading areas
E_{LA2}	= efficiency of loading area 2 with only three nominated loading areas
E_{LA3},	= efficiency of loading area 3 with only three nominated loading areas
f_{bbi}	= bus-bus interference factor
k	= door opening and closing time; (s)
LT_n	= n^{th} loading area bus lost time; (s)
m	= number of time intervals during study period when loading area 2 OR loading area 3 OR loading areas 2 and 3 were occupied AND loading area 4 was not occupied

n = number of time intervals during study period when loading area 2 OR loading area 3 OR loading areas 2 and 3 were occupied AND loading area 1 was not occupied AND loading area 4 was not occupied (from Figure 5-6; $\sum_{i=2} t_i + \sum_{i=7}^{10} t_i$)

N = number of passengers board and alight

N_{EL} = empirical factor reflecting number of effective loading areas

N_{la} = actual number of loading areas on platform, equal to 3 for study station

o = number of time intervals during study period when loading area 2 OR loading area 3 OR loading areas 2 and 3 were occupied AND loading area 4 was occupied

p = number of time intervals during study period when loading area 2 OR loading area 3 OR loading areas 2 and 3 were occupied AND loading area 1 was not occupied AND loading area 4 was occupied

P_b, P_a = number of passenger boarding and alighting

P_{nsb} = proportion of non-stopping buses

q = number of time intervals during study period when loading area 4 was occupied.

Q_{av} = upstream average queue length; (bus)

st_{av} = average time spent in the system; (s)

t_a = service time per passenger alighting; (s)

t_b = service time per passenger boarding; (s)

t_{bl} = boarding lost time; (s)

t_c = average clearance time; (s)

t_d = average dwell time; (s)

$t_{d|est}$ = estimated dwell time; (s)

$t_{h,4}$ = duration of the h^{th} time interval when loading area 4 was occupied; (s)

t_i = dwell time value that will not be exceeded more often than the desired failure rate; (s)

$t_{i,3\bar{\wedge}4}$ = duration of the i^{th} time interval when loading area 3 was occupied AND loading area 4 was not occupied; (s)

$t_{i,(2\vee3\vee(2\wedge3))\bar{\wedge}4}$ = duration of the i^{th} time interval when loading area 2 OR loading area 3 OR loading areas 2 and 3 were occupied AND loading area 4 was not occupied; (s)

$t_{j,(2\vee3\vee(2\wedge3))\bar{\wedge}1\bar{\wedge}4}$ = duration of the j^{th} time interval when loading area 2 OR loading area 3 OR loading areas 2 and 3 were occupied AND loading area 1 was not occupied AND loading area 4 was not occupied (from Figure 5-6;$\sum_{i=9}^{10} t_i$) ; (s)

$t_{j,3\bar{\wedge}1\bar{\wedge}4}$ = duration of the j^{th} time interval when loading area 3 was occupied AND loading area 1 was not occupied AND loading area 4 was not occupied; (s)

$t_{k,3\wedge4}$ = duration of the k^{th} time interval when loading area 3 was occupied AND loading area 4 was occupied; (s)

$t_{k,(2\vee3\vee(2\wedge3))\wedge4}$ = duration of the k^{th} time interval when loading area 2 OR loading area 3 OR loading areas 2 and 3 were occupied AND loading area 4 was occupied (from Figure 5-6;$\sum_{i=3}^{5} t_i$); (s)

$t_{l,3\bar{\wedge}1\wedge4}$ = duration of the l^{th} time interval when loading area 3 was occupied AND loading area 1 was not occupied AND loading area 4 was occupied; (s)

$t_{l,\bar{\wedge}4}$ = duration of the l^{th} time interval when loading area 4 was occupied AND loading area 3 was not occupied; (s)

$t_{l,(2\vee3\vee(2\wedge3))\bar{\wedge}1\wedge4}$ = duration of the l^{th} time interval when loading area 2 OR loading area 3 OR loading areas 2 and 3 were occupied AND loading area 1 was not occupied AND loading area 4 was occupied (from Figure 5-6;$\sum_{i=4}^{5} t_i$); (s)

t_{oc} = door opening and closing time (2-5 seconds)

t_{om} = operating margin; (s)

$t_{pf,max}$ = maximum passenger flow time of all door channels; (s)

t_q = bus queuing transaction time; (s)

$t_{sg}(t_d)$ = gross smart card transaction time corresponding to t_d; (s)

$t_{sn}(t_d)$ = net smart card transaction time corresponding to t_d; (s)

t_{st} = smart card transaction time; (s)

$\bar{t}_{d|meas}$ = average measured dwell time; (s)

$\bar{t}_{d|est}$ = average estimated dwell time using Equation 6-1; (s)

T = system time, equal to 1h (3600s)

$T_{1,b}$ = total time that loading area 1 was empty while a bus occupied loading area 2 OR loading area 3 OR both loading areas 2 and 3; (s)

$T_{2,b}$ = total time that loading area 2 was empty while a bus occupied loading area 3 during time T; (s)

$T_{2,3}$ = total time that loading area 2 OR loading area 3 OR loading areas 2 and 3 are occupied during time T; (s)

T_3 = total time that loading area 3 is occupied during time T; (s)

v = bus cruise speed; (km/h)

X_{in} = degree of saturation; (demand/capacity)

Z = standard normal variate corresponding to a desired failure rate

δ_i = delay time at a i^{th}stop; (s)

α = acceleration rate; (m/s^2)

η_{LA1} = efficiency of loading area 1 with *temporary* loading area

η_{LA2} = efficiency of loading area 2 with *temporary* loading area

η_{LA3} = efficiency of loading area 3 with *temporary* loading area

$\eta_{LA4\,(t)}$ = efficiency of fourth *(temporary)* loading area

β = deceleration rate; (m/s^2)

σ_{t_d} = standard deviation of dwell times

Appendix B: Ethical Clearance

University Human Research Ethics Committee

HUMAN ETHICS APPROVAL CERTIFICATE

NHMRC Registered Committee Number EC00171

Date of Issue: 16/4/13 (supersedes all previously issued certificates)

Dear Mr Rakkitha Widana Pathiranage

A UHREC should clearly communicate its decisions about a research proposal to the researcher and the final decision to approve or reject a proposal should be communicated to the researcher in writing. This Approval Certificate serves as your written notice that the proposal has met the requirements of the *National Statement on Research involving Human Participation* and has been approved on that basis. You are therefore authorised to commence activities as outlined in your proposal application, subject to any specific and standard conditions detailed in this document.

Within this Approval Certificate are:

* Project Details
* Participant Details
* Conditions of Approval (Specific and Standard)

Researchers should report to the UHREC, via the Research Ethics Coordinator, events that might affect continued ethical acceptability of the project, including, but not limited to:

(a) serious or unexpected adverse effects on participants; and
(b) proposed significant changes in the conduct, the participant profile or the risks of the proposed research.

Further information regarding your ongoing obligations regarding human based research can be found via the Research Ethics website http://www.research.qut.edu.au/ethics/ or by contacting the Research Ethics Coordinator on 07 3138 2091 or ethicscontact@qut.edu.au

If any details within this Approval Certificate are incorrect please advise the Research Ethics Unit within 10 days of receipt of this certificate.

Project Details

Category of Approval:	Human non-HREC		
Approved From:	16/04/2013	**Approved Until:**	16/04/2016 (subject to annual reports)
Approval Number:	1300000074		
Project Title:	Comparison of bus rapid transit operations between local route joins corridor versus local route interchange with line haul		
Experiment Summary:	Develop a model to obtain Bus stop capacity with stopping and non-stopping buses.		

Investigator Details

Chief Investigator: Mr Rakkitha Widana Pathiranage

Other Staff/Students:

Investigator Name	Type	Role
A/Prof Jonathan Bunker	Internal	Supervisor
Dr Ashish Bhaskar	Internal	Supervisor

Participant Details

Participants:
Passenger counting only

Location/s of the Work:
Buranda, Garden City and Eight mile Plains Busway stations

University Human Research Ethics Committee

HUMAN ETHICS APPROVAL CERTIFICATE

NHMRC Registered Committee Number EC00171

Date of Issue: 16/4/13 (supersedes all previously issued certificates)

Conditions of Approval

Specific Conditions of Approval:
None apply

Standard Conditions of Approval:
The University's standard conditions of approval require the research team to:

1. Conduct the project in accordance with University policy, NHMRC / AVCC guidelines and regulations, and the provisions of any relevant State / Territory or Commonwealth regulations or legislation;

2. Respond to the requests and instructions of the University Human Research Ethics Committee (UHREC);

3. Advise the Research Ethics Coordinator immediately if any complaints are made, or expressions of concern are raised, in relation to the project;

4. Suspend or modify the project if the risks to participants are found to be disproportionate to the benefits, and immediately advise the Research Ethics Coordinator of this action;

5. Stop any involvement of any participant if continuation of the research may be harmful to that person, and immediately advise the Research Ethics Coordinator of this action;

6. Advise the Research Ethics Coordinator of any unforeseen development or events that might affect the continued ethical acceptability of the project;

7. Report on the progress of the approved project at least annually, or at intervals determined by the Committee;

8. (Where the research is publicly or privately funded) publish the results of the project is such a way to permit scrutiny and contribute to public knowledge; and

9. Ensure that the results of the research are made available to the participants.

Modifying your Ethical Clearance:
Requests for variations must be made via submission of a Request for Variation to Existing Clearance Form (http://www.research.qut.edu.au/ethics/forms/hum/var/var.jsp) to the Research Ethics Coordinator. Minor changes will be assessed on a case by case basis.

It generally takes 7-14 days to process and notify the Chief Investigator of the outcome of a request for a variation.

Major changes, depending upon the nature of your request, may require submission of a new application.

Audits:
All active ethical clearances are subject to random audit by the UHREC, which will include the review of the signed consent forms for participants, whether any modifications / variations to the project have been approved, and the data storage arrangements.

End of Document